# TEXTILE RESEARCH JOURNAL

*Publication of*

TEXTILE RESEARCH INSTITUTE

VOLUME XXVIII MAY 1958 NUMBER 5

# TEXTILE RESEARCH JOURNAL

VOL. XXVIII *May 1958* NUMBER 5



*Editor:* **Julian S. Jacobs**

*Production Editor:* **Candida Frenking**

*Advisory Board*

**H. J. Ball**
**Earl E. Berkley**
**Henry Eyring**
**W. J. Hamburger**
**Milton Harris**
**K. L. Hertel**
**Harold P. Lundgren**
**H. Mark**
**E. R. Schwarz**



TEXTILE RESEARCH JOURNAL, published monthly at Prince and Lemon Streets, Lancaster, Pa., is devoted to the interest of research in textile and allied industries. It is published by Textile Research Institute.

Entered as second-class matter, April 27, 1945, at the post office at Lancaster, Pa., under the Act of August 24, 1912. Accepted for mailing at special rate of postage provided for in paragraph (d-2), Section 34.40, P. L. & R. of 1948, authorized May 9, 1950.

Manuscripts and communications should be sent to the Publications Department, P.O. Box 625, Princeton, N. J.

Subscription rates: $20.00 per year; additional for postage, 50 cents to Canada, $1.00 to all other countries. Single copies, $2.00 each.



Contents copyrighted © 1958 by Textile Research Institute. Advertising rates supplied on request.


## IN THIS ISSUE


Microscopical Study of a Multilayer Nylon Body Armor Panel After Impact. *G. Susich, L. M. Dogliotti, and A. S. Wrigley* ..... 361

The Amino Acid Composition of Fractionated Cortical Cells From Wool. *David H. Simmonds and John J. Bartulovich* ..... 378

Applications of Infrared Absorption Spectroscopy to Investigations of Cotton and Modified Cottons. Part I: Physical and Crystalline Modifications and Oxidation. *Robert T. O'Connor, Elsie F. DuPré, and Donald Mitcham* .... 382

The Effect of Temperature on the Rate of Creep Failure for 66 Nylon. *Bernard D. Coleman, Andrew G. Knox, and William F. McDevit* ..... 393

A Two-Dimensional Load–Estension Tester for Fabrics and Film. *P. B. Checkland, T. H. Bull, and E. J. Bakker* .. 399

Some Relationships Between Supermolecular Structure and Mechanical Behavior of Native and Chemically Modified Cotton Cellulose. *Verne W. Tripp, Rollin S. Orr, Hilda M. Ziifle, and Carl M. Conrad* ..... 404

Changes in the Weight Distribution of Fiber Lengths of Cotton as a Result of Random Fiber Breakage. *W. J. Byatt and J. P. Elting* ..... 417

The Reliability of the Soil Burial Method for Evaluating Textile Preservative Treatments. *J. M. Ashcroft* ..... 422

Punched-Card Methods for Studying Fiber–Yarn Relationships. *Helmut Wakeham and La Dean Steward* ..... 431


### LETTERS TO THE EDITOR


Micronaire Reading as a Close Approximation to Fiber Thickness. *K. L. Hertel* ..... 442

The Occurrence of Myrothecium on Field Cotton. *A. N. J. Heyn* ..... 444

*BOOK REVIEWS* ..... 446


REPRINT REQUESTS SHOULD BE DIRECTED TO THE AUTHORS
SEE ARTICLES FOR ADDRESSES

MAY 1958
VOL. XXVIII NO. 5

TEXTILE RESEARCH JOURNAL

# Microscopical Study of a Multilayer Nylon Body Armor Panel After Impact

**G. Susich, L. M. Dogliotti, and A. S. Wrigley**

*Pioneering Research Division, Quartermaster Research and Engineering Center, Natick, Massachusetts*

**Abstract**

A body armor panel consisting of twelve identical layers of 2 × 2 basket weave nylon fabric was investigated after impact by a fragment simulator .22-caliber steel missile in the range of 330–420 m./sec. (1100–1400 ft./sec.) striking velocities. The kinetic energy of the projectile was either slightly higher or lower than that the panel could absorb (706,000 g.-cm.).

Completely and partially penetrated holes were investigated. The area surrounding the bullet holes was studied to learn about the various types of deformations and damages in each layer. The microscopic observations were obtained at various magnifications (5, 10, and 200 ×) from cross sections of the panel and from individual layers removed from the panel.

Cross sections at various levels were made in three directions, either perpendicular or parallel to the panel surface. In these sections the distortion of the fabric pattern, alignment of extended, unravelled, and broken yarns into the direction of bullet movement, compression of yarns, softening, heat relaxation, fusion, decomposition, and fibrillation of nylon filaments were observed. It was recognized that the permanent damage was localized to a small area close to the path of the fast-moving missile.

After separating the panel into individual layers, the stoppage of the projectile was studied. A slight dissipation of the stress was observed in those layers which were exposed to the bullet after it was slowed down. Some damages to nylon filaments were caused by the transient and localized heat generated during the impact of the missile. Fibrillation indicates the vigorous movements of filaments which took place in the panel during penetration. The restriction of permanent deformations and defects to small regions was explained by the presence of cross yarns. They prevent the propagation of the stress from the impacted spot to any considerable length along the yarns.

## Introduction

The impact behavior of textile fabrics generally is studied in ballistic tests by firing missiles at the fabric under well controlled conditions. The ballistic resistance is obtained readily by observing the penetration of missiles under increasingly severe conditions. The conditions of ballistic tests are determined by the material, weight, dimensions (shape), and velocity of the missile striking the fabric, by the direction of incidence and of penetration, and by environmental conditions, such as tempera-

ture, humidity, backing, etc. It is preferable to keep all these factors in ballistic tests constant except for the velocity of the missile. The ballistic resistance of a fabric can then be expressed conveniently by the highest striking velocity at which retention of the projectile occurs. The ballistic test by itself does not provide any information on the way in which the textile material fails or resists. Since the fabric and its elements (yarns and single fibers) are deformed by the impact, they can be studied by microscopical methods.

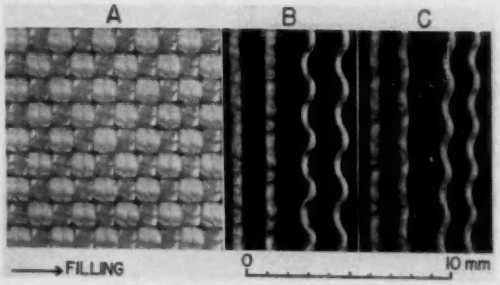


**Fig. 1.** Fabric surface and yarns removed from the fabric. (A) 2 × 2 basket weave; (B) warp yarns; (C) filling yarns. Two left yarns seen normal, two right yarns seen parallel to the fabric surface.

The alterations of the fabric are either temporary or permanent. If deformations are caused by relatively low stresses, they do not exceed the elastic limit, and the fabric may recover after the impacting process has ceased. High stresses cause deformations which remain and represent damages to the fabric. They are predominant at sufficiently severe conditions when a hole appears in the textile material.

The microscopical examination of fabrics during the impact of the bullet would be extremely instructive. It could reveal temporary as well as permanent deformations of the material, including movement of the fabric and any other alterations at different stages of the impact. The high speed at which deformations take place and the limitations of conventional microscopes, such as short working distance, small depth of focus, etc. make these examinations unfeasable. If instead of a single fabric layer a fabric panel consisting of many layers has to be studied, the microscopical observation would be necessarily restricted to the first and last layers. This is a great disadvantage, because no information would be gained on the performance of individual layers within the panel. It is, therefore, more practical and yet informative to examine the behavior of a fabric panel after it was

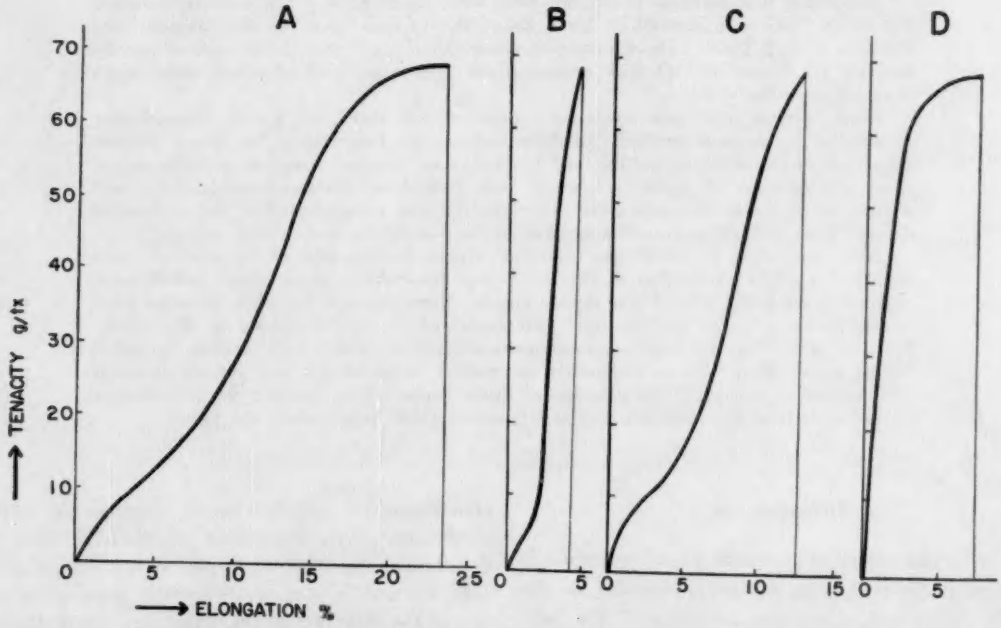


**Fig. 2.** Stress-strain relationship and recovery behavior of 5-ply 210/34 nylon yarn Type 300. (A) stress-strain curve; (B) immediate elastic recovery; (C) delayed elastic recovery; (D) permanent set.

impacted by missiles. It must be mentioned that the impact of a multilayer panel hardly can be considered as a superposition of the impact on a number of single fabric layers. The simultaneous presence of many layers in close contact with each other influences the penetration of each individual layer markedly.

If the nylon body armor panel is hit by a steel missile at a sufficiently high striking velocity, the first layer is severely damaged and penetrated. This occurs after it was extended or compressed, depending upon the resistance of the layers backing the fabric. During penetration the missile loses part of its original velocity and kinetic energy. The velocity of the projectile is reduced as it passes through the first and subsequent layers, since each layer absorbs a portion of the energy. Thus a deceleration of the missile takes place until either the energy of the missile has been fully absorbed or all layers have been penetrated. In the case of complete penetration, the missile leaves the panel with a residual velocity and kinetic energy usually much lower than the original, and the panel provides some protection to the human body. If the kinetic energy of the missile diminishes to such an extent that it is no longer able to emerge from a layer, the missile is stopped. A partial penetration takes place; nevertheless, unpenetrated layers become deformed by the pressure of the projectile. In this case the panel gives full protection to the human body.

The slowing down of the missile and the extraction of its energy cannot occur without substantial alterations of the fabric. The most obvious of them is the appearance of holes. They represent the path of the fast-moving projectile and remain in the panel after the missile emerges from the last layer or is stopped. During penetration, of course, much movement takes place in the area surrounding the holes, causing dislocations and deformations of yarns and filaments. These are partly reversible and can recover either immediately or after a while, depending upon the elastic and creep properties of the textile material. An essential portion of alterations in the area close to the missile movement is irreversible. Therefore, the fabric around holes appears drastically deformed. Yarns are extended, bent, compressed, unravelled, partially or completely ruptured, and are no longer in their original locations. These can be recognized in impacted panels to some extent with the naked eye. They can be better studied by microscopic techniques after making cross-sections or after separating the panel into individual layers. Both methods were used in this investigation, in which the surrounding area of holes was studied at appropriate magnifications. The holes served as "footprints" of the fast-moving projectile. They revealed the permanent alterations caused by the impact of the projectile.

## The Nylon Panel Tested

The body armor panel tested consists of twelve layers of the same nylon fabric, assembled in identical positions and button-stitched together. The dimensions of the panel were approximately 30 × 40 cm. (12 × 16 in.), its weight was 18.6 oz./sq. ft. (5677 g./m.$^2$), and its thickness varied from 11 to 13 mm. depending upon the airspaces between the layers.

The fabric was made to meet the Military Specification "Cloth Nylon Duck, Lightweight" MIL-C-12369 (QMC) of 4 December 1952. It is a 2 × 2 basket weave nylon fabric, shown in Figure 1A, having a weight of 14.0 oz./sq. yd. (474 g./m.$^2$) and an approximate thickness of 0.8 mm. The fabric contains 49 ends and 44 picks/in. (19.3 and 17.3 threads/cm. respectively) of 5-ply 210/34 nylon Type 300 (Du Pont) multifilaments with low twist. Warp and filling yarns are identical, their size being 116.6 tex [1, 2] (1050 den.), each containing 170 single filaments of 0.67 tex (6 den.).

The tensile properties, including the elastic behavior of the nylon yarns, are illustrated in Figure 2 and Table I. They represent average values from ten specimens tested under standardized conditions (21.2° C. = 70° F. and 65% R.H.) at a strain rate of 100%/min., using the Instron Tensile Tester TTB and a testing technique described in more detail previously [11].

The nylon yarn was highly drawn. It is a strong fiber, with a remarkable extensibility and consequently high energy absorption compared to other textile materials. It is also a very elastic fiber, since a considerable portion of its elongation recovers after the tension is released. The major part of this recovery does not take place immediately, however, but requires some time, and is known as delayed elastic recovery (see Table I).

The tensile properties of nylon characterize the mechanical resistance of the yarns when extended in a direction parallel to the fiber length at a strain

rate essentially lower than prevailing in ballistic tests. In ballistic tests yarns are subjected to stresses practically normal to the fiber length. The behavior of yarns in the fabric is greatly affected by the presence of two yarn systems. The impact of the missile and its movement elongate the yarns in the panel. Their extension is restricted, however, by the cross yarns and the resistance of layers backing the fabric. Extension of yarns is, of course, not the only deformation which takes place in an impacted fabric; yarns are also compressed, bent, and sheared. Therefore it can be expected that the tensile properties of yarns are not sufficient for interpreting the ballistic behavior of the panel.

Warp and filling yarns are set (permanently fixed) in the fabric by the heat treatment at 163° C. (325° F.) prescribed in the specification. The yarns have a two-dimensional crimp which is very uniform and different in the two yarn systems. This can be recognized in Figures 1B and C, where warp and filling yarns, removed from the fabric, are illustrated as seen from two directions. The crimp plane of warp and filling are mutually perpendicular to each other and both are normal to the fabric surface. The fabric is slightly unbalanced due to its texture. In the final setting operation warp yarns obtain a more pronounced crimp. The wave length of the crimp, its amplitude, and the flattening of warp are higher than for filling. The flattening of yarns in each system can be recognized by comparing the yarn diameters as they appear normal and parallel to the fabric surface in Figures 1B and C. The "ellipticity" of yarns is more readily observable from fabric cross sections, shown in Figure 3. Here the two yarns appear pressed together to form elliptical double yarns. Warp yarns are slightly more flattened than filling yarns. The ratio of minor to major axis in the elliptical cross sections is approximately 1 : 3.2 for warp and 1 : 2.4 for filling.

**TABLE I**

Tensile Properties of 5-Ply 210/34 Nylon Type 300 Yarn (Du Pont) (116.6 tex) [1, 2]

| | |
|---|---|
| Breaking load | 7900 g. |
| Breaking tenacity | 67.7 g./tex |
| Elongation at break | 23.6% |
| Initial modulus of elasticity | 324 g./tex |
| Total energy of rupture | 860 g.-cm./tex/m. |

Recovery Behavior at the Breaking Point [11]

| | Elongation | | Energy | |
|---|---|---|---|---|
| | % | % of total | g.-cm./ tex/m. | % of total |
| Immediate elastic recovery | 4.25 | 18 | 101 | 12 |
| Delayed elastic recovery (Primary creep) | 12.25 | 52 | 371 | 43 |
| Permanent set | 7.05 | 30 | 388 | 45 |
| Total | 23.6 | | 860 | |

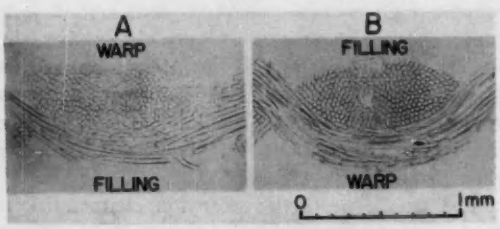


**Fig. 3.** Cross sections of the 2 × 2 nylon fabric. (A) warp cross section; (B) filling cross section.

## Ballistic Tests

The ballistic resistance of the panel was tested using the .22-caliber (5.6 mm.) 17 grain (1.052 g.) fragment simulator steel missile T-37 in the range of 330–420 m./sec. (1100–1400 ft./sec.) striking velocities. The missile has a rectangular (chisel-shaped) nose; its dimensions are shown in Figure 4.

The locations of holes representing 20 shots fired into the panel approximately 5 cm. (2 in.) apart from each other are illustrated diagrammatically in Figure 5A. Looking in the direction of projectile movement, the top of the panel is marked north, the bottom south, the right side east, and the left west. These designations were useful for defining locations in the panel. They were necessary in discussing the cross sections made in different directions and were also suitable for describing both sides of individual layers after they were taken out from the panel.

Of the 20 holes, 12 were complete and 8 were partial penetrations. Figures 5B and C are X-ray

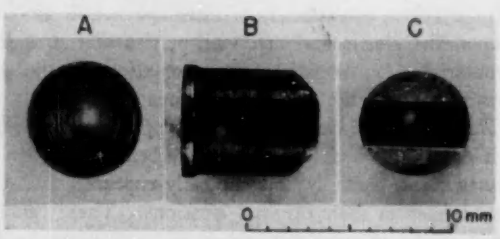


**Fig. 4.** Fragment simulator steel missile. (A) back view with rim; (B) side view; (C) front view.

pictures of the impacted panel taken from two directions perpendicular to each other. They illustrate the position of the 8 bullets after they were stopped by the panel. These missiles could not penetrate the panel, partly because of their too low striking velocity and kinetic energy [1] and partly because of their tumbling. None of them had a striking velocity higher than 374 m./sec. (1226 ft./sec.), equivalent to a kinetic energy of 748,000 g.-cm., while corresponding values for complete penetrations were as high as 426 m./sec. (1398 ft./sec.) and 971,000 g.-cm., respectively. In spite of the relatively small distance (a few feet) between muzzle and panel, the majority of the bullets deviated during penetration more or less from their original direction. It is obvious that a greater number of yarns will resist the missile if its movement is not perpendicular to the panel surface, following the shortest distance through the panel, but goes in oblique directions, which may even change during penetration. As a result of this tumbling, the chance to stop the missile increases by the resistance of a larger number of yarns directly hit by the bullet, because each of them is able to absorb a certain amount of energy.

The microscopical study started after the ballistic test of the panel, and all but four of the twenty holes were studied. Only nine holes will be discussed here —six complete (No. 3, 5, 7, 9, 10, and 13) and three partial penetrations (No. 16, 18, and 20). Their location can be recognized on Figure 5A. They

[1] The kinetic energy is the capacity of moving objects to perform work; it can be expressed conveniently either by ergs, absolute work units of the CGS system, or by gravitational work units. In this study gram-centimeter, a gravitational unit of the metric system, will be used. Energy values are obtained from the equation $E = \frac{1}{2}\ w\ v^2\ \frac{1}{981}$ where $E$ is the kinetic energy in g.-cm., $w$ the weight of the bullet in grams (1.052 g.), $v$ the velocity of the bullet in cm./sec., and 1/981 a conversion factor.

Energy values in g.-cm. can be transformed by multiplication with $7.23 \times 10^{-8}$ into ft.-lb. (gravitational units of the English system) or with $2.34 \times 10^{-5}$ into calories (units of thermal energy).

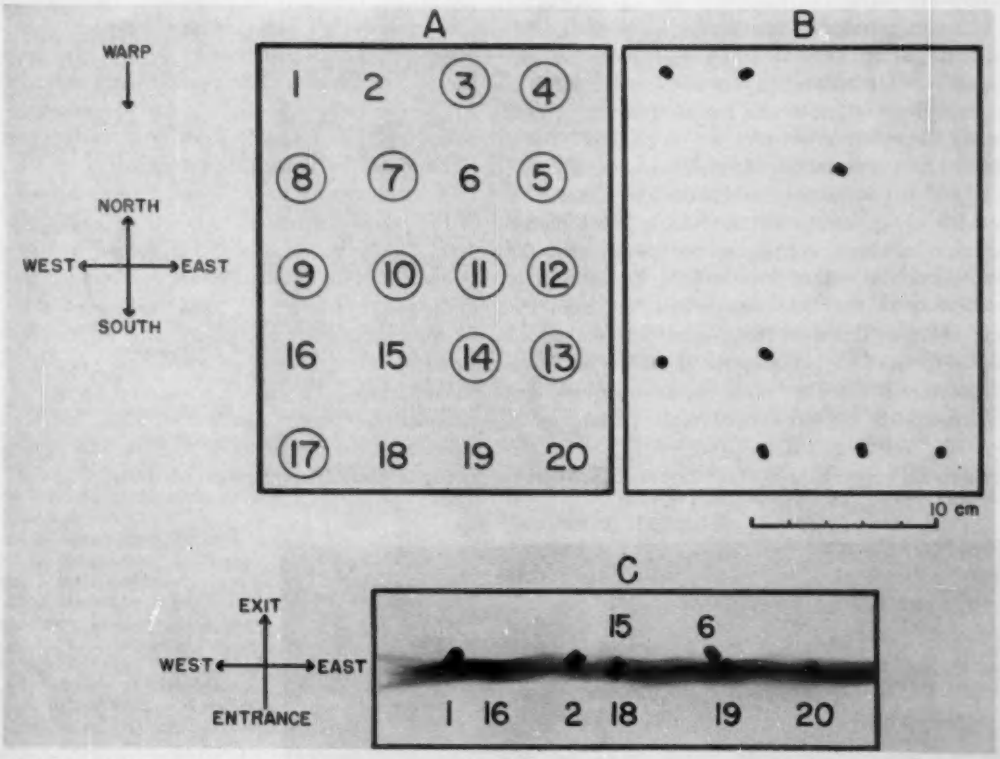


**Fig. 5.** Nylon body armor panel after impact. (A) position of holes (encircled numbers represent complete penetrations); (B) X-ray picture from the front; (C) X-ray picture from the top (north).

were examined either by the sectioning or by separating techniques.

## Sectioning Technique

*Experimental Procedure*

Sections of the panel were made perpendicular and parallel to the fabric surface at different levels. For this purpose the panel was embedded in a plastic material. The embedding was slightly different for complete and partial penetrations, because in the latter case the missile had to be removed before sectioning.

After an area 2.5 cm. (1 in.) square around a completely penetrated hole was stitched through all layers, it was cut out from the panel with a sharp razor blade. It was marked by one or two dyed threads, necessary for identifying the original position of sections. The small rectangular part of the panel containing the hole was sewn together firmly with overcast stitches and then soaked in a liquid mixture of methyl-methacrylate and a plasticizer (37% Santicizer M17) in a beaker for several days. It was frequently evacuated in a dessicator to eliminate air bubbles between layers and yarns. After a few days the wet panel was transferred into a new mixture to which a polymerization catalyst (0.8% Luperco AC) was added. It was then heated (47° C. = 117° F.) until polymerization took place. In about 20 hr. a transparent and fairly hard plastic block was obtained containing the panel with the hole. After the beaker was broken, the immediate surrounding of the hole was sawed out from the block, trimmed down to the proper size, embedded again in the methyl-methacrylate plasticizer mixture, and polymerized. The block finally obtained was then embedded in moderately hard paraffin wax (melting point 56–58° C. = 133–136° F.) to fit into the specimen holder of a Spencer Sliding Microtome, where the cross sections were made. The sections obtained were relatively thick (100–250 $\mu$). Although it was possible to make thinner sections, they were uneven and did not entirely cover the area we were interested in.

The first step in embedding a partially penetrated hole was identical to that for a completely penetrated hole. After a plastic block was obtained, it was cut into two halves around the bullet. The missile was removed from one half shell; this was then re-embedded and treated in the same way as described previously. It is obvious that the preparation of cross sections from partial penetrations is even more timeconsuming than that of complete penetrations. It also requires some experience and skill, because it is essential to remove the projectile after the first embedding without damaging those yarns which are in contact with the missile.

The different steps of the embedding process are illustrated by seven samples in Figure 6; (A) shows the surrounding area of a complete penetration (Hole No. 3) cut out from the panel and sewn together before embedding. (B) is the entrance view of a completely penetrated hole (No. 13) after polymerization in a beaker. The vertical black thread to the left of the hole is a marking for identification purposes. (C) is a plastic block after cutting out and eliminating the immediate surrounding of the hole. (No. 9, discussed later.) Only unpenetrated parts of the panel are visible. (D) is an embedded hole (No. 10) with black marking thread to the right, re-embedded in plastic for sectioning perpendicular to the panel surface. (E) is an embedded hole (No. 7), re-embedded in the plastic and in paraffin after a number of cross sections were made parallel to the panel surface. (F) is the remaining (west) shell of an embedded partial penetration (No. 16) with the bullet after the plastic block was cut into two halves. Sections shown in Figures 9A–D were made from

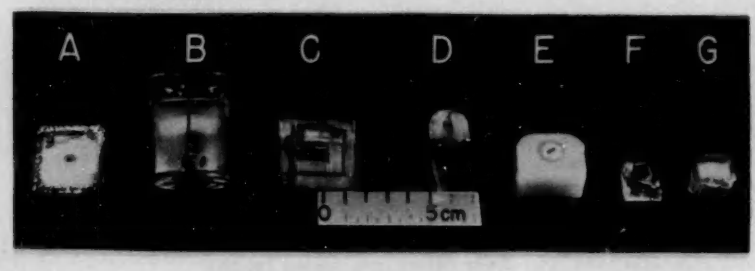


**Fig. 6.** Demonstration of the embedding technique. (A) panel before embedding; (B) panel in beaker after polymerization; (C) rest of plastic block after removal of the embedded hole; (D) embedded hole with marking thread re-embedded in plastic; (E) embedded hole re-embedded in plastic and paraffin; (F) embedded partial penetration with missile; (G) unpenetrated part of panel after sectioning.

the other (east) half shell. (G) is the remainder of a plastic block after the cross sections through a completely penetrated hole (No. 5) were made and after removal of the surrounding paraffin. Cross sections through unpenetrated fabric layers are visible. Their locations were below the hole (to south) shown in Figure 7A.

*Warp Cross Sections of a Complete Penetration* [2]

The entrance and exit views of a completely penetrated hole (No. 5) are shown in Figures 7A and B. The entrance hole is smaller than the circular cross-section of the bullet and is relatively well defined. The longitudinal opening indicates the rectangular shape of the missile nose. The exit hole is rather large and less distinct, since it is covered by numerous loose yarns protruding from the panel surface. Some of them are broken, while others form loops. They were pulled out from the last layers of the panel. The dissimilarity of the entrance and exit holes reflects the markedly different conditions under which they were formed. The first layer was hit at a velocity of 409 m./sec. (1342 ft./sec.) equivalent to a kinetic energy of 895,000 g.-cm. The missile was slowed down and lost an essential part of its originally high energy. The panel absorbed approximately 706,000 g.-cm., or 79% of the impact energy.[3] The missile left the panel with a residual velocity of 188 m./sec. (616 ft./sec.) corresponding to a kinetic energy of 189,000 g.-cm., or 21% of the original impact energy.

In the first layer, hit at high velocity, sharp bending and rupture of yarns by shear and extension took place. The permanent deformation is localized to the path of the bullet. The resistance of the first layer was enhanced by the other layers backing (stiffening) the first. In the exit layers, where the missile moved much slower and no backing exists,

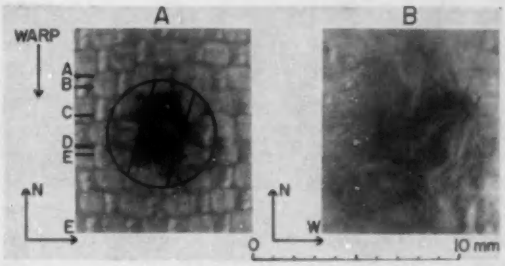


**Fig. 7.** Completely penetrated hole (No. 5). (A) entrance view; (B) exit view.

the extension and pulling out of yarns prevail instead of rupture. The stress is dissipated to an area larger than the cross section of the bullet.

The holes through the first and last layers of the panel are the only ones visible. In order to observe the damage in other layers, a series of warp cross sections were made at different levels of the hole, as indicated in Figure 7A. Five sections are demonstrated in Figures 8A–E, the distance between section (A) and (E) being approximately 4 mm.

The photographs were made at the relatively low original magnification of ten diameters. The cross sections of the panel are shown in the same positions; this is indicated by the two black marking threads in the upper right and lower left corners. In each picture, sections through the twelve individual fabric layers appear. The entrance layer is on the bottom and the exit on the top.

The sections start above the hole in the first layer (north of the panel) and proceed from north to south. Section (A) shows an unaffected fabric pattern in the first four layers. Warp yarns follow a direction practically normal to the plane of the pictures; they appear moderately flattened. Filling yarns lay horizontally (in the west-east direction) and exhibit their regularly crimped state. While only slight alterations can be seen in the following two layers, the middle part of the seventh, eighth, and ninth layer is already distorted. Yarns are bent in a direction parallel to the movement of the missile, which is from bottom to top on the picture. The crimp of filling deviates here from its originally regular waviness. These distortions suggest that this area of the panel was not too far away from the path of the missile. In the last three layers the disturbance of the fabric pattern diminishes. Behind the panel (in the upper left corner of the picture) loose yarns and single filaments are visible. They

[2] In warp cross sections of the panel, warp yarns are cut through perpendicular to the yarn length, while filling yarns are sectioned longitudinally (parallel to the yarn axis).

[3] The energy extracted from the projectile indicates the resistance of the panel and varies depending upon the path (length, direction) and the position of the missile during penetration. Neither was known exactly for the holes formed in the panel. Although the exit velocities of the missiles were not measured in the ballistic tests performed, it could be estimated that the panel was able to absorb approximately 706,000 ± 42,000 g.-cm. energy. This value corresponds to a missile velocity of 363 ± 11 m./sec. (1190 ± 36 ft./sec.).

were pulled out by the missile at levels lower than this section and were cut through by the microtome. We can conclude that the projectile formed this hole by moving first upward (to the north) and turning then downward (to the south) in the middle layers of the panel. The tumbling of the missile appears clearer in Section (B), made slightly above the hole of the entrance layer. While the first two layers remained almost unaffected, the following layers are more or less distorted, and a channel through the panel can be recognized starting at the fifth layer. (C) shows a section across the hole; the channel goes through all twelve layers. It represents the path of the bullet at this level. In the first layers, unravelled warp and filling yarns are bent around the corners of the opening. They are aligned in the direction of projectile movement similar to the orientation of longitudinal bodies into the direction of flow in an air or liquid stream. The intrusion of yarn ends into the hole makes the channel markedly narrower than the diameter of the circular cross section of the bullet which passed through the hole. Some of the aligned yarns are broken, and their ends appear curled (as a result of heat relaxation) or even fused. In Section (D) the hole started to close from the exit side. The first five layers were penetrated. Their opening became increasingly narrower, because of the upward motion of the missile discussed above. The layers following the fifth remained unbroken; their middle portion is markedly disturbed. In Section (E), cut through the lower part of the entrance hole, only the first two layers appear ruptured. In the following layers the middle portion is still distorted, indicating that the path of the bullet must have been close and above this part of the panel. A part of the last layers, not backed sufficiently by others, appears extended and bulged out from the panel due to the pressure exerted by the projectile.

*Filling Cross Sections through a Partial Penetration*

A sequence of four cross sections through a partially penetrated hole (No. 16) is illustrated in Figures 9A–D. They are perpendicular to the fabric surface and to the sections shown in Figure 8. Here filling yarns are cut transversely and warp yarns longitudinally.

The bullet hit the first layer with a velocity of 360 m./sec. (1180 ft./sec.) corresponding to a kinetic energy of 693,000 g.-cm., which is much lower than for the previously discussed complete penetration. The panel entirely absorbed the energy of the missile. The bullet penetrated the first six layers and ruptured some yarns in the following two layers without emerging from them. Although the last four layers remained unbroken, they were extended. They protrude slightly from the panel, indicating the pressure of the bullet. After the bullet was stopped, a cavity, corresponding to the shape of the missile, remained in the panel. Sectioning started in the middle of this cavity and proceeded from west to east. The first and last sections were approximately 4 mm. apart.

A sack-like hole can be seen in Section (A), open

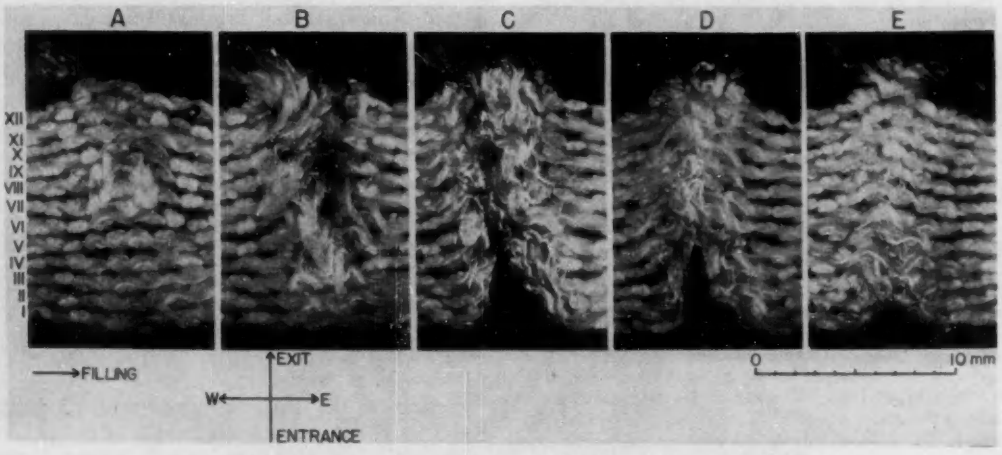


**Fig. 8.** Warp cross sections through a completely penetrated hole (No. 5).

at the entrance side. Sharply bent yarns are aligned in the direction of the missile movement, forming an envelope around the resting projectile. Compressed residues of the sixth and following layers are visible at the level of the ninth layer. Although the last four layers are not ruptured, their pattern is disturbed. The crimp in warp yarns is diminished due to tension. Filling yarns are very much flattened; their ellipticity is substantially increased up to a ratio 1 : 4 of minor to major axis. In Section (B) the hole is closed. Apparently the missile turned with its nose slightly to the south-east (as indicated by the position of the missile in Figures 5B and C) before it was stopped. Similar to the previous section, ruptured and compressed residues of the sixth and subsequent layers are visible at the end of the hole, followed by the unpenetrated last four layers. They are bent, and their deformation is revealed by extremely flattened filling and straightened-out warp yarns. In Section (C) the hole is small and the distortion of the fabric pattern is somewhat diminished. The hole disappears entirely in the last section—(D). The middle part of the fifth to eighth layers is still much affected, suggesting that the missile moved close (probably 1 mm. west) to this area. In all sections a considerable gap appears between the fifth and sixth; a smaller one occurs between the following two layers. These gaps reflect the pressure of the projectile forcing these layers apart.

### *Cross Sections Parallel to the Panel Surface Through a Complete Penetration*

In the series discussed so far, 12 layers of the panel were cut through simultaneously. If sections are prepared parallel to the panel surface, it is possible to cut through one layer and to prepare sections in the same sequence as the missile progressed. This will be illustrated for a completely penetrated hole (No. 9), impacted at 379 m./sec. (1244 ft./sec.) striking velocity, corresponding to a kinetic energy of 768,000 g.-cm., which was more than the panel could absorb.

Sections through the first, third, sixth, ninth, and twelfth layers are demonstrated in Figures 10A–E; the first and last sections were approximately 11 mm.

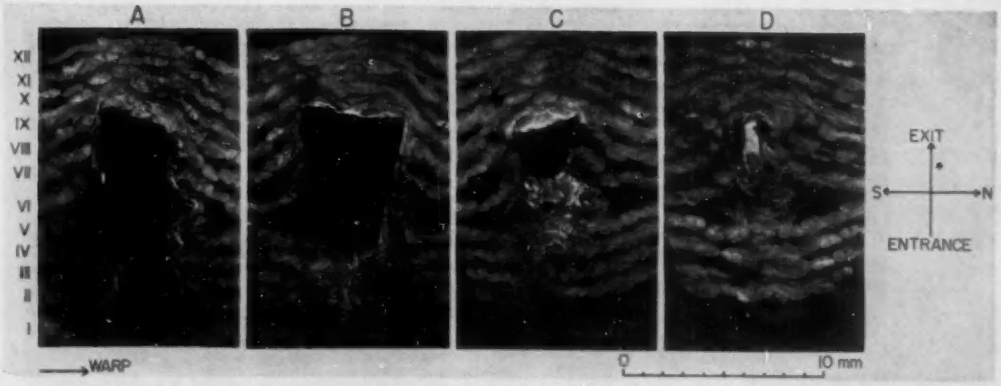


**Fig. 9.** Filling cross sections through a partially penetrated hole (No. 16).

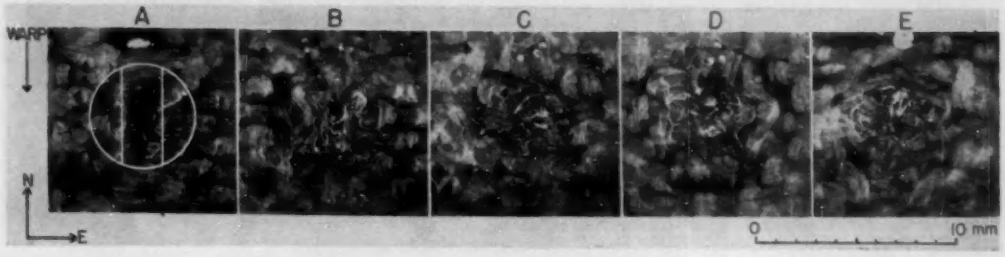


**Fig. 10.** Cross sections parallel to the panel surface through a completely penetrated hole (No. 9). (A) first layer; (B) third layer; (C) sixth layer; (D) ninth layer; (E) twelfth layer.

apart in the panel. Yarns of both systems are cut parallel to the yarn length. Warp yarns are vertical (from north to south) in the pictures.

In the first layer—(A)—the hole is longitudinal and similar to the rectangular nose of the missile. The opening appears much smaller in the third layer —(B)—because of loose yarn ends intruding into the hole from the first and second layers. The opening diminishes even more in the following sections (C, D, and E), and it is difficult to recognize exactly its boundaries because a great number of fibers appear in the impacted area. These cross sections also prove that the permanent distortion of the fabric structure remains restricted to a small area very close to the path of the projectile. The fabric pattern barely 4–5 mm. away from the center of the hole is practically unaffected even in the exit layer.

### Damage to Nylon Filaments Due to Impact

The cross sections of the panel discussed above reveal the distortion of the fabric pattern, dislocations, deformations, and rupture of yarns. They also indicate other damage to nylon which becomes more clearly visible at a higher magnification. They will be illustrated by microphotographs taken at the original enlargement of 200 diameters at suitable locations of four previously-described cross sections, as shown in Figures 11a–d.

In the channel formed by the bullet, some broken fiber ends appear thickened and have a mushroom-like shape. Figures 12A–D show such filaments with thick fiber tips. They are similar to the fibers of a longitudinally impacted nylon yarn[4] studied by Stone, Schiefer, and Fox [10]. Stretched nylon contracts when heated [6], and this increases the fiber diameter. This phenomenon is known as heat shrinkage or heat relaxation; it occurred in the panel after the tension was released. It appears that only the fiber ends were heated. Their temperature must have been higher than 215° C. (419° F.), where softening and shrinkage of the yarns starts.

Single filaments in the nylon fabric are independent and separated (or at least separable) from each other within the yarn structure. In the impacted area, however, filaments frequently stick together and are fused into larger clumps or a compact mass,

[4] Figure 13, p. 527 [10].

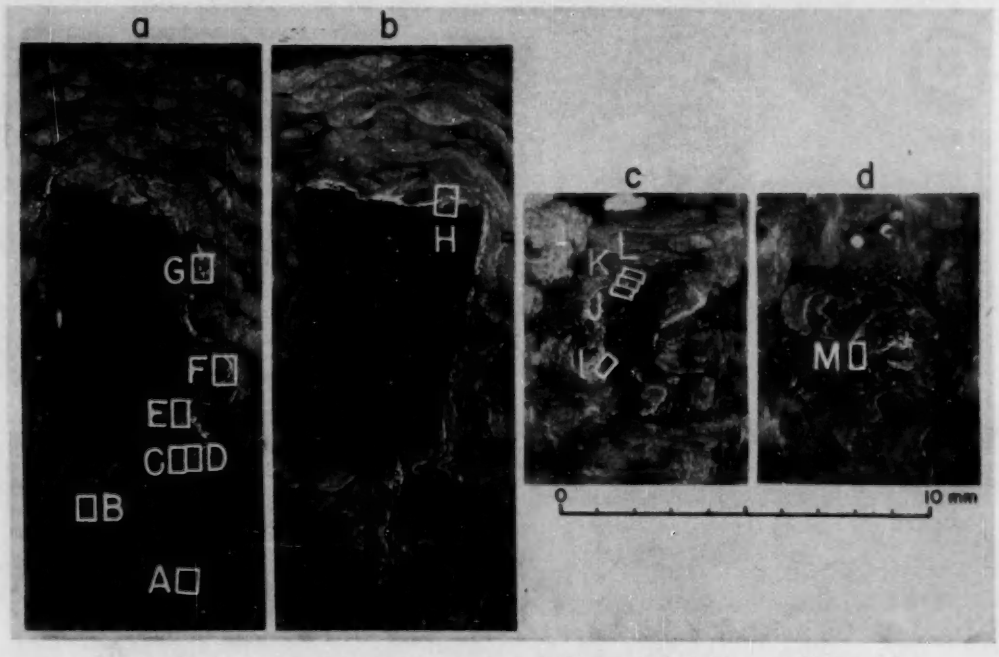


**Fig. 11.** Locations of the enlarged pictures shown in Figures 12–15. (a) part of Figure 9A; (b) part of Figure 9B; (c) part of Figure 10A; (d) part of Figure 10C.

as demonstrated in Figures 13A–C. They prove that fibers were subjected to considerable compression and heat in localized areas of the panel. This is also evident from the yarn ends which intrude into the hole and are best observable after separation of the panel into layers (see *Separating Technique*). Since yarns around the hole are fused, the individual layers of the panel can hardly be separated. They suggest that here the temperature reached the melting point of nylon—254° C. (489° F.). The temperature increase of nylon during penetration was so high in some areas that decomposition and pyrolysis [8] of nylon took place. This is apparent from dark spots on and between the filaments, as illustrated in Figures 14A–C. The oxidation of 6,6 nylon already starts above 120° C. (248° F.) [6]. It is not limited to the path of the bullet, where fibers came in direct contact with the missile, because it can be observed sometimes on the surface of remote yarns. Here excessive heat was developed by the friction between yarns moving along or across each other at high speed. According to Bowden and Thomas [3] the heat is transient and localized in "hot spots" when solids slide over each other. A high surface temperature was observed by these authors in rubbing metals against glass. The temperature increased markedly with the sliding speed and was in the range of 1000° C. (1832° F.). It was limited by the melting point of metals, except when oxidation in air (burning) occurred. In this case it even exceeded the melting point, since "the heat evolved is not primarily due to friction but to exothermic oxidation." It is evident that an analogous process took place in localized areas of the panel, where surpris-

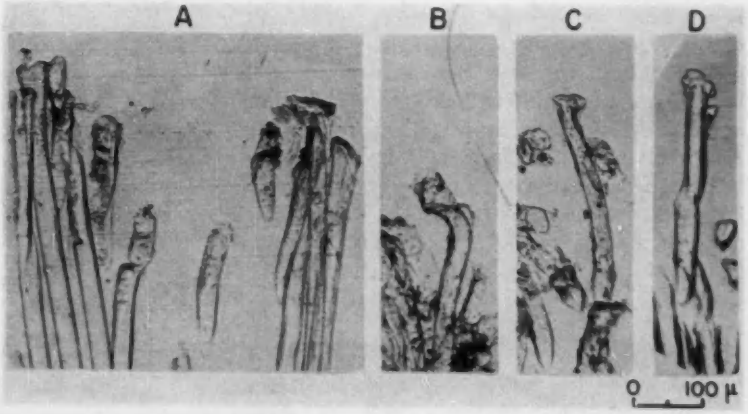


**Fig. 12.** Thickening of filament ends. (A) is (A) in Figure 11a; (B) is (I) in Figure 11c; (C) is (J) in Figure 11c; (D) is (L) in Figure 11c.

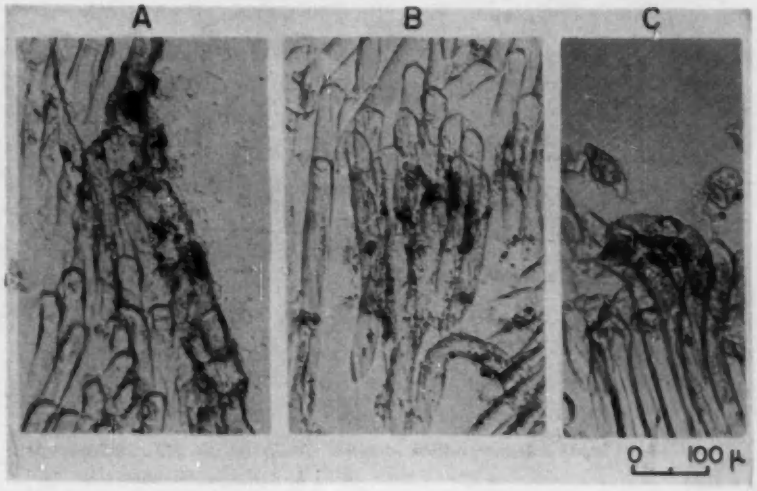


**Fig. 13.** Fusion of filaments into clumps. (A) is (B) in Figure 11a; (B) is (D) in Figure 11a; (C) is (K) in Figure 11c.

ingly high temperatures were reached for short intervals.

Heat is generated when fibers are extended. Brauer and Mueller [4] observed a temperature increase of 40° C. (104° F.) during extension of unstretched polyamide films at a relatively low strain rate (8 mm./min.). In the nylon panel, high temperatures can be expected due to impact, because yarns were extended at a very rapid rate.

Heat also develops when the fast-moving missile passes through the panel as a result of friction between the bullet and the fabric. We have to remember that the fabric is tightly woven and the channel formed by the projectile is very much narrowed by the intrusion of broken yarn ends. A part of the kinetic energy of the missile is thus transformed into heat during penetration.

It is obvious that the heat generated in the panel is very much concentrated [8] and cannot be readily dissipated. This causes the softening, fusion, and decomposition of nylon in localized regions. Nylon is a thermoplastic material, and its mechanical resistance decreases appreciably at higher temperatures. According to Coplan [5], at 177° C. (350° F.) the breaking tenacity of nylon Type 300 multifilament is 26 g./tex, its extensibility is 29.4%, and its initial modulus of elasticity 150 g./tex in comparison to 65 g./tex, 16.2%, and 350 g./tex respectively at 21.2° C. (70° F.).[5] The ballistic resistance of the panel is substantially diminished because of the heat generated in localized spots where an excessive elongation and rupture of yarns can easily occur.

In the microscopic study of the cross sections, fibrillation of nylon filaments was recognized, as illustrated in Figures 15A–C. Fibrillation is the breakdown of single filaments into numerous extremely fine fiber units called fibrils. This is not uncommon for highly oriented synthetic fibers, and its origin is generally the overstretching of the fiber skin.

Nylon filaments are cylindrical, their cross section is circular (diameter 27$\mu$), and they have a relatively smooth fiber surface. After fibrillation, however, a great number of extremely thin fibrils of approximately 1$\mu$ diameter appear partially separated from the main filament. They protrude from the fiber and roughen its surface. Fibrillation starts at the fiber periphery. It can be limited to one side and may also cause the splitting of filaments into two or more finer fibers. Fibrillation was observed mainly close to the path of the missile, where yarns were extended and were rapidly moved along or across each other.

Fibrillation is also demonstrated in Figure 16, where filaments removed from the second layer of a

[5] These values were obtained from a 210-den. (23.3-tex) multifilament and are comparable to those listed in Table I for the 5-ply 210/34 yarn.

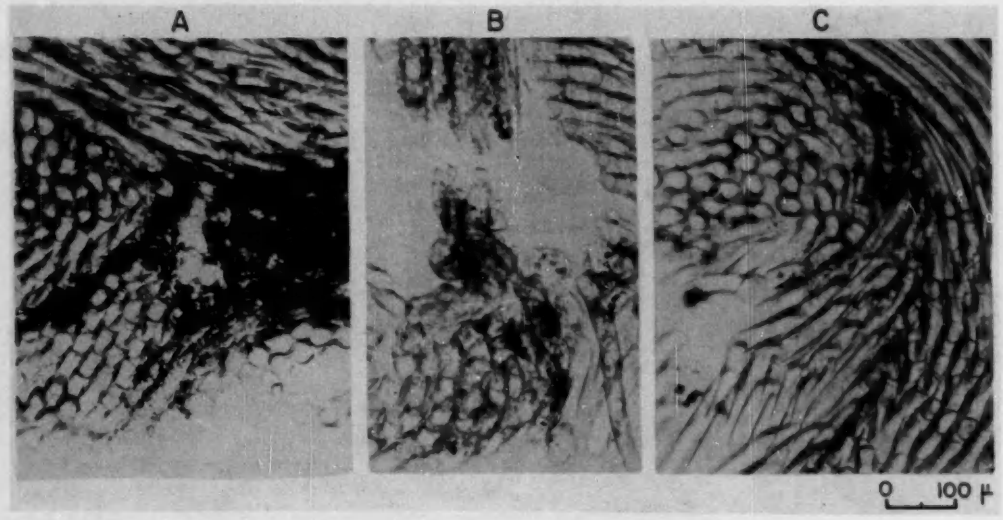


**Fig. 14.** Decomposition of nylon fibers. (A) is (H) in Figure 11b; (B) is (G) in Figure 11a; (C) is (F) in Figure 11a.

partially penetrated hole (No. 20) are shown after the fabric was dyed. Dye uptake of 6,6 nylon depends mainly on the number and the accessibility of relatively scarce amine endgroups. High degree of order (crystallinity) and high orientation of nylon reduce the diffusion of dye molecules to the proper sites. Therefore, the dye uptake of highly stretched nylon filaments, particularly with pronounced skin structure, is low compared to undrawn fibers. The rate of dyeing of drawn filaments increases when the fiber surface is damaged by fibrillation and after disorientation of the stretched fiber through the action of heat. Fibrillation increases the fiber surface through which diffusion of the dye occurs; it also exposes the core of filaments to the dye bath. Differences in dye uptake can best be detected by anionic or dispersed dyes having comparatively long molecules [7]. According to Munden and Palmer [9], Durazol Fast Blue 2R, a trisulfonated cotton dye, is very sensitive to differences in stretching of nylon. A similar dye in pure form (sample designation: MDD 3456, Du Pont) was used in this study to recognize structural changes of nylon filaments. If a penetrated fabric layer is dyed with this compound, the impacted area appears darker blue than the unaffected part. It was convenient to use 0.25% dye in a liquor bath ratio 1 : 50 at pH 3 (acetic acid) for 1 hr. at 90° C. (194° F.) to stain the damaged part of fabrics. Figure 16A shows fibrillated filaments, while in 16B and C heavily damaged fibers with mushroomlike fiber tips are visible after removal from a stained fabric. The fibrils and the damaged part of the filaments appear dark compared to the unaffected fiber surface. In the thickened fiber tips,

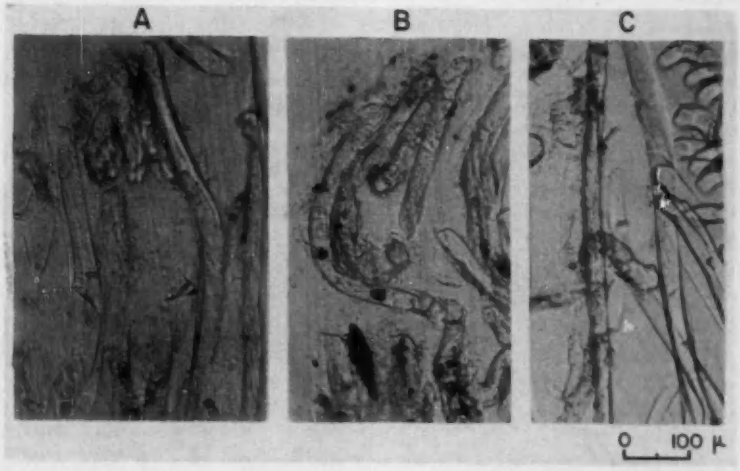


**Fig. 15.** Fibrillation of impacted filaments. (A) is (C) in Figure 11a; (B) is (E) in Figure 11a; (C) is (M) in Figure 11d.

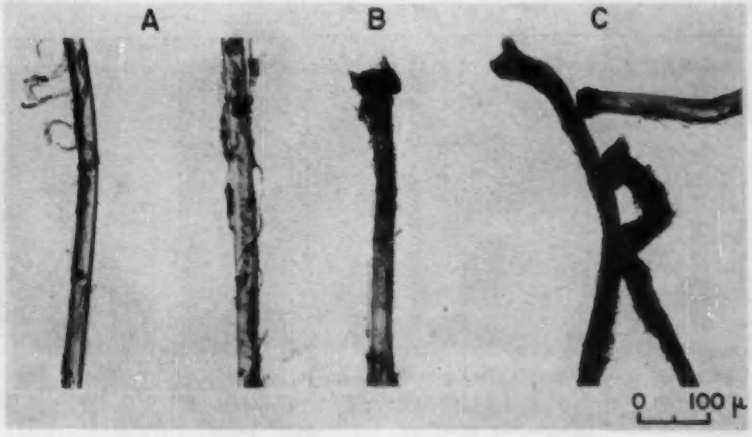


**Fig. 16.** Filaments removed from the hole of an impacted fabric layer after dyeing. (A) fibrillation; (B) and (C) softened ends.

softening and melting caused a randomization of the originally well-aligned crystallites, and this markedly increased the dye uptake. The disorientation as a result of heat relaxation was corroborated by the X-ray diffraction pattern. In the yarn ends removed from holes, a random distribution of crystallites was observed instead of the well-pronounced fiber diagram of unimpacted nylon yarns.

### Separating Technique

Despite the useful information gained from cross sections of the panel, their study did not disclose how each individual layer as a whole behaved. This can be investigated, however, after separating the impacted panel into single layers. It should be remembered that each layer was hit with a decreasing velocity of the missile and in a direction which was not always the same. The stiffening of individual layers by backing decreased in the direction of the missile motion. It can be understood, therefore, that the deformation was different in each layer.

The separation of an impacted panel into layers probably requires as much care and experience as preparing cross sections; nevertheless, it is somewhat less timeconsuming. Yarn ends around holes are frequently fused and adhere to each other through many layers. These must be separated without affecting the fabric pattern. Some yarns are unraveled, pulled apart, or broken, while others are just bent or form loops. They all intrude into the hole of subsequent layers and protrude occasionally from the last one. The layers have to be separated, preserving the distorted pattern around the hole without causing additional defects to the fabric.

One completely and two partially penetrated holes were investigated by this technique. The observations made were essentially identical and will be described only for the two partial penetrations. Here the separation is informative because it shows—better than any other method—how many layers were penetrated, which way they failed, and also the deformation of those layers which resisted penetration.

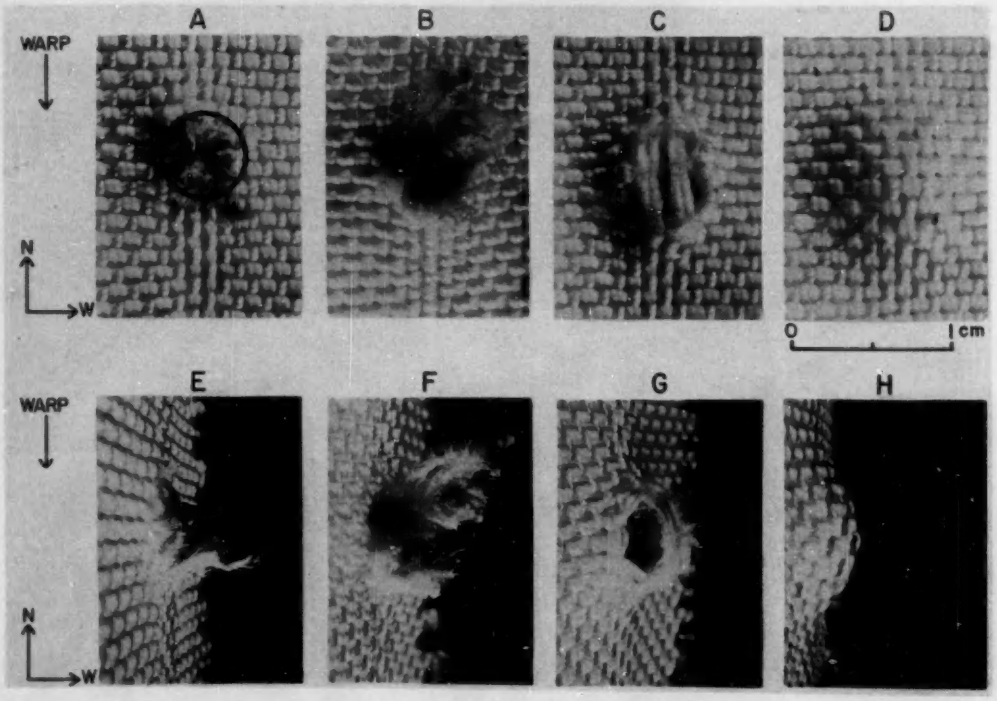


**Fig. 17.** Fabric layers after partial penetration (Hole No. 20). Upper row: perpendicular view of exit; lower row: side view of exit. (A) and (E) first layer; (B) and (F) fourth layer; (C) and (G) sixth layer; (D) and (H) ninth layer.

In the first partially penetrated hole studied (No. 20), the missile had the relatively low striking velocity of 355 m./sec. (1165 ft./sec.) corresponding to a kinetic energy of 674,000 g.-cm. It did not deviate appreciably from its perpendicular incidence during penetration (see Figures 5B and C). After five layers were completely penetrated, in the following two layers very few yarns were ruptured. The last four layers remained entirely unbroken, although they were extended by the projectile. These layers were practically unbacked (unstiffened). Their permanent deformation was conical, resembling that observable in conventional burst tests not carried out to complete failure of the fabric. The height of the bulged area decreased (from 5 to ½ mm.), while its diameter increased (from 6 to 13 mm.) in the last four layers. The deformation of the fabric spread thus to an area larger than the cross section of the bullet. This is in contrast to observations in the entrance layers and indicates some dissipation of the missile energy.

Photographs made at a low original magnification (five diameters) of the exit side of the first, fourth, sixth, and ninth layers are shown in Figures 17A–H. They are demonstrated from a direction perpendicular and oblique to the fabric surface after removal of the missile. The first and fourth layers (A and B) show rather large holes, covered by unravelled and broken yarn ends. A slight distortion of the original fabric pattern around the hole and some tensioned yarns are also visible. In the sixth layer(C), which stopped the bullet, four fairly straight warp yarns appear extended but unbroken. They were in front of the bullet and stopped its movement. Other warp yarns in the path of the bullet were displaced; they apparently slid down from a tilted part of the nose. Some filling yarns in this layer were broken, others pushed aside; the missile dislodged them by its motion. After yarns were extended and tensioned by the moving projectile, some of them must have slipped from the slanted surface of the bullet to release their tension long before rupture could occur. The dislodged yarns fail, of course, to develop fully their resistance to the missile. This phenomenon is more common in the panel than generally anticipated. It seems to prevail in those layers where the velocity of the missile is reduced and the yarns can be easily extended. Pushing aside yarns from the path of the bullet probably is the origin of the frequently observed tumbling, because the resistance to missile movement becomes suddenly distributed unevenly. In the ninth layer—(D)—all yarns remained unbroken. Some of them were extended, however; therefore, small open spaces can be seen at several intersections of warp and filling yarns in the bulged area.

In the oblique views of the first and fourth layer (E and F) broken yarn ends protruding from the fabric surface are visible. They are at the periphery of the opening sharply bent in the direction of missile movement and intrude considerably into the hole of following layers. They lost their crimp, are stuck together, and their tips are fused. They are "set" by the heat produced during penetration. The broken yarn ends are frequently much longer (8–12 mm.) than expected. Most likely the enhanced extensibility of softened filaments is the origin of the yarn length observed. It can be assumed that the length of impacted yarns was even longer before their rupture than that which could be observed. Shrinkage (heat relaxation) must have taken place to a certain extent immediately after the stress was released by rupture [6].

The separation of the panel into individual layers also reveals the progression of stoppage. This is illustrated in Figures 18A–H, where perpendicular views of the entrance sides and oblique views of the exit sides of some layers are shown. The projectile hit the panel in this partially penetrated hole (No. 18) at a slightly lower velocity than previously discussed, namely at 335 m./sec. (1098 ft./sec.) corresponding to 601,000 g.-cm. kinetic energy. It deviated from its perpendicular incidence and turned to the south-east, which is recognizable from its final position, shown in Figures 5B and C. The hole is almost circular in the fifth layer (A). Half-moon-shaped holes appear in the sixth, seventh, and eighth layers (B, C, and D). The size of these openings decreases markedly in the direction of missile motion, indicating the diminished energy of the projectile. While six yarns were broken and many others dislodged in the fifth layer, four yarns were ruptured in the sixth and seventh, and only two yarns failed in the eighth layer. In all these layers the surface area of broken yarns (confined by cross yarns) is a surprisingly low fraction of the circular cross section of the bullet. In the ninth and following layers no yarns were ruptured. These layers were deformed and remained bulged, as observable by the small

interstices between yarns in the extended area of the ninth layer (E).

The side views of the fifth, sixth, and seventh layers (F, G, and H) illustrate that the fabric deformation is first cylindrical and later conical. Its height decreases, while its base increases in the direction of missile movement. This suggests that the dissipation of stress began after the velocity of the projectile dropped to a certain level.

It is evident that the bullet was decelerated and stopped by the combined resistance of several layers. Looking at the size and shape of holes as they appear in this series, one is able to decide which layer prevented the further movement of the projectile. This did not occur in the ninth layer, where yarns were not ruptured at all, but in the eighth layer. Here, a half-moon-shaped small hole appears, resulting from the failure of two filling yarns, broken by a protruding edge of the missile. It seems not too arbitrary to consider that this layer has actually retained the projectile, despite its penetration by a minor part of the bullet. The markedly diminished size of the opening and the rupture of only two yarns suggest that the missile did not go through this layer in the same way as it did the preceding ones.


## Summary

The microscopical study revealed permanent deformations and damages in the impacted area. Dislocations, flattening, straightening out, extension, unravelling, and rupture in both yarn systems and various types of defects of nylon filaments were observed. These consisted of softening, melting accompanied by disorientation, heat relaxation, even decomposition, burning, and fibrillation of nylon filaments. These phenomena represent damage because they alter fiber properties essential for protection against the impact of the missile. In order to recognize them, cross sections were made and the panel was separated into single layers. The impacted layers removed from the panel confirmed and supplemented the observations gained from cross sections; they permitted the study of fabric deformations within the panel and the progression of stoppage of the bullet.

It became evident that the permanent alterations of the fabric due to impact were limited to a region close to the path of the projectile. The impact remains confined in the panel to a relatively small area, because the presence of two yarn systems prevents the propagation of the stress wave along the whole yarn length. Apparently cross yarns behave like


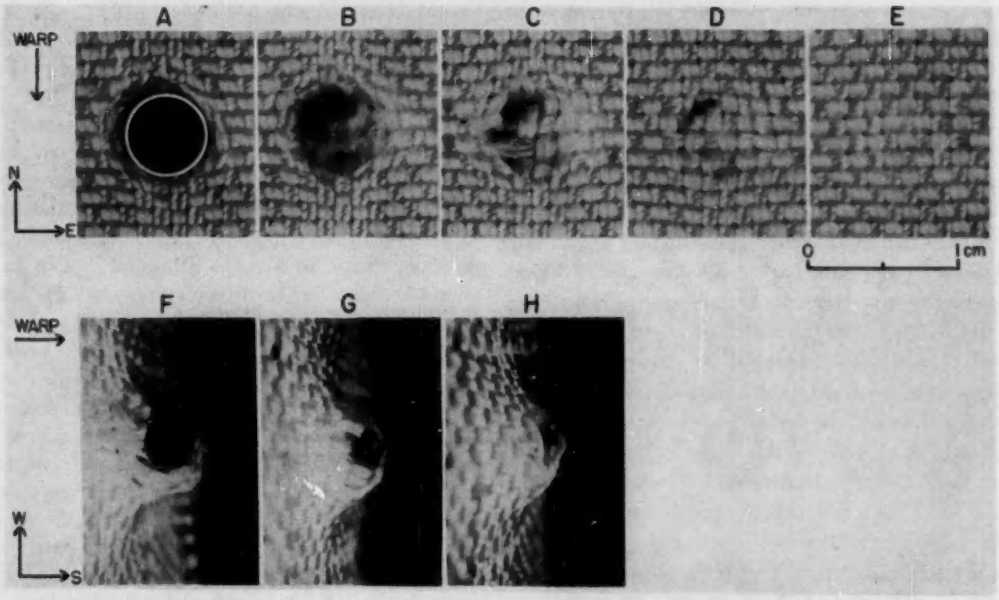


**Fig. 18.** Layers of a partial penetration showing the stoppage of the missile (Hole No. 18). Upper row: perpendicular view of entrance; lower row: side view of exit. (A) and (F) fifth layer; (B) and (G) sixth layer; (C) and (H) seventh layer; (D) eighth layer; (E) ninth layer.

clamps, limiting the stress to the neighborhood of the impacted spot. The cross yarn closest to the impact may not act completely; however, the next or the one after does. This restricts the impact to that area of the fabric which was in close contact with the missile. An exception to this behavior is the slight dissipation of stress in layers exposed to the essentially decelerated missile without appreciable backing. These layers were either insignificantly ruptured or remained entirely unbroken. They did not contribute much to the ballistic resistance of the panel.

### Acknowledgments

The authors are indebted to Dr. W. J. Hamburger, Fabric Research Laboratories, Dedham, Mass., and his group for suggestions in the discussion of results and to Dr. O. Stallmann, E. I. Du Pont de Nemours & Co., Wilmington, Del., for furnishing the dye sample used in this study.

It is a pleasure to acknowledge the assistance and cooperation of the Textile, Clothing, and Footwear Division of the Quartermaster Research and Engineering Center.

Thanks are due to Mrs. G. Hynek for preparing the fabric cross sections of Figure 3, to Lt. J. Moore for evaluating tensile properties and performing dyeing tests of nylon, and to Mrs. G. W. Seligsberger for her assistance in preparing the manuscript.

### Literature Cited

1. American Society for Testing Materials, 1955 Book of ASTM Standards, Part 7, "ASTM Standards on Textiles" ASTM Designation D861–52 Philadelphia, Pa.
2. Bayes, A. W., *J. Textile Inst.* **48**, P255–67 (1957).
3. Bowden, F. P. and Thomas, P. H., *Proc. Roy. Soc.* **A223**, 29–40 (1954).
4. Brauer, P. and Mueller, F. H., *Kolloid Z.* **135**, 65–7 (1954).
5. Coplan, M. J., A Study of the Effect of Temperature on Textile Materials. Wright Air Development Center Technical Report 53–21, March 1953.
6. Forward, M. V. and Palmer, H. J., *J. Textile Inst.* **45**, T510–68 (1954).
7. Forward, M. V. and Simmens, S. C., *J. Textile Inst.* **46**, T671–4 (1955).
8. Gruntfest, I. J., Textile Research Journal **25**, 966–7 (1955).
9. Munden, A. R. and Palmer, H. J., *J. Textile Inst.* **41**, P609–34 (1950).
10. Stone, W. K., Schiefer, H. F., and Fox, G., Textile Research Journal **24**, 520–7 (1955).
11. Susich, G. and Backer, S., Textile Research Journal **21**, 482–509 (1951).

*Manuscript received September 30, 1957.*

---

## Note

The small amplitude oscillations described in the text of the paper by Grignet and Monfort (Some Dynamometric Applications of an Electronic Integrator-Differentiator, January 1958, pp. 47–59) do not appear in Figure 5.1 because of the loss of detail due to reduction of the illustration to column width.

# The Amino Acid Composition of Fractionated Cortical Cells From Wool

**David H. Simmonds**[1]

*Biochemistry Unit, Wool Textile Research Laboratories, CSIRO, Victoria, Australia*

**John J. Bartulovich**

*Western Utilization Research and Development Division, Agricultural Research Service, USDA, Albany, California*

**Abstract**

Two cortical cell fractions separated from wool after treatment at 30° C. with 6 *N* HCl for 50 hr. have been analyzed for their amino acid composition. The heavy fraction was significantly richer than the light fraction in amide nitrogen, cystine, serine, and proline, but was deficient in alanine, glutamic acid, glycine, leucine, lysine, phenylalanine, and tyrosine. Both cortical cell fractions were richer than the original wool in cystine, lysine, and proline, while the material dissolved by the acid treatment was richer in glycine, phenylalanine, serine, and tyrosine.

## Introduction

The amino acid composition of wool and its biological variation are now well established [3, 14, 15, 17, 21, 22]. In addition, analyses of various histological and protein fractions derived from wool have established that such structural components differ in composition both among themselves and from the original wool [5, 11, 16, 18, 21].

These results suggest that the variations which have been noted in the composition of whole wool [15] may be explained in part at least by variations in the proportions of distinct components present. The development of methods for separating cortical cell fractions obtained after acid treatment of whole wool [20] has enabled us to prepare samples of different density for amino acid analysis.

## Experimental

### *Preparation of Cortical Cells*

Cortical cell residues were obtained from Australian Merino wool of 70s fineness which had been washed successively with ether, ethanol, tap water, benzene, and distilled water at room temperature. Hand carding to remove foreign matter preceded the final rinse. The clean wool (1 g. conditioned at 65% relative humidity) was soaked in 6 *N* HCl (40 ml.) at 30° C. for 50 hr. After separation of the acid by filtering through cheesecloth, the residue was broken down by beating with water in a Waring blendor. The liberated cortical cell residues were repeatedly washed and recovered by centrifuging until the wash water gave no turbidity with silver nitrate. They were then fractionated by centrifuging with a solution of chloral hydrate, following procedures already described [20]. The separated fractions after repeated washing with water to rid them of bound chloral hydrate were recovered by centrifuging. Each fraction was finally washed with approximately 1 l. of 0.1% Sequestrene NA2[2] (disodium ethylenediaminetetraacetate) per gram of residue and rinsed with glass-distilled water.

### *Analytical Procedures*

Amino acid analyses were carried out by the rapid procedure referred to by Spackman, Stein, and Moore [19].[3] Effluent fractions from the Dowex 50-X8 chromatographic columns were collected in the fraction-measuring device described by Simmonds (*Anal. Chem.*, in press) and dispensed into

[1] Present address: Waite Agricultural Research Institute, Adelaide, South Australia.

[2] Mention of specific products does not imply endorsement over others of similar nature.

[3] The authors are indebted to Dr. S. Moore of the Rockefeller Institute for Medical Research for supplying details of this procedure prior to its publication.

test tubes on a motor-driven fraction-collector turntable. Manual colorimetric assay of the individual fractions followed the procedure of Moore and Stein [12].

Cystine was estimated by amperometric titration ([9] and Human, in preparation) and also after 5 hr. of hydrolysis in 5 *N* HCl in a sealed tube at 125° C. by the method of Folin and Marenzi [4] as modified by Shinohara [13].

Tyrosine and tryptophan were estimated by the method of Goodwin and Morton [7] and proline by the method of Simmonds and Stell [18] and Simmonds (in preparation). Shortage of material prevented analyses' being carried out for methionine.

## Results

Table I gives the amino acid composition, with standard errors, for 16-hr. hydrolysates of the light and heavy cortical cell fractions, while Figure 1 compares, in terms of grams of amino acid from 100 grams of dry protein, the composition of the two cortical fractions and whole wool of the same breed and fineness as that used in the present investigation [17].

Separate experiments have shown that with this method of fractionation 43.8 ± 0.7% of the intact dry wool was dissolved in the HCl, 2.6 ± 0.2% was soluble in the chloral hydrate fractionating medium, 26.1 ± 2.0% was recovered as the light fraction, 20.2 ± 1.8% as the heavy fraction, while 7.3% was unaccounted for. The losses presumably are due to processing and are known definitely to include at least 2.2 ± 0.3% insoluble material which could not be removed readily from the glassware. These values are averages of at least six trials.

Nitrogen recovery after analysis is essentially complete for both fractions: 102% of the total nitrogen in the light fraction and 101% of that in the heavy fraction was accounted for, and it is therefore unlikely that large amounts of tryptophan and methionine are present. The total sulfur known to be present from elementary analysis, however, was

**TABLE I. Amino Acid Composition of Light and Heavy Cortical Cell Fractions**
(Amino acid nitrogen expressed as a percentage of total nitrogen)

| | Heavy fraction | | | | | Light fraction | | | | | Level of significance, % |
|---|---|---|---|---|---|---|---|---|---|---|---|
| Amino acid | *n* | Mean | SE* | 95% Fiducial limits of mean | LSD† (5%) | *n* | Mean | SE* | 95% Fiducial limits of mean | LSD† (5%) | |
| Alanine | 5 | 3.67 | 0.32 | 2.91– 4.43 | 1.12 | 4 | 4.83 | 0.35 | 4.00– 5.66 | 1.12 | 5 |
| Ammonia‡ | 4 | 4.78 | 0.04 | 4.68– 4.88 | 0.14 | 4 | 4.30 | 0.04 | 4.20– 4.40 | 0.14 | 0.1 |
| Arginine | 4 | 22.05 | 0.28 | 21.77–22.33 | 0.97 | 4 | 22.51 | 0.28 | 22.23–22.79 | 0.97 | NS |
| Aspartic acid | 4 | 5.08 | 0.44 | 4.00– 6.16 | 1.52 | 4 | 4.87 | 0.44 | 3.79– 5.95 | 1.52 | NS |
| Cystine | 4 | 12.48 | 0.12 | 12.19–12.77 | 0.42 | 4 | 10.23 | 0.12 | 9.94–10.52 | 0.42 | 0.1 |
| Glutamic acid** | 4 | 8.94 | 0.52 | 7.67–10.21 | 1.80 | 4 | 11.20 | 0.52 | 9.93–12.47 | 1.80 | 5 |
| Glycine | 5 | 3.32 | 0.07 | 3.16– 3.48 | 0.26 | 4 | 4.11 | 0.08 | 3.92– 4.30 | 0.26 | 0.1 |
| Histidine | 4 | 1.65 | 0.09 | 1.43– 1.87 | 0.31 | 4 | 1.43 | 0.09 | 1.21– 1.65 | 0.31 | NS |
| Isoleucine | 5 | 2.30 | 0.06 | 2.16– 2.44 | 0.23 | 4 | 2.45 | 0.07 | 2.29– 2.61 | 0.23 | NS |
| Leucine | 5 | 4.76 | 0.09 | 4.55– 4.97 | 0.32 | 4 | 6.14 | 0.10 | 5.90– 6.38 | 0.32 | 0.1 |
| Lysine | 4 | 4.32 | 0.18 | 3.88– 4.76 | 0.62 | 4 | 5.20 | 0.18 | 4.76– 5.64 | 0.62 | 5 |
| Phenylalanine | 5 | 0.94 | 0.05 | 0.83– 1.05 | 0.17 | 4 | 1.27 | 0.05 | 1.15– 1.39 | 0.17 | 1 |
| Proline | 7 | 7.62 | 0.17 | 7.23– 8.01 | 0.54 | 8 | 5.97 | 0.18 | 5.60– 6.34 | 0.54 | 0.1 |
| Serine‡ | 4 | 8.12 | 0.26 | 7.48– 8.76 | 0.90 | 4 | 7.01 | 0.26 | 6.37– 7.65 | 0.90 | 5 |
| Threonine‡ | 4 | 5.18 | 0.36 | 4.30– 6.06 | 1.24 | 4 | 4.62 | 0.36 | 3.74– 5.50 | 1.24 | NS |
| Tryptophan | | 0 | | | | | 0 | | | | |
| Tyrosine | 5 | 1.74 | 0.05 | 1.62– 1.86 | 0.20 | 4 | 1.99 | 0.06 | 1.85– 2.13 | 0.20 | 5 |
| Valine | 5 | 4.00 | 0.32 | 3.26– 4.74 | 1.03 | 5 | 3.71 | 0.32 | 2.97– 4.46 | 1.03 | NS |
| Total nitrogen accounted for | | 100.95 | | | | | 101.84 | | | | |
| Nitrogen, % | | 15.9 | | | | | 15.9 | | | | |
| Sulfur, % | | 5.65 | | | | | 4.21 | | | | |
| Chlorine, % | | 0.17 | | | | | 0.09 | | | | |

* Standard error.
† Least difference for significance at 5% level.
‡ Not corrected for loss during hydrolysis.
** Corrected for pyrolidone carboxylic acid formation on the ion exchange columns.

not quantitatively accounted for by the sulfur-containing amino acids found. Cystine sulfur accounted for 3.72% sulfur in the light fraction and 4.54% in the heavy fraction. The contribution of methionine sulfur as well as those of cysteic acid and lanthionine, known to be minor components of normal wool hydrolysates, should not change these figures substantially. The amount of sulfur unaccounted for in the light fraction is therefore 0.49% by weight and in the heavy fraction 1.11%. It is possible that some of this sulfur is present in the form of a reaction product with chloral hydrate, although the chlorine content of the cells is so low that extensive loss from this cause is unlikely.

## Discussion

The two fractions differ significantly in their contents of alanine, amide nitrogen, cystine, glutamic acid, glycine, leucine, lysine, phenylalanine, proline, serine, and tyrosine. The differences range from 11% to 28% of the amount present in the light fraction. Alanine, cystine, glutamic acid, glycine, leucine, phenylalanine, and proline show the largest—although not necessarily the most significant—differences between the two preparations. The most significant differences are shown by ammonia, cystine, glycine, leucine, and proline.

Comparison of the composition of the two fractions with that of the original wool shows that the acid treatment has caused substantial enrichment of the total residue in cystine, lysine, and proline, with corresponding decreases in the amounts of glycine, phenylalanine, serine, and tyrosine present. The evidence for this is illustrated in Figure 1 and Table II. The latter shows the composition of the solubilized and unaccounted-for parts of the fiber (Columns 4–6) calculated by difference from the combined yields of light and heavy fractions.

It is interesting to note that the fraction dissolved or unaccounted for in this study does not correspond closely in composition to the soluble fractions of other workers. Lindley [10], Blackburn [1], and Leach [8], for example, have found that aspartic acid is the main amino acid released from wool by short treatment with warm dilute hydrochloric acid, although later Blackburn and Lee [2] found that concentrated HCl at 37° C. does not show the same specific action on the aspartic acid residues as the more dilute acid at a higher temperature. Zahn and Meienhofer [23] have reported that peptides of alanine, aspartic acid, glutamic acid, glycine, leucine, serine, threonine, and valine are extracted from wool by hot water. Of this list, only glycine and serine appear to be *selectively* dissolved by acid under our conditions. The absence of aspartic acid under these conditions confirms the observations of Blackburn and Lee [2].

As would be expected, the amide content has been reduced by the acid treatment to about 60% of the amount present in the original wool. The enrichment of the light and heavy fractions in cystine is interesting, since it contrasts with analyses carried out on preparations obtained by extracting wool with 0.1 *M* potassium thioglycollate at pH 10.5 and 50° C. [16]. These have shown that the readily soluble material is very rich in cystine. The extraction with HCl must therefore solubilize different components of the fiber, leaving the cystine-rich fraction in the

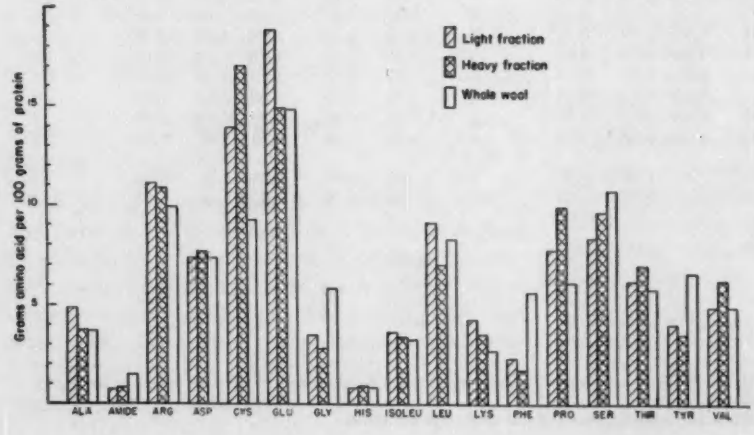


**Fig. 1.** Amino acid composition of light fraction, heavy fraction, and whole wool.

**TABLE II. Amino Acid Composition of Soluble Fraction by Difference**

| Amino acid | Weight in 26.1 g. of light fraction, g. | Weight in 20.2 g. of heavy fraction, g. | Weight in 100 g. of whole wool, g. | Weight in 53.7 g. of fraction dissolved or unaccounted for (by difference), g. | Composition of protein dissolved or unaccounted for % by weight | Fraction of amino acid dissolved from original wool |
|---|---|---|---|---|---|---|
| Alanine | 1.27 | 0.75 | 3.70 | 1.68 | 3.13 | 0.45 |
| Amide | 0.20 | 0.18 | 1.50 | 1.12 | 2.09 | 0.75 |
| Arginine | 2.90 | 2.20 | 9.96 | 4.86 | 9.05 | 0.49 |
| Aspartic | 1.92 | 1.55 | 7.36 | 3.89 | 7.24 | 0.53 |
| Cystine | 3.64 | 3.44 | 9.24 | 2.16 | 4.02 | 0.23 |
| Glutamic | 4.88 | 3.02 | 14.86 | 6.96 | 12.96 | 0.47 |
| Glycine | 0.91 | 0.57 | 5.86 | 4.38 | 8.16 | 0.75 |
| Histidine | 0.22 | 0.20 | 0.90 | 0.48 | 0.89 | 0.53 |
| Isoleucine | 0.95 | 0.69 | 3.30 | 1.66 | 3.10 | 0.50 |
| Leucine | 2.39 | 1.43 | 8.33 | 4.51 | 8.40 | 0.54 |
| Lysine | 1.12 | 0.72 | 2.76 | 0.92 | 1.71 | 0.33 |
| Phenylalanine | 0.62 | 0.36 | 5.62 | 4.64 | 8.64 | 0.83 |
| Proline | 2.04 | 2.01 | 6.19 | 2.14 | 3.99 | 0.35 |
| Serine | 2.18 | 1.96 | 10.73 | 6.59 | 12.27 | 0.61 |
| Threonine | 1.64 | 1.42 | 5.83 | 2.77 | 5.16 | 0.48 |
| Tyrosine | 1.07 | 0.72 | 6.62 | 4.83 | 8.99 | 0.73 |
| Valine | 1.29 | 1.07 | 4.93 | 2.57 | 4.78 | 0.52 |

cortical cell residues. The low glutamic acid and high glycine, phenylalanine, and tyrosine contents of the pH 10.5 thioglycollate extracts contrast sharply with the composition of the light and heavy cell fractions which, apart from having less amide, aspartic acid, and phenylalanine and more cystine and proline, are rather similar to kerateine 2 [6] in their general composition [16].

## Acknowledgments

We are gratefully indebted to Miss G. E. Secor and Mr. L. M. White for sulfur and nitrogen analyses. We particularly appreciate the advice, encouragement, and criticism of Dr. W. H. Ward and Dr. H. P. Lundgren. One of us (D.H.S.) wishes to thank Miss M. McShane for expert technical assistance with amino acid analyses by the ion exchange chromatographic procedure and Mr. W. B. Hall of the CSIRO Division of Mathematical Statistics for assistance with the statistical analysis of the results.

## Literature Cited

1. Blackburn, S., *Biochem. J.* **47**, xxviii (1950).
2. Blackburn, S. and Lee, G. R., *Biochem. J.* **58**, 227 (1954).
3. Corfield, M. C. and Robson, A., *Biochem. J.* **59**, 62 (1955).
4. Folin, O. and Marenzi, A.D., *J. Biol. Chem.* **83**, 103 (1929).
5. Geiger, W. B., *J. Research Nat. Bur. Standards* **32**, 127 (1944).
6. Gillespie, J. M. and Lennox, F. G., *Aust. J. Biol. Sci.* **8**, 97 (1955).
7. Goodwin, T. W. and Morton, R. A., *Biochem. J.* **40**, 628 (1946).
8. Leach, S. J., *Proc. Int. Wool Text. Res. Conf. Aust.* **C1**, 198 (1955).
9. Leach, S. J., *Proc. Int. Wool Text. Res. Conf. Aust.* **C2**, 469 (1955).
10. Lindley, H., *Nature* **160**, 190 (1947).
11. Mercer, E. H., Golden, R. L., and Jeffries, E. B., TEXTILE RESEARCH JOURNAL **24**, 615 (1954).
12. Moore, S. and Stein, W. H., *J. Biol. Chem.* **211**, 907 (1954).
13. Shinohara, K., *J. Biol. Chem.* **109**, 655 (1935); **110**, 263 (1935); **111**, 435 (1935); **112**, 671, 683, 697, 709 (1935); **120**, 743 (1937).
14. Simmonds, D. H., *Aust. J. Biol. Sci.* **7**, 98 (1954).
15. Simmonds, D. H., *Proc. Int. Wool Text. Res. Conf. Aust.* **C1**, 65 (1955).
16. Simmonds, D. H., *Aust. J. Biol. Sci.* **8**, 114 (1955).
17. Simmonds, D. H., *Aust. J. Biol. Sci.* **8**, 537 (1955).
18. Simmonds, D. H. and Stell, I. G., *Proc. Int. Wool Text. Res. Conf. Aust.* **C1**, 75 (1955).
19. Spackman, D. H., Stein, W. H., and Moore, S., *Fed. Proc.* **15**, 358 (1956).
20. Ward, W. H. and Bartulovich, J. J., TEXTILE RESEARCH JOURNAL **25**, 889 (1955).
21. Ward, W. H., Binkley, C. H., and Snell, N. S., TEXTILE RESEARCH JOURNAL **25**, 314 (1955).
22. Ward, W. H. and Lundgren, H. P., in "Advances in Protein Chemistry," Academic Press, New York, Vol. IX, 244 (1954).
23. Zahn, H. and Meienhofer, J., TEXTILE RESEARCH JOURNAL **25**, 738 (1955).

*Manuscript received November 26, 1957.*

# Applications of Infrared Absorption Spectroscopy to Investigations of Cotton and Modified Cottons

## Part I: Physical and Crystalline Modifications and Oxidation

**Robert T. O'Connor, Elsie F. DuPré, and Donald Mitcham**

*Southern Regional Research Laboratory,[1] New Orleans, Louisiana*

**Abstract**

The KBr technique to obtain spectra of cotton cellulose has been applied satisfactorily to an investigation of physical and crystalline modifications and to changes resulting from oxidation. Several experiments to illustrate applications are described. The potential applications to investigations suggested in the literature are reviewed.

It has been shown that infrared absorption spectra of cotton cellulose can be used to follow changes in hydrogen bonding by the classical method of observing the exact wavelengths of the O-H stretching vibrations. Degree of crystallinity can be measured quantitatively by use of ratios of intensities of preselected absorption bands. Oxidation changes can be followed only where such processes result in the formation of C = O groups *per se* in the oxidized cotton.

INFRARED absorption spectroscopy has been widely ignored in investigations of the structure and reactions of cotton. Monographs and reference texts on the chemistry of cellulose either make no mention of this tool or refer only incidentally to an isolated application. Heuser [11] refers to infrared absorption only to support the theory of the existence of hydrogen bridges in the reaction of cellulose with water. Neither Ott [19] nor Hermans [10] mentions infrared spectra, and Timell [31] limits references to applications to the single sentence "Infrared absorption spectra indicate that nearly all the hydroxyl groups are involved in the formation of hydrogen bonds of varying strengths."

The few articles which have appeared in technical journals dealing with applications of infrared absorption spectroscopy to investigations of cotton can be divided into two groups; (a) those dealing with the use of infrared spectra to deduce or support theories regarding the structure of the cellulose molecule, such as studies of hydrogen bonding [3, 5, 14], degree of crystallinity [7, 14, 32], and cross-linkage [28] and (b) those dealing with investigations of modifications of cellulose, such as the oxidation studies of Rowen et al. [20] and the determination of acetyl content by Mitchell et al. [17].

All of these papers are somewhat preliminary in character and all bear testimony of the difficulties in obtaining satisfactory, quantitatively reproducible, infrared spectra. Infrared absorption spectra are undoubtedly capable of yielding considerably more information regarding the structure of the cellulose molecule than has yet been made available, such as the nature of hydrogen bonding, changes in crystallinity, products formed by cross-linking or oxidation, or for qualitative identification or quantitative analysis.

The purpose of this paper is to describe the usefulness of infrared absorption spectroscopy, and, in particular, the application of a newly-described technique for measuring the infrared absorption spectra of cotton and modified cottons to these types of problems.

### KBr Disc Technique for Obtaining Infrared Absorption Spectra of Cotton

Undoubtedly one of the principal reasons for the lack of a more widespread use of infrared absorption in research investigations into the structure and the reactions of cotton has been the difficulty in obtaining satisfactory spectra simply and rapidly. Cotton cannot be dissolved in a solvent suitable for absorption

[1] One of the laboratories of the Southern Utilization Research and Development Division, Agricultural Research Service, U. S. Department of Agriculture.

measurements, at least not without considerable modification. Thus the common solvent techniques are not available, except for measurements over very limited portions of the spectra, such as the use by Mitchell et al. [17] of pyrrole in the near infrared, from about 0.7 to 2.0$\mu$. Mulling with a mineral oil such as Nujol [2] is one of the older procedures for measuring the spectra of insoluble materials. But mulls of cotton with mineral oil are not easily prepared. Such mulls do not permit very accurate quantitative measurements of band intensities. The grinding necessary to prepare a mull which will yield a satisfactory spectrum will cause change in structure of the cotton, as evidenced by loss of crystallinity.

A technique which has been more popular in England than in this country is the preparation of thin films of the sample cast on glass plates, frequently employing ground glass to avoid interference patterns in double-beam instruments [3, 14, 20, 29]. This technique is not entirely satisfactory, as precise quantitative measurements of band intensities cannot be obtained because film thickness and uniformity can only be estimated. Brown et al. [3], for example, recommend the lengthy procedure of measuring such films at several positions and using average readings to overcome lack of homogeneity. A more serious limitation is that suitable fibers cannot be made from the several types of modified cottons.

Recently, O'Connor, DuPré, and McCall [18] described a use of the now well-known KBr disc technique [6, 9, 24, 30] for obtaining spectra of cellulose and modified cellulose. They showed that such discs can be prepared quickly and easily and, of utmost importance, that satisfactory spectra can be obtained by the KBr disc technique without the requirements for excessive grinding; hence, spectra can be obtained of cottons without modification. Briefly the procedure consists of (a) cutting the cotton or modified cotton fiber, yarn, or fabric in a Wiley [2] mill to pass a 20-mesh screen; [3] (b) mixing with a mortar and pestle or with a mechanical mixer such as the Wig-L-Bug,[2] 2 mg. of a cotton sample and 300 mg. of potassium bromide; (c) pressing this mixture in a laboratory-type press under vacuum with a die especially designed for the purpose; and (d) measuring the spectra of the resulting disc, which should be entirely transparent, in a double-beam spectrophotometer against a similar disc, containing no sample, in the reference beam.

In Figures 1 and 2 are shown the KBr disc spectra of raw or native cotton in the rock salt region, from 2 to 15$\mu$, in comparison with several other natural fibers (Figure 1) and synthetic fibers (Figure 2). It should be noted that the KBr disc technique yields spectra with clear sharp bands and a relatively low degree of scattered radiation.

Infrared absorption spectra can be used to identify most natural and synthetic fibers. Cannon [4] recently has described infrared techniques used in such

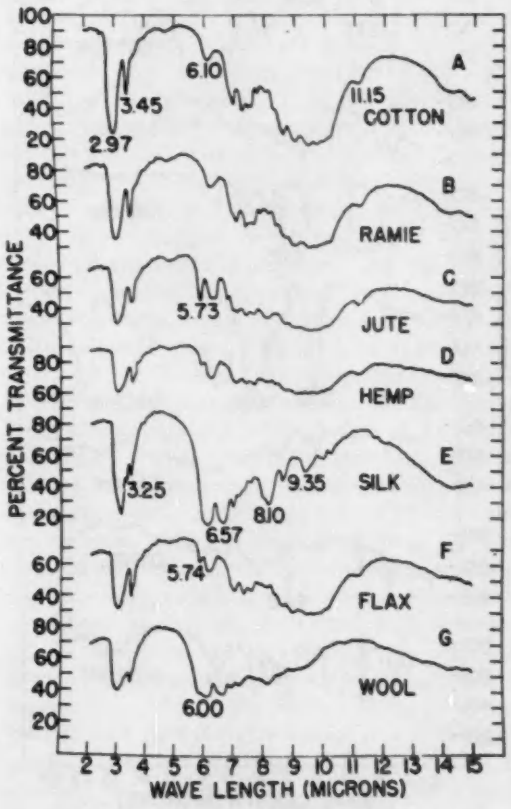


**Fig. 1.** Infrared spectra of natural fibers.

[2] Mention of names of firms or trade products does not imply that they are endorsed or recommended by the U. S. Department of Agriculture over other firms or similar products not mentioned.

[3] A 20-mesh screen was adopted for uniformity in the procedure and because, in agreement with conclusions of Schwenker and Whitwell [25] that "cotton yarn is not degraded significantly by a single passage through a Wiley mill fitted with a 20-mesh screen," it was found that spectra of samples passing through such a screen were identical to spectra prepared using considerably larger particles.

investigations and reviewed the general applications.

Directly from the infrared spectra shown in Figure 1, jute and flax, for example, could be differentiated readily from cotton or ramie. The spectra of jute and of flax reveal the weak 6.95$\mu$ and 11.15$\mu$ bands ($CH_2$ symmetrical bending and $CH_2$ rocking, respectively) characteristic of the cellulosic moeity. In addition, they reveal the 5.73−4$\mu$ band characteristic of C=O stretching. Jute can be distinguished from flax by the appearance of bands in the spectrum of the former at 6.25 and 6.65$\mu$. Silk and wool are differentiated readily from cotton, as they reveal no bands at 6.95$\mu$ nor at 11.15$\mu$ and the characteristic broad band of cellulosic fibers extending from 8 to 10$\mu$ is replaced, in the spectra of these fibers, by a transparency region. In addition, the spectra of both silk and wool exhibit the expected 6.0 and 6.57$\mu$ bands arising from C=O stretching and N−H bending of the CONH group. Silk can be distinguished from wool by the appearance in its spectrum of sharp bands with maxima at 8.10 and 9.35$\mu$.

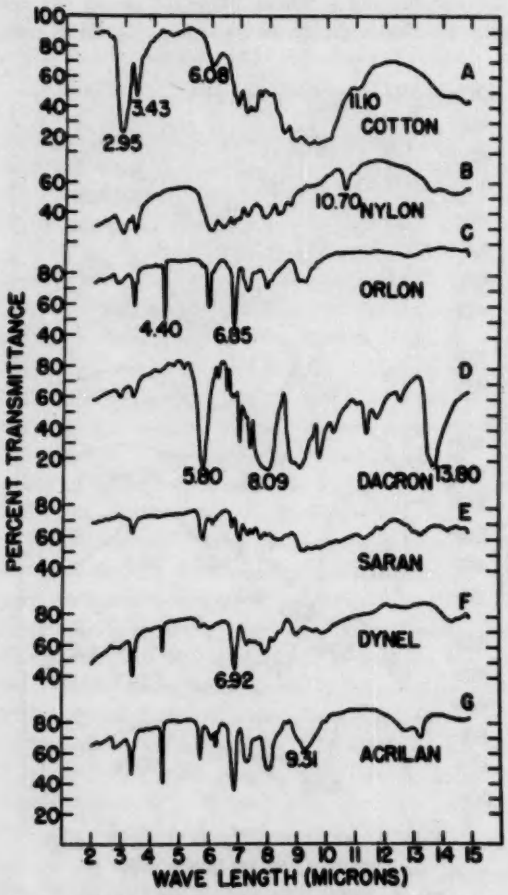


Fig. 2. Infrared spectra of cotton and synthetic fibers.

In the spectra of the synthetic fibers (Figure 2) Orlon,[4] Dynel, and Acrilan are differentiated readily by the appearance of the sharp bands with maxima at 4.40$\mu$ owing to a C≡N stretching. Within this group further differentiation is possible. Acrilan is the only fiber which reveals a band with maximum at 5.72$\mu$, C=O stretching of the acetate group, as well as the weaker but very characteristic bands at 12.75 and 13.25$\mu$, probably arising from vibrations of this same functional group. Orlon can be distinguished from either Dynel or Acrilan by the appearance of the strong, sharp band with maximum at 5.95$\mu$.

Of the nonacrylic type fibers, Dacron can be differentiated readily from nylon or Saran by the strong C=O stretching band in its spectrum at 5.80$\mu$ or by the characteristic bands arising from the aromatic moeity, C=C stretchings at 6.35 and 6.65$\mu$, and C−H bendings about the benzene ring at 13.0$\mu$. Dacron can also be recognized by the characteristic sharp bands in its spectrum with maxima at 9.85, 10.35, and 11.47$\mu$, which arise from aromatic C−H in-plane and out-of-plane deformations and which are not observed in the spectra of any of the other synthetic fibers examined. Nylon is identified by its very characteristic "crystalline" band at 10.70$\mu$, and Saran is characterized by a lack of any sharp bands consistent with its structure, which allows only various C−H stretchings and deformations. C−Cl vibrations would appear at wavelengths beyond the limits of these measurements. All of the synthetic fibers are differentiated from cotton by the nonappearance of the 6.95 and 11.15$\mu$ bands and of the broad absorption region from about 8$\mu$ to 10$\mu$, characteristic of cellulose.

Infrared absorption spectra can be used to identify qualitatively both natural and synthetic fibers. By selection of specific characteristic bands, quantitative measurements of the proportions of a particular fiber could be obtained. Thus, infrared spectra can be a very useful tool in identifying and measuring the relative proportions of components in blended fabrics. The KBr disc technique, as used in these investigations, is an ideal procedure for such measurements, especially where quantitative accuracy is required.

[4] Du Pont trademark.

### Hydrogen Bonding

In the spectrum of cotton in the rock salt region (Figure 1A or 2A) the bands at the shortest wavelengths, 2.8 to 3.0$\mu$, arise from fundamental stretching vibrations of the O—H groups. These are the groups that are responsible for hydrogen bonds in the cellulose molecule. Their bands are of greatest interest in the investigation of hydrogen bonding. As early as 1926 Sponsler and Dore [27] postulated that the orientation of cellulose chains in the cell walls was stabilized by hydrogen bonding of the hydroxyl groups of the glucose residues. Hilbert and coworkers [12], in an extensive series of careful experiments, showed how infrared spectra could be used as criteria for the determination of the existence or nonexistence of hydrogen bonding. As a result of their work, the detection of hydrogen bonding became one of the earliest triumphs of infrared spectroscopy.

Free O—H stretching gives rise to an absorption band with maximum about 2.70$\mu$. Hydrogen bonding causes a shift of this band to longer wavelengths, the magnitude of the shift becoming a rough estimation of the degree or type of hydrogen bonding [26]. Ellis and Bath [5] used near infrared absorption spectra, from 1 to 2.5$\mu$, to investigate hydrogen bonding in cellulose. They report two bands, one near 1.5$\mu$, an overtone of the fundamental O—H stretching vibration seen in Figures 1A and 2A at approximately 3.0$\mu$, and a combination valence-deformation band near 2.0$\mu$. A sharp but weak band near 1.4$\mu$ was correlated with the unperturbed (free) hydroxyl stretching overtone and bands with maxima at 1.49, 1.54, and 1.58$\mu$ with bonded O—H stretching. Similarly, bands at approximately 2.02 and 2.11$\mu$ arise from free and bonded O—H stretching respectively. In ramie fiber the 2.02$\mu$ band is absent, indicating that all or practically all of the hydroxyl groups in natural cellulose fiber are bonded. Mercerization resulted in disappearance of the 1.54$\mu$ band and a progressive shifting of the 2.11$\mu$ band to 2.09$\mu$, indicating that mercerization results in an increase in the absorption representing the lesser degree of hydrogen bonding.

In Figure 3 are shown the spectra in the 2–3$\mu$ region of the fundamental O—H stretchings, obtained with NaCl optics. Obviously, the bands are unresolved at the dispersion possible with the optics used. The shifting of the wavelength position of the unresolved maxima to shorter wavelengths with

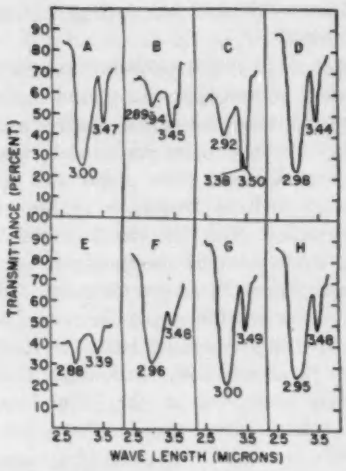


**Fig. 3.** Infrared spectra in the OH stretching region, 2.5–3.75$\mu$: (A) cotton linters control; (B) methyl cellulose; (C) ethyl cellulose; (D) cotton, Stoneville 2B control; (E) cellulose acetate; (F) carboxymethyl cotton; (G) cotton control; (H) mercerized cotton.

various treatments is observed in these spectra, in agreement with the results reported by Ellis and Bath from their observations in the near infrared region. Figure 3A is the spectrum of cotton linters and 3B and 3C of methyl- and ethylcellulose, respectively, prepared from them. The position of the unresolved O—H stretching fundamental shifts from 3.00$\mu$, in the spectrum of the raw linters, to 2.89–2.94$\mu$ in the spectrum of methylcellulose and to 2.92$\mu$ in that of ethylcellulose. A sample of commercial cellulose acetate (Figure 3E) exhibits a maximum at 2.88$\mu$, compared to the 2.98$\mu$ position of raw cotton (Figure 3D). The spectrum of a carboxymethylated cotton cloth (Figure 3F) exhibits a maximum at 2.96$\mu$, compared to the 3.00$\mu$ position of the control (Figure 3G). Figure 3H is the spectrum of the cotton after mercerization, exhibiting a similar shift of the position of maximum from 3.00 to 2.95$\mu$. These spectra indicate clearly that all of these processes result in a lessening of the degree of hydrogen bonding. It seems probable that the reactions involve the amorphous regions of the cotton and remove a greater proportion of the more highly hydrogen bonded O—H groups in this region. The result, as observed, is a shift in the position of the unresolved band toward the less highly bonded crystalline O—H groups at shorter wavelengths. Rowen et al. [20] observed the converse effect, the increase in wavelength position of the maximum of the O—H stretch-

ing band from 2.86 to 2.94$\mu$ during deacetylation of cellulose acetate.

Brown et al. [3] have published results of one of the very few investigations of cotton in the fundamental O−H vibration region of the infrared spectra, about 3.0$\mu$. From samples prepared by casting thin films on finely ground glass plates they found that the shape as well as frequency of the absorption bands associated with the fundamental hydroxyl stretching modes can be used to give considerable information about hydrogen bonding conditions. With the higher resolution possible with LiF optics, bands were observed arising from O−H stretching vibrations at about 2.98, 3.05, and 3.08$\mu$, with shoulders on both sides of the 2.98$\mu$ band. Free O−H stretching gives rise to sharp symmetrical bands, while bonded O−H stretchings are unsymmetrical with broadening toward the lower frequency sides. A measure of the symmetry index [5] is thus some criterion of hydrogen bonding. However, as seen from the spectra in Figure 3, obviously band shapes and symmetry indices have no significance in the unresolved NaCl spectra.

Marrinan and Mann [15] investigated hydrogen bonding by examining the infrared spectra of cellulose before and after deuteration. They explain the results of their experiments on the basis that deuteration at ordinary conditions results in substitution of deuterium for hydrogen in the hydroxyl groups of the amorphous regions only. In these amorphous regions there is a range of hydrogen bonds of varying strengths and hence a broad unresolved band. This is the band observed before deuteration. In crystalline regions, however, there are a discrete number of hydrogen bonds, each giving rise to a definite absorption band. Thus the spectrum from about 2.8 to 3.3$\mu$, measured with LiF optics, after deuteration exhibits four discrete bands. A new band appears about 3.9$\mu$, attributable to O−D stretching, and a band with maximum at 3.4$\mu$, arising from C−H stretching, is unchanged. Removal of the unresolved bonds arising from hydroxyl groups in the amorphous regions by converting them to O−D bonds makes it possible to observe the bands which are attributable to the O−H stretching arising from the hydroxyl groups in the crystalline regions.

[5] Symmetry index is defined as the ratio of the band widths on the low and on the high frequency side of the maximum at half band absorbance. The symmetry index for a symmetrical band is thus unity and is greater than unity for bands which are broadened on the low frequency side [3].

The KBr disc technique is ideal for investigations of hydrogen bonding, as spectra can be obtained with no change in bonding or degree of crystallinity during the process of obtaining them, they can be obtained quickly and simply, and quantitative measurements can be obtained with high precision. Considerably additional measurements of the KBr disc spectra in the region of the fundamental O−H (and O−D) stretchings with resolution greater than that obtained with NaCl optics, together with corresponding measurements of the overtone and combination bands in the near infrared, are needed. The papers

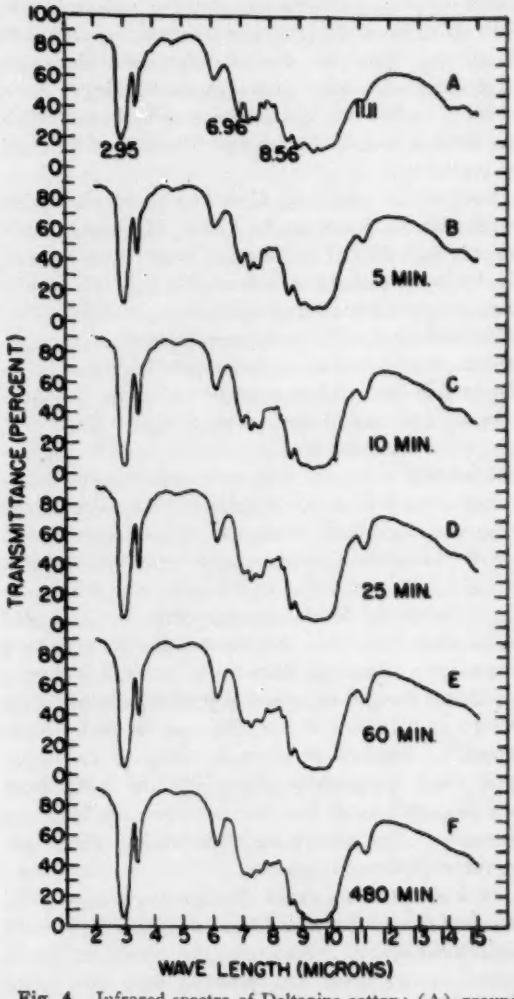


**Fig. 4.** Infrared spectra of Deltapine cotton: (A) ground to pass 2 mm. mesh in Wiley mill; (B), (C), (D), (E), and (F) ground in vibratory ball mill.

of Ellis and Bath [5], Brown, Holliday, and Trotter [3], and Marrinan and Mann [15] have indicated clearly that such measurements would be a fruitful source of data for further investigations of hydrogen bonding of cellulose and modified celluloses.

### Crystallinity

In Figure 4 are shown the spectra of a Deltapine raw cotton before and after a series of grindings in a vibratory ball mill of the type described by Forziati et al. [7]. The effects of the decrystallization accompanying this grinding can be observed. The broad unresolved band at 2.95$\mu$, arising from O—H stretchings, progressively increases in intensity. The rather weak but distinct bands in the region between 7.0 and 9.0$\mu$ become less and less distinct. Presumably various bendings can occur at a multitude of frequencies in the amorphous cotton. The more rigorously fixed vibrations of the crystalline cotton give rise to a series of sharp bands which disappear on decrystallization, gradually giving way to a broad absorption band. In particular the band at 6.9$\mu$, arising from C—H bending, disappears. In the region near 11.00$\mu$, a very weak band in the raw cotton increases in intensity as the crystallinity decreases.[6] Both the changes at about 7 and 11$\mu$ are very small, but they are in opposite directions. A ratio of absorptivities at these two wavelengths is thus a reasonably sensitive measure of degree of crystallinity. Values of this ratio, called crystallinity index,[7] are given in Table I for the series of cottons decrystallized in the vibratory ball mill. Conrad and coworkers [2] have shown that values of crystallinity measured in this manner are directly proportional to data obtained from X-ray diffraction measurements. Appearance of a band at about 7.0$\mu$ and no distinct band at 11.0$\mu$, or conversely, no band exhibited at about 7.0$\mu$ but a distinct band at 11.0$\mu$, are reasonably sensitive criteria of crystalline and decrystallized cotton cellulose, respectively.

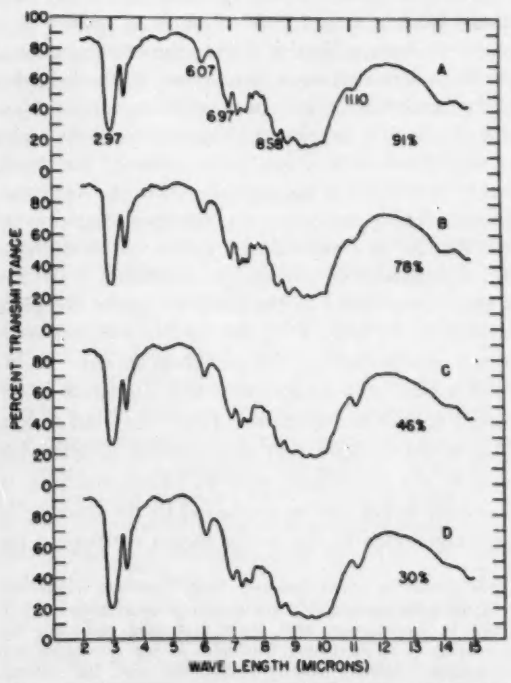


Fig. 5. Infrared spectra of chemically decrystallized cotton (crystallinity measured by acid hydrolysis).

Several workers engaged in investigations of polymers by means of their infrared absorption spectra have assigned specific absorption bands as "crystalline" or "amorphous." A "crystalline" band is defined as one which decreases in intensity progressively with increase in temperature and finally disappears completely when the polymer becomes molten. Conversely an "amorphous" band is one which does not appear in the spectra of the crystalline polymer and becomes more intense with increased amorphous character. Sandeman and Keller

[6] Forziati et al. [7] noted an increase in this band at about 11$\mu$ in converting cellulose I to cellulose II and to amorphous cellulose.

[7] Crystallinity index is defined as the ratio of the absorbance of the band maximum at about 6.9$\mu$ to the absorbance of the maximum about 11.0$\mu$. Absorbancies used to calculate the indices reported in Table I were obtained from measurements at these two wavelengths by the usual baseline technique.

**TABLE I. Measurements of Crystallinity from Infrared Absorption Spectra**

| Mechanical decrystallization | | Chemical decrystallization (ethylamine) | |
|---|---|---|---|
| Time grinding in vibratory ball mill, min. | Crystallinity index | Crystallinity by acid hydrolysis, % | Crystallinity index |
| 0 (Control) | 2.73 | 91 (Control) | 2.88 |
| 5 | 1.18 | 78 | 2.49 |
| 10 | 0.75 | 63 | 1.65 |
| 25 | 0.40 | 39 | 1.27 |
| 60 | 0.21 | 28 | 0.93 |
| 480 | 0.11 | 26 | 0.78 |

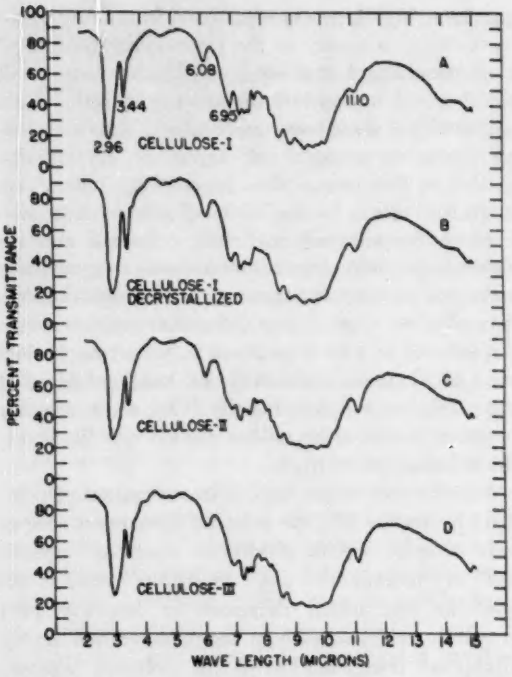


**Fig. 6.** Infrared spectra of polymorphic forms of cellulose.

[23], for example, assign absorption bands at 10.70$\mu$ in the spectra of nylon 6, at 10.67$\mu$ in the spectra of nylon 6.6, and at 10.64$\mu$ in the spectra of nylon 6.10 as "crystalline" bands and describe how these bands may be used to estimate degree of crystallinity in these polymers. Under these definitions the bands at 6.9$\mu$ and at 11.0$\mu$ in the spectrum of cellulose may be called "crystalline" and "amorphous" bands, respectively.

Cotton decrystallized chemically with ethylamine shows changes which, although much smaller, parallel those found by mechanical decrystallization, as shown in Figure 5. Crystallinity indices from these spectra are included in Table I.

In Figure 6 are shown spectra of the three polymorphic forms of cellulose—cellulose I, II, and III. Identity of these celluloses have been confirmed by X-ray diffraction. As seen in this figure, infrared spectra from KBr discs in the rock salt region from 2 to 15$\mu$ are not very satisfactory to differentiate the three polymorphic forms. Any small differences observed in sharpness of individual bands can be accounted for by small changes in degree of crystallinity.[8]

Mann and Marrinan [14] have described a method for estimating the crystallinity of cellulose by infrared spectra based on the reaction between the cellulose and heavy water. Results are expressed as the ratio of the absorbance at the maximum of the O–D (amorphous) band at 3.95$\mu$ to that of the O–H (crystalline) band at 2.98$\mu$. While this method has the obvious disadvantage of requiring the additional step of deuteration, it undoubtedly has the advantage of being a most sensitive method and may afford the most satisfactory procedure for obtaining crystallinity measurements by means of infrared spectroscopy.

## Cross-Linkage

The spectra of a series of mercerized cottons cross-linked with epichlorohydrin are given in Figure 7. The effect of cross-linkage on the infrared spectra follow rather closely the effects of decrystallization. There is, however, a small *decrease* in the intensity of the O–H stretching band at about 3.0$\mu$. The very gradual decrease is observed in intensity of the progression of sharp distinct bands in the region 7.0–9.0$\mu$ and, in particular, the decrease in the intensity of the band at 6.9$\mu$ (weak in all these spectra as a result of decrystallization during the mercerization). An important difference is observed in the behavior of the band near 11.0$\mu$. In progressive decrystallization this band is developed (Figure 4). In the series of epichlorohydrin cross-linked cottons, the band, rather prominent in the control, due to the decrystallization during mercerization, becomes progressively less intense as cross-linkage, measured as decrease in cuprammonium solubility, increases. In the sample cross-linked to the point of almost complete insolubility (Figure 7F), this 11.0$\mu$ band has completely disappeared. Cross-linking appears to involve a band with maximum near 11.0$\mu$ which is observed only in the spectrum of decrystallized cotton. This might indicate that cross-linking is occurring only in the amorphous regions. Disappearance of this band might also be explained by the increase in total absorption in the 8–11$\mu$ region enveloping the

[8] It should be noted, however, that Marrinan and Mann [16], using the considerably higher resolution afforded by LiF optics in conjunction with their deuterium technique for separating O–H stretching vibrations in the crystalline and amorphous regions, have demonstrated that the various polymorphic forms of cellulose can be differentiated readily by means of their infrared absorption spectra.

specific maximum. Steele [28] investigated the reaction of formaldehyde with cellulose by means of infrared absorption spectra and also noted an increase in total absorption in this region, attributing it to additional C−O linkages resulting from cross-linkage. Curves published by Steele clearly indicate the disappearance of the 11.0$\mu$ band during the cross-linking process. Steele found that the 2.92$\mu$ O−H stretching vibration band was reduced in intensity and that the 3.43$\mu$ band, arising from C−H stretching, was slightly increased. He interpreted these changes as indicating that, of the probable processes involved, the formation of methylene ether cross-links

$$\text{Cell}-\text{O}-\text{CH}_2-\text{O}-\text{Cell}$$

occurs predominately.

The intensities of the bands near 6.9 and 11.0$\mu$ are, unfortunately, never very strong, and any measurements of cross-linkage using NaCl infrared spectra could not be made very sensitive. The intensity of the 11.0$\mu$ band decreases more rapidly during cross-linking than does the band at 6.9$\mu$. Thus (Figure 7), the crystallinity index increases with increased cross-linking. However, except to follow the course of a specific cross-linking process, this index could not be helpful in determining the amount of cross-linkage, as it is more influenced by the amount of decrystallization of the particular sample than by the extent of cross-linkage.

## Oxidation

Oxidation of cotton cellulose can produce several products, depending upon the conditions of the oxidative attack. Unruh and Kenyon [33] have listed six products, all containing aldehyde, ketone, or carboxyl groups, which might be expected. The strong C=O stretching of each of these groups should permit their ready identification and quantitative measurement with a high degree of sensitivity by means of infrared absorption spectra. Rugg et al. [22], for example, have shown from detailed study of the oxidation of polyethylene how various C=O groups can be differentiated by means of the infrared spectra of polymers.

The spectra of periodate oxidized cotton (Figure 8) indicate C=O stretching in the region of 5–6$\mu$. From chemical evidence it has been shown that with periodate oxidative attack is mainly at the secondary carbons, at positions 1 and 2 in the cellulose molecule [33]. This would be expected to result in aldehyde formation, as in the case of dialdehyde starch. However, not until excessive oxidation has taken place are any C=O bands observed in the infrared spectra (Figure 8).

Forziati, Rowen, and Plyler [8] have shown that the carboxyl group can be detected and determined quantitatively by means of infrared absorption measurements to a sensitivity of 0.1 mmole/g. They claim that their "results indicate that the intensity of the absorption of the oxidized celluloses at 5.84$\mu$ constitutes a fairly satisfactory measure of their carboxyl content even in the presence of appreciable amounts of non-carboxylic carbonyl." In one sample they found and measured as little as 0.19 mmole/g.

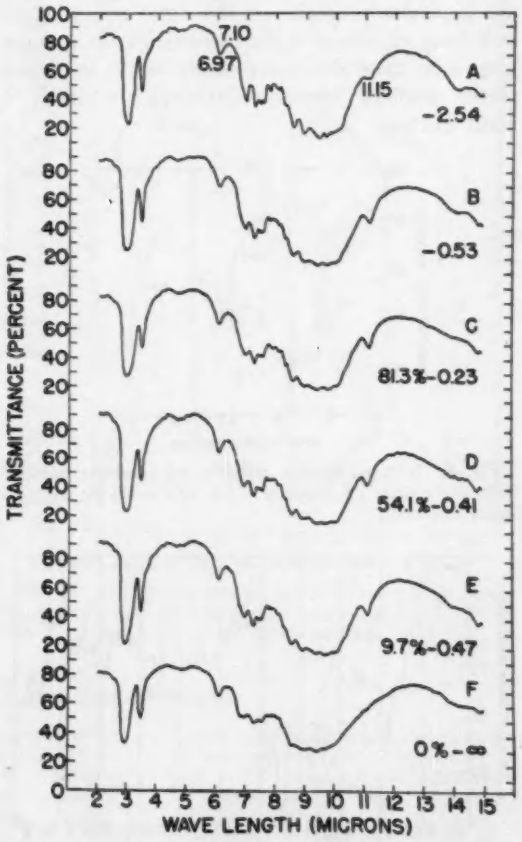


**Fig. 7.** Infrared spectra of cross-linked cotton: (A) control; (B) mercerized control; (C), (D), (E), (F) epichlorohydrin cross-linked (percent cuprammonium solubilities and crystallinity indices are given).

of carboxyl in the presence of 7.37 mmole/g. of noncarboxylic carbonyl (by hydroxylamine hydrochloride method). In view of the known positions and intensities of the C=O stretching vibrations of aldehydes and ketones (as demonstrated by Rugg et al. [22]), this conclusion is untenable without further qualification.

Thus, two anomalous results are encountered in the examination of infrared spectra of oxidized cotton cellulose; (a) it can be oxidized under conditions which produce relatively large concentrations of aldehyde (or ketone) groups, but the spectra exhibit no evidence of the well-known, intense C=O stretching vibrations of these groups; and (b) the carboxyl content can be obtained satisfactorily with quantitative accuracy by measurement of the 5.8$\mu$ C=O stretching vibration of the carboxyl group in the apparent presence of the very strong C=O stretching vibrations of the carbonyl group at wavelengths so close that these bands would be incompletely resolved from the carboxyl stretchings in NaCl spectra.

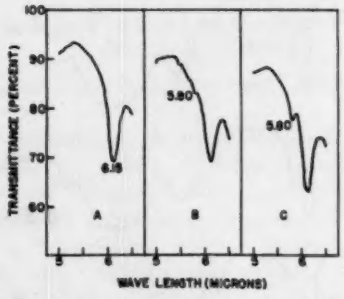


**Fig. 8.** Infrared spectra, 5.0–6.5$\mu$, of periodate oxidized Deltapine cotton: (A) control; (B) 10% oxidized; and (C) highly oxidized.

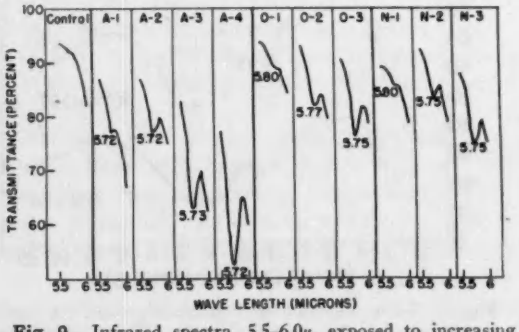


**Fig. 9.** Infrared spectra, 5.5–6.0$\mu$, exposed to increasing dosages of gamma radiation in atmospheres of air, oxygen, and nitrogen.

Rowen, Forziati, and Reeves [21] have given a reasonable explanation for these anomalous findings. They postulate that either or both of the free aldehyde groups of the oxidized cellulose are hydrated by reaction with water as suggested by Malaprade [13] as an intermediate in the periodate oxidation of adjacent hydroxyl and carbonyl groups.

Very probably the first stage in the periodate oxidation of cellulose is the formation of the aldehyde hydrate, which, although it would react as a carbonyl group with certain chemical reagents, gives rise to no C=O stretching bands in its infrared spectra, as this group is not present in the oxidized molecule. In fact, little change would be expected from the spectra of the original nonoxidized sample with two secondary hydroxyl groups, and none is observed. On further oxidation, either the aldehyde is converted to carboxyl or oxidative attack is initiated at the primary hydroxyl of the molecule to produce a carboxyl group. This is readily detected by the appearance, in the infrared spectra, of the characteristic C=O stretching of the carboxyl group. The method of Forziati, Rowen, and Plyler [8] for the quantitative determination of carboxyl groups in oxidized cellulose is not valid, as claimed, in the presence of large quantities of carbonyl. They were able to obtain satisfactory quantitative results only because none of their oxidized cottons contained carbonyl groups *per se*. Only if all the carbonyl is tied up as a hydrate or hemiacetal can infrared measurements with rock salt optics be used for quantitative determination of carboxyl content.

The spectra of a series of cottons exposed to gamma radiation in atmospheres of air, oxygen, and nitrogen for a series of increasing dosages are given in Figure 9. The carboxyl and carbonyl contents determined chemically are presented in Table II with the intensities of the infrared band about 5.8$\mu$. As in the periodate oxidations, the intensities bear no relation to the carbonyl concentrations, but above the limiting sensitivity (in agreement with Forziati, Rowen, and Plyler [8]) of about 0.1 mmole/g. the absorbances follow the chemically measured carboxyl groups. The postulations of Rowen, Forziati, and Reeves [21] afford a complete explanation of these results. Blouin and Arthur [1] used infrared absorption data in their studies of the effects of gamma radiation on cotton.

Obviously, if infrared absorption spectra are to be used for the determination of carboxyl group con-

tent, the absence of carbonyl groups (i.e., proof of the existence of hydrates or hemiacetals) must be established. With NaCl optics this usually can be accomplished by careful examination of the C=O stretching band, as aldehyde and carboxyl groups, although not completely resolved, exhibit maxima at somewhat different positions. The resulting band is less sharp when both are present. Use of higher resolution, as for example with CaF optics, should permit the simultaneous determination of both aldehyde and carboxyl groups by means of infrared absorption spectra. If the carbonyl is tied up as a hydrate, obviously its determination could be accomplished from infrared absorption measurements only after the hydrate linkage has been broken. This could be accomplished most easily by measurement of the spectra of some simple derivative of the hydrated aldehyde.

## Heat Damage of Cotton

A problem of considerable interest to the textile industry is the heat damage of cotton. Heat damage might be expected to arise from some oxidation which could be detected and determined by means of an examination of the infrared absorption spectra of the heat damaged sample. However, as seen in Figure 10, either the concentration of oxidized materials is too small for detection by means of infrared or the oxidized product is again a hydrated aldehyde which could not be detected. No C=O stretchings are observed until the cotton has been heated to temperatures and for periods of time far in excess of any encountered in actual commercial practice. The C=O stretchings observed in the spectra of these excessively heated samples may be a secondary oxidation to give carboxyl groups. In any case, lack of any observable C=O stretching bands in the spectra of several heated cottons examined means that their carboxyl content is less than 0.1 mmole/g.


## Summary

The infrared absorption spectra of cotton cellulose by means of the recently described application of the KBr disc technique can be used to investigate changes in physical and crystalline properties. Experiments are described illustrating how the technique can be employed to follow changes in hydrogen bonding or to measure the degree of crystallinity. Application of the technique to the few uses of infrared spectra suggested by earlier workers has been reviewed. It has been shown that oxidation of cotton can be detected and measured by means of infrared absorp-


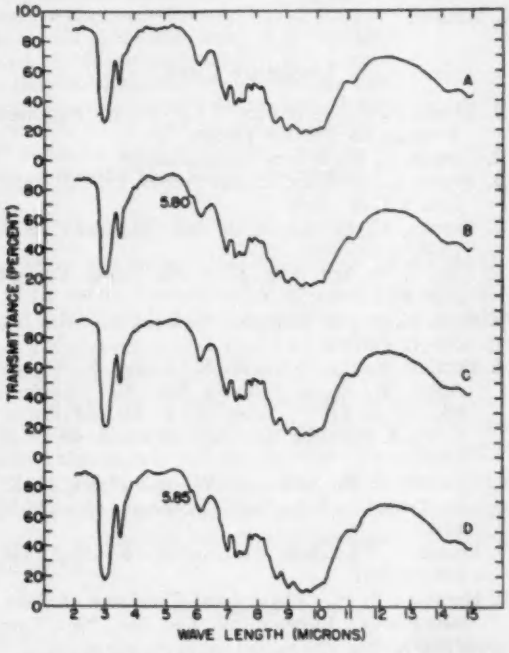


**Fig. 10.** Infrared spectra of heated cottons: (A) Deltapine, control; (B) Deltapine, heated 48 hr. at 162° C.; (C) Pima 32, control; (D) Pima 32, heated 48 hr. at 162° C.

**TABLE II. Infrared Spectra of Gamma Irradiated Cottons**

| Irradiated in an atmosphere of air | | | | Irradiated in an oxygen atmosphere | | | | Irradiated in a nitrogen atmosphere | | | |
|---|---|---|---|---|---|---|---|---|---|---|---|
| Gamma radiation, roentgens | Carbonyl groups, mmoles/g. | Carboxyl groups, mmoles/g. | Infrared absorptivity, 5.7–8μ | Gamma radiation, roentgens | Carbonyl groups, mmoles/g. | Carboxyl groups, mmoles/g. | Infrared absorptivity, 5.7–8μ | Gamma radiation, roentgens | Carbonyl groups, mmoles/g. | Carboxyl groups, mmoles/g. | Infrared absorptivity, 5.7–8μ |
| $3.3 \times 10^7$ | 1.14 | 0.101 | 0.066 | $5 \times 10^6$ | 0.28 | 0.022 | No band | $5 \times 10^6$ | 0.22 | 0.015 | No band |
| $6.3 \times 10^7$ | 2.08 | 0.211 | 0.066 | $1 \times 10^7$ | 0.58 | 0.039 | No band | $1 \times 10^7$ | 0.36 | 0.023 | No band |
| $1.2 \times 10^8$ | >3.00 | 0.38 | 0.116 | $5 \times 10^7$ | 1.91 | 0.107 | 0.048 | $5 \times 10^7$ | 1.30 | 0.070 | 0.044 |
| $1.9 \times 10^8$ | >3.00 | 0.63 | 0.161 | $1 \times 10^8$ | 3.02 | 0.155 | 0.067 | $1 \times 10^8$ | 2.66 | 0.139 | 0.070 |

tion spectra only if a C=O is produced *per se* by the oxidation process.

### Acknowledgment

The authors are indebted to several staff members of this laboratory for the samples used in these investigations—Fred S. Perkerson, Leon H. Chance, Manuel D. Cruz, George L. Drake, Jr., Carl Hamalainen, Wilson A. Reeves, Walter T. Schreiber, Ricardo Wade, Carl M. Conrad, Mary L. Nelson, Elias Klein, Leon Segal, David J. Stanonis, Ines V. DeGruy, John G. Frick, Jr., Robert M. Reinhardt, James E. Snowden, Jr., Florine A. Blouin, and Jett C. Arthur.

### Literature Cited

1. Blouin, F. A. and Arthur, J. C., TEXTILE RESEARCH JOURNAL **28**, 198–204 (1958).
2. Conrad, C. M., private communication.
3. Brown, L., Holliday, P., and Trotter, I. F., *J. Chem. Soc.* 1532–9 (1951).
4. Cannon, C. G., *Chem. & Ind.* (London) 29–33 (1957).
5. Ellis, J. W. and Bath, J., *J. Am. Chem. Soc.* **62**, 2859–61 (1940).
6. Ford, M. A. and Wilkinson, G. R., *J. Sci. Instr.* **31**, 338–41 (1954).
7. Forziati, F. H., Stone, W. K., Rowen, J. W., and Appel, W. D., *J. Research Nat. Bur. Standards* **45**, 109–13 (1950); Forziati, F. H. and Rowen, J. W., *J. Research Nat. Bur. Standards* **46**, 38–42 (1951).
8. Forziati, F. H., Rowen, J. W., and Plyler, E. K., *J. Research Nat. Bur. Standards* **46**, 288–91 (1951).
9. Hausdorff, H., *Appl. Spectroscopy* **8**, 131–2, 134, 136 (1954).
10. Hermans, P. H., "Physics and Chemistry of Cellulose Fibres," Elsevier Pub. Co., Inc., New York (1949).
11. Heuser, E., "The Chemistry of Cellulose," Wiley, New York, 1944.
12. Hilbert, G. E., Wulf, O. R., Hendricks, S. B., and Liddel, U., *Nature* **135**, 147–8 (1935), *J. Am. Chem. Soc.* **58**, 548–55 (1936); Hendricks, S. B., Wulf, O. R., Hilbert, G. E., and Liddell, U., *J. Am. Chem. Soc.* **58**, 1991–6 (1936); Wulf, O. R., Liddel, U., and Hendricks, S. B., *J. Am. Chem. Soc.* **58**, 2287–93 (1936).
13. Malaprade, L., *Bull. Soc. Chim.* (France) (5) **1**, 833–52 (1934).
14. Mann, J. and Marrinan, H. J., *Trans. Faraday Soc.* **52**, 481–7, 487–92, 492–7 (1956).
15. Marrinan, H. J. and Mann, J., *J. Appl. Chem.* (London) **4**, 204–11 (1954).
16. Marrinan, H. J. and Mann, J., *J. Polymer Sci.* **21**, 301–11 (1956).
17. Mitchell, J. A., Bockman, C. D., Jr., and Lee, A. V., *Anal. Chem.* **29**, 499–502 (1957).
18. O'Connor, R. T., DuPré, E. F., and McCall, E. R., *Anal. Chem.* **29**, 998–1005 (1957).
19. Ott, E., Spurlin, H. M., and Grafflin, M. W., ed. "Cellulose and Cellulose Derivatives," 2nd ed. 3 pts. (High Polymers, Vol. 5), Interscience, New York (1954–55).
20. Rowen, J. W., Hunt, C. M., and Plyler, E. K., *J. Research Nat. Bur. Standards* **39**, 133–40 (1947); TEXTILE RESEARCH JOURNAL **17**, 504–11 (1947); Rowen, J. W. and Plyler, E. K., *J. Research Nat. Bur. Standards* **44**, 313–320 (1950).
21. Rowen, J. W., Forziati, F. H., and Reeves, R. E., *J. Am. Chem. Soc.* **73**, 4484–7 (1951).
22. Rugg, F. M., Smith, J. J., and Bacon, R. C., *J. Polymer Sci.* **13**, 535–47 (1954).
23. Sandeman, I. and Keller, A., *J. Polymer Sci.* **19**, 401–35 (1956).
24. Schiedt, U. and Reinwein, H., *Z. Naturforsch.* **7b**, 270–7 (1952).
25. Schwenker, R. F., Jr. and Whitwell, J. C., TEXTILE RESEARCH JOURNAL **23**, 804–8 (1953).
26. Smith, F. A. and Creitz, E. C., *J. Research Nat. Bur. Standards* **46**, 145–164 (1951).
27. Sponsler, O. L. and Dore, W. H., *Colloid Symposium Monograph* **4**, 174–202 (1926).
28. Steele, R., TEXTILE RESEARCH JOURNAL **25**, 545–8 (1955).
29. Steele, R. and Pacsu, E., TEXTILE RESEARCH JOURNAL **19**, 790–3 (1949).
30. Stimson, M. M. and O'Donnell, M. J., *J. Am. Chem. Soc.* **74**, 1805–8 (1952).
31. Timell, T., "Studies on Cellulose Reactions," Esselte Aktiebolag, Stockholm (1950).
32. Tsuboi, M., *J. Polymer Sci.* **25**, 159–71 (1957).
33. Unruh, C. C. and Kenyon, W. O., TEXTILE RESEARCH JOURNAL **16**, 1–12 (1946).

*Manuscript received December 2, 1957.*

# The Effect of Temperature on the Rate of Creep Failure for 66 Nylon

**Bernard D. Coleman[1], Andrew G. Knox, and William F. McDevit**

*E. I. du Pont de Nemours and Company, Carothers Research Laboratory, Wilmington, Delaware*

**Abstract**

Measurements have been made of the lifetime under dead load behavior of high tenacity bright nylon yarn in dry nitrogen at eight temperatures in the range 30–125° C. The data obtained have been interpreted using a previously published absolute reaction rate theory of the creep failure of oriented crystalline polymeric fibers. The prediction of the theory that the logarithm of the lifetime should be a linear function of the sustained dead load was found to be consistent with the experimental results at all temperatures investigated. The data were used to calculate estimates at each temperature for the displacement volume $\delta$ and the free energy of activation $\Delta F^*$ for the breakdown process. An examination of the temperature dependence of $\Delta F^*$ has yielded the conclusion that the negentropy of activation $-\Delta S^*$ makes a negligible contribution to $\Delta F^*$. The best estimate for the heat of activation for breakdown $\Delta H^*$ was found to be ~49 kcal.

## Introduction

In previous publications [1, 3] a simplified absolute reaction rate theory was presented which permitted calculations of breaking times for partially oriented polymeric filaments bearing time-dependent tensile loads. This theory is only approximate in that it neglects some statistical considerations which have been discussed elsewhere [2] and will be discussed in more detail in future publications. It is believed, nevertheless, that the reaction rate theory furnishes an adequate basis for calculating average lifetimes for ensembles of fibers under loading histories which cause creep failure. The theory should be particularly applicable to such materials as drawn nylon, cotton, rayon, and drawn Dacron[2] polyester fibers.

The present paper is concerned with lifetime under dead load measurements; that is, measurements of times required for breaking $t_B$ for yarns subjected to constant tensile stresses $f$. Yarn lifetimes have been determined as a function of $f$ for high tenacity bright nylon at selected temperatures through the range 30–125° C. The data and their interpretation are to be presented here.

We shall make no attempt to summarize the previous theoretical and experimental work on the temperature dependence of the strength of nylon and other textile fibers, except to mention a paper by Illingworth and Kilby [4] which gives recent results of careful and extensive measurements of the tensile strength, under loads that are proportional to time, for polyamide, polyester, and cellulose yarns throughout the temperature range 20–160° C. These authors present a rate process theory and give references to earlier experimental investigations on the temperature dependence of tensile strength.

[1] Present address: Mellon Institute, Pittsburgh 13, Pennsylvania.

[2] Du Pont trademark.

## Theory

The discussion given below is based on the theory presented previously [1, 3]. According to this theory, the lifetime of a fiber which is bearing a constant tensile stress $f$ (in dynes cm.$^{-2}$) is given by

$$t_B = \frac{\gamma_B}{\lambda}\frac{h}{kT}e^{\Delta F^*/RT}e^{-f\delta/2kT} \qquad (1)$$

Here $\Delta F^*$ (in kcal. mole$^{-1}$) is the free energy of activation for the displacement of force centers, $\lambda$ (jump distance) is the separation between the positions of minimum potential of mean force, $\delta$ (displacement volume) is equal to the product of the effective cross-sectional area per force center and the jump distance, $\gamma_B$ (in cm.) is a measure of

the critical amount of irreversible distortion that the microstructure can tolerate before the breakdown process occurs with catastrophic rapidity, $T$ is the absolute temperature, $R$ is the gas constant, $k$ is Boltzmann's constant, and $h$ is Planck's constant. In deriving Equation 1 it is assumed that $f\delta$ is at least two or three times greater than $2kT$. Other restrictions on Equation 1 are discussed at length elsewhere [3].

It is common practice in the textile industry to express tension in the units of grams per denier, where the denier is the weight in grams of 9000 meters of the unloaded yarn at room temperature. We shall use the symbol $f'$ to denote tension in these units. If a fiber, at temperature $T$, is bearing a free-hanging weight $W$ (in g.) and has a denier $d$ as measured for a relaxed sample at room temperature, the value of $f'$ is defined by

$$f' \equiv W/d \tag{2}$$

regardless of the value of $T$ or the elongation $E$ caused by $W$. On the other hand, the true tensile stress $f$ in c.g.s. units is

$$f = Wg/A \tag{3}$$

where $g$ is the gravitational constant ($\sim$ 980 cm. sec.$^{-2}$) and $A$ is the cross-sectional area (in cm.$^2$) of the yarn at the moment under consideration. To a very good approximation, for those fibers whose density is relatively insensitive to temperature or stretching, we can write for $A$ in Equation 3:

$$A = \frac{d}{\rho 9 \times 10^5 (1 + E)(1 - S)} \tag{4}$$

where $S$ is the free shrinkage of the yarn on going from room temperature to $T$ and $\rho$ is the mean density (g. cm.$^{-3}$) of the yarn. If the weight $W$ is sufficiently large so that the yarn will eventually break ($t_B$ finite), yet small enough so that the yarn lasts for several seconds, then for most of the time $t_B$ the fiber will have an elongation $E$ that is very close to the elongation at break $E_B$. When this is the case, the value of $f$ for insertion into Equation 1 can be calculated from $f'$ by means of Equations 2, 3, and 4:

$$f = f'\rho g(1 + E_B)(1 - S)9 \times 10^5 \tag{5}$$

For many textile fibers, $E_B$, at constant $T$, has been observed to be independent of $f$ and $t_B$. Indeed, for 66 nylon [1] near room temperature, $E_B$ appears to be independent of the functional form of $f$ for a large class of general loading histories, $f(t)$. Thus, if we plot $\log_{10} t_B$ versus $f'$ at a particular temperature, according to Equations 1 and 5 we should expect to get a straight line:

$$\log_{10} t_B = a - bf' \tag{6}$$

Here, $a$ and $b$ are functions only of $T$. Equations 1, 5, and 6 yield

$$a = \log_{10}\left(\frac{\gamma_B h}{\lambda k T}\right) + 0.4343\,\frac{\Delta F^*}{RT} \tag{7}$$

$$b = 0.4343\,\frac{\rho g(1 + E_B)(1 - S)9 \times 10^5}{2kT}\,\delta \tag{8}$$

Equation 7 permits us to calculate the standard free energy of activation $\Delta F^*$ from $a$ if we make an assumption about the magnitude of $\gamma_B/\lambda$. For the calculations reported in Table III, it has been assumed that $\gamma_B/\lambda$ has the same order of magnitude as $E_B$. The calculated values of $\Delta F^*$ are not very sensitive to $\gamma_B/\lambda$. If the estimate for $\gamma_B/\lambda$ were to be changed by a factor of $10^2$, the tabulated values of $\Delta F^*$ would change by, at most, 3.7 kcal.

The standard free energy of activation may be resolved into entropy ($\Delta S^*$) and enthalpy ($\Delta H^*$) components:

$$\Delta F^* = \Delta H^* - T\Delta S^* \tag{9}$$

If it can be assumed that throughout the temperature range under consideration $\Delta H^*$ and $\Delta S^*$ are independent of $T$, then a plot of $\Delta F^*$ (as determined from Equations 6 and 7) versus $T$ will yield $\Delta H^*$ for its apparent intercept and $\Delta S^*$ for its slope.

According to Equation 8, once $E_B$ and $S$ are known for a given yarn, an estimate for the magnitude of the displacement volume $\delta$ can be obtained from the slope $b$ of a plot of $\log_{10} t_B$ versus $f'$. If it is assumed that the hydrogen bonds are the most important force centers in nylon, and that the potential of mean force is distorted in a symmetrical manner by the applied tension, then a lower bound may be calculated [1] for $\delta$ from purely geometrical considerations. For 66 nylon the lower bound is $\sim$150 Å$^3$ or, roughly, $\frac{1}{2}$ the volume of a unit cell. This value of 150 Å$^3$ applies only to a "perfect" fiber which has no stress concentrating defects and whose fine structure consists solely of triclinic crystallites whose $c$ axes are parallel to the fiber axis.

A multiplicity of reasons may be invoked to explain why experimentally observed values of $\delta$ exceed the theoretical lower bound. For example, the presence of only partially oriented crystallites [1] and regions of incomplete crystallization must give rise to an increase in $\delta$ over its lower limit. Stress-concentrating defects will make the microstress greater than the apparent tension $f$, and will yield anomalously high values of $\delta$ when experimental data are interpreted with Equations 6 and 8. Also, thermal motion of the force centers in plastic materials, such as nylon, can be expected to cause a slight dependence of $\delta$ on temperature. To a first approximation, we can expect $\delta$ to be a linear function of $T$:

$$\delta = \alpha + \beta T \tag{10}$$

When the experimental data are examined it will be seen that the precision is not sufficient to establish definitely the functional form of $\delta(T)$.

If we wish to consider the dependence of $t_B$ on $T$ at constant stress,[3] $f$, it is convenient to use Equation 10 to write Equation 1 in the form

$$\log_{10} t_B = \left\{ \log_{10} \frac{\gamma_B h}{\lambda k T} - 0.4343\left( \frac{\Delta S^*}{R} - \frac{f\beta}{2k} \right) \right\} + \frac{1}{T}\left\{ 0.4343\left( \frac{\Delta H^*}{R} - \frac{f\alpha}{2k} \right) \right\} \tag{11}$$

For practical purposes the first term in Equation 11 may be regarded as being independent of $T$. If we plot $\log_{10} t_B$ versus $1/T$ we should expect to get a straight line whose slope, when multiplied by 2.303, is

$$\frac{\Delta H^*}{R} = \frac{\Delta H^*}{R} - \frac{f\alpha}{2k} \tag{12}$$

This apparent enthalpy of activation $\Delta H^*$ depends on $f$, and cannot be regarded as a fundamental fiber property. To obtain $\Delta H^*$ from $\Delta H^*$, one must either know $\alpha$ precisely or one must calculate $\Delta H^*$ at several values of $f$ and extrapolate to zero $f$. But $\alpha$ is not known precisely (it is not even known whether or not $\delta$ is really a linear function of $T$), and the latter course of extrapolation is not feasible for those strong fibers for which human patience requires that measurements be restricted to a small range of relatively large values of $f$, lest one be forced to measure extraordinarily large values of $t_B$.

The above considerations have led the authors to suggest the following method of determining $\Delta H^*$, $\Delta S^*$, and the other fundamental strength parameters for a yarn in a given range of $T$:

1. Perform lifetime under dead load measurements at constant $T$, varying $f'$ so that a convenient range of $t_B$ is covered.
2. Determine the parameters $a$ and $b$ in Equation 6 by least squares analysis, assuming that the error in $f'$ is negligible compared to that in $\log_{10} t_B$.
3. Repeat steps 1 and 2 at different temperatures in the prescribed range of $T$. It will be noticed that the range in $f$ must be changed as $T$ is changed if $t_B$ is to be limited to conveniently measured values.
4. Measure the free shrinkage $S$ on going from room temperature to the values of $T$ under consideration.
5. Measure the elongation at break $E_B$ at each temperature, starting with relaxed yarn at that temperature. If $E_B$ is nearly independent of $f(t)$, this can be done using any convenient loading history.
6. Compute $\Delta F^*$ and $\delta$ at each temperature using Equations 7 and 8.
7. Plot $\Delta F^*$ versus $T$. If a reasonably good straight line is not obtained, a first or second order phase transition is indicated. If the plot appears linear, perform the least squares analysis suggested by Equation 9, thus obtaining $\Delta H^*$ and $\Delta S^*$.

The remainder of this paper contains a description of the application of steps 1 through 7 to 66 nylon.

## Experimental Details

The lifetime under dead load measurements were made in a nitrogen atmosphere whose temperature was controlled to within 0.1° C. The dead-loading curves (plots of $\log_{10} t_B$ versus $f$) were determined at the following temperatures in the order listed: 50.0, 75.0, 100.0, 125.0, 30.0, 65.0, 110.0, 50.0 (repeat), and 85.0° C.

The yarn tested came from a single pirn of 210 den. high tenacity bright nylon consisting of 34 continuous filaments. Prior to the tests, the yarn was transferred to a new pirn and in the process twisted to a total twist of 3.75 turns/in. It was

[3] Note that this does not correspond to constant $f'$ or constant total load $Wg$.

then stored in a nitrogen atmosphere at room temperature. When the first set of measurements at 50.0° C. was started, the yarn had been kept in nitrogen for one week. Throughout the entire period of this work, while samples were being tested, the remaining yarn was stored in nitrogen. The second run at 50.0° C. was started about three months after the first run at 50.0° C. was completed. The reasonably good agreement between the data obtained in the two experiments at the same temperature indicates that the pertinent physical properties of the yarn did not change appreciably while the intermediate tests were in progress. Denier measurements were made on the dry yarn periodically throughout the course of this work; all the results obtained were within the range 210.5 ± 1.

The dead load values were selected so as to cover the range $2.9 \leq \log_{10} t_B \leq 5.4$ with 45 ± 10 breaks.

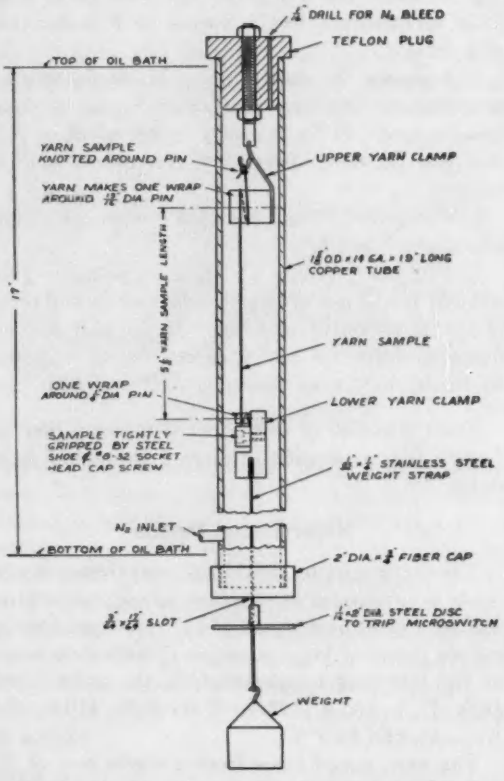
DRILL FOR N₂ BLEED
TEFLON PLUG
TOP OF OIL BATH
YARN SAMPLE KNOTTED AROUND PIN
UPPER YARN CLAMP
YARN MAKES ONE WRAP AROUND DIA. PIN
OD × 14 GA. × 19" LONG COPPER TUBE
19"
5" YARN SAMPLE LENGTH
YARN SAMPLE
ONE WRAP AROUND DIA. PIN
LOWER YARN CLAMP
SAMPLE TIGHTLY GRIPPED BY STEEL SHOE & 6-32 SOCKET HEAD CAP SCREW
STAINLESS STEEL WEIGHT STRAP
N₂ INLET
BOTTOM OF OIL BATH
2" DIA. FIBER CAP
SLOT
DIA. STEEL DISC TO TRIP MICROSWITCH
WEIGHT

**Fig. 1.** Diagram of contents of copper tube containing clamping assembly for lifetime under dead load measurements. Four such tubes, and the copper coils for the $N_2$ supply, were mounted in a large oil bath whose temperature was regulated to ±0.05° C.

The yarn samples were tested in groups of four, using electric timers to record the breaking times. The length of all the test samples was 14 cm.

A line drawing of the method of clamping is shown in Figure 1. The yarn and clamps were enclosed in a copper tube which was immersed in an oil bath; the oil bath contained four such tubes. The temperature of the oil bath was regulated to within 0.05° C. Dry Seaford nitrogen was passed through a copper coil immersed in the bath and thus brought into thermal equilibrium with the oil. A five-way tee at the bottom of the bath distributed the moving nitrogen equally into each of the copper tubes. A $\frac{1}{16}$-in. hole in the Teflon plugs at the top of the tubes insured a net upward flow of nitrogen. Thus, any air that may have gotten into the tubes during the clamping operation was quickly driven out. It will be noticed that the apparatus was designed to insure that both the atmosphere about the yarn (the nitrogen) and the wall of the immediate container (the copper tube) were at the same temperature.

About 5% of the time the yarn broke either at the steel pin surface of one of the clamps or within 0.25-in. of the surface (as measured on the relaxed yarn after fracture). When this occurred the data were rejected and the break repeated. If three such clamp breaks occurred consecutively at the same clamp, the pin surface was repolished. This always corrected the situation.

The measurements of the shrinkage and elongation used to prepare Table I were made in air. The values of $E_B$ are the average of Instron measurements at three rates of strain: 0.02, 0.10, and 0.60 minute$^{-1}$. No significant trend was found for the variation of $E_B$ with rate of strain at the temperatures studied. Prior to each measurement of $E_B$ the samples were allowed to shrink under zero load at the temperature listed until no further observable length changes occurred. Thus, the $E_B$ values were determined on samples which previously had been equilibrated with their environment.

## Discussion

Plots of $\log_{10} t_B$ versus $f'$ for the dead-loading experiments are shown in Figures 2 and 3. Each point represents a single break. It will be noticed that, within the precision of the data, Equation 6 is obeyed throughout the temperature range investigated. Values of $a$ and $b$ were calculated by the

method of least squares. The results are shown in Table II. The probable errors for $a$ and $b$ and standard errors of estimate are also listed. These data, when combined with the phenomenological relationships reported earlier [3], can be used for the precise estimation of safety limits in the design of textile components for use at elevated temperatures. The precision limits reported here for $a$ and $b$ are not due to experimental errors, but rather to the extreme sensitivity of the lifetime under dead load experiment to slight fluctuations in fiber properties. Tenacity measurements on the same yarn, if made with loads proportional to time, would show a much smaller relative statistical variation [2].

The data in Tables I and II were used, in conjunction with Equations 7 and 8, to compute the values of $\Delta F^*$ and $\delta$ listed in Table III. For these calculations it was assumed that for drawn dry nylon $\rho = 1.14$ g. cm.$^{-3}$ (approximately); this yields $9 \times 10^5 \rho g = 1.0_0 \times 10^9$. The value of $E_B$ at each $T$ was used as an estimate for $\gamma_B/\lambda$. When values of $E_B$ or $(1 - S)(1 + E_B)$ were not available at a particular temperature, they were obtained by linear interpolation of the neighboring values.

The calculated values of $\delta$ do not exhibit any systematic dependence on temperature. It appears that the best one can do with the values listed is to say that the mean value of $\delta$ for dry high tenacity

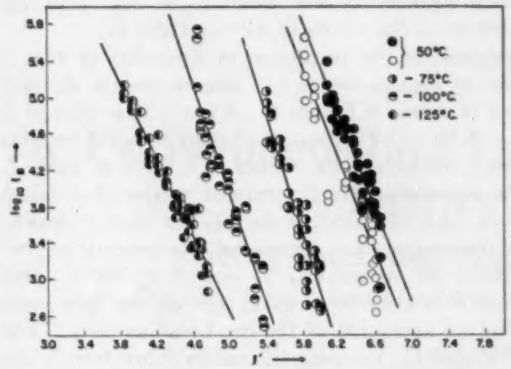


**Fig. 2.** Plot of experimental values of the logarithm of the lifetime in seconds versus the dead load in grams per denier. Deniers were measured at room temperature using the relaxed, unloaded yarn. Open circles are data for the first run at 50.0° C. Solid circles pertain to the second (and more reliable) run at 50.0° C.

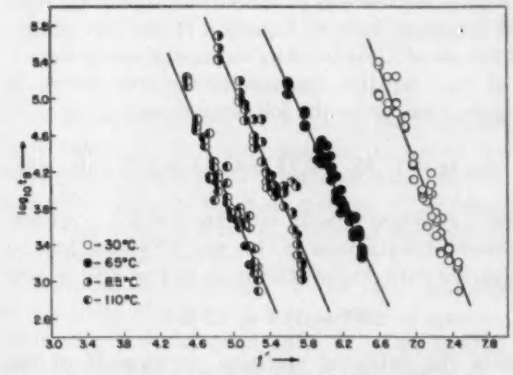


**Fig. 3.** Plot of experimental values of the logarithm of the lifetime in seconds versus the dead load in grams per denier.

**TABLE I. Values of $E_B$ and $(1 - S)(1 + E_B)$ for High Tenacity Bright Nylon with 3.75 Turns/In.**

| $T$, °C. | $E_B$ | $(1 - S)(1 + E_B)$ |
|---|---|---|
| 24 | $0.15_0$ | $1.14_5$ |
| 50 | $0.16_7$ | $1.14_6$ |
| 75 | $0.18_5$ | $1.14_8$ |
| 100 | $0.20_4$ | $1.14_7$ |
| 150 | $0.29_8$ | $1.19_1$ |

**TABLE II. Summary of Lifetime Under Dead Load Measurements**

(Assuming $\log_{10} t_B = a - bf'$; indicated limits are probable errors [5]; $\sigma$ is the standard error of estimate.)

| $T$, °C. | $a$ | $b$, den. g.$^{-1}$ | $\sigma$ |
|---|---|---|---|
| 30.0 | 22.57 ± 0.41 | 2.61 ± 0.06 | 0.167 |
| 50.0 | 20.46 ± 0.89 | 2.61 ± 0.14 | 0.347 |
| 50.0 | 21.15 ± 0.71 | 2.64 ± 0.11 | 0.204 |
| 65.0 | 17.74 ± 0.23 | 2.24 ± 0.04 | 0.091 |
| 75.0 | 23.51 ± 0.88 | 3.46 ± 0.15 | 0.266 |
| 85.0 | 17.34 ± 0.37 | 2.43 ± 0.07 | 0.180 |
| 100.0 | 19.06 ± 0.65 | 3.03 ± 0.13 | 0.285 |
| 110.0 | 16.03 ± 0.30 | 2.45 ± 0.06 | 0.154 |
| 125.0 | 13.06 ± 0.20 | 2.08 ± 0.05 | 0.138 |

**TABLE III. Free Energies of Activation and Displacement Volumes**

| $T$, °C. | $\Delta F^*$, kcal. | $\delta$, Å$^3 \times 10^3$ |
|---|---|---|
| 30.0 | $50._2$ | 4.4 |
| 50.0 | $50._3$ | 4.7 |
| 50.0 | $51._4$ | 4.7 |
| 65.0 | $48._5$ | 4.2 |
| 75.0 | $59._1$ | 6.7 |
| 85.0 | $50._6$ | 4.8 |
| 100.0 | $55._7$ | 6.3 |
| 110.0 | $51._9$ | 4.5 |
| 125.0 | $48._4$ | 4.7 |
| | Average = $51._8$ | Average = $5.0 \times 10^3$ |

bright nylon, in the temperature range 30–125° C., is ~500 Å³. If one, nevertheless, tries out Equation 10, a least squares analysis yields

$$\delta = 235 \pm 236 - T(0.770 \pm 0.67) \quad (13)$$

with a standard error of estimate of 88. In Equation 13, $\delta$ is in Å³ and $T$ in degrees Kelvin; the indicated limits for the linear parameters are probable errors.

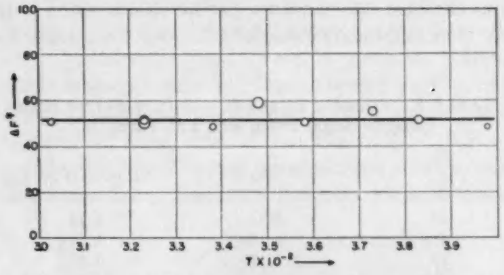


**Fig. 4.** Plot of $\Delta F^*$ in kcal. versus the thermodynamic temperature. The values of $\Delta F^*$ were calculated from the data shown in Figures 2 and 3, using Equation 7.

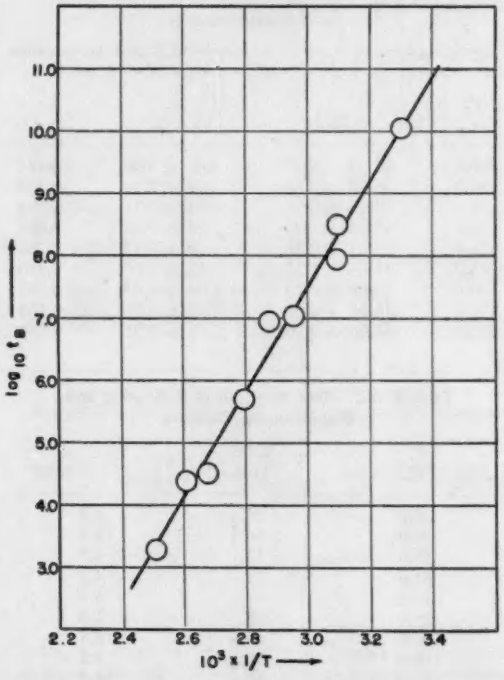


**Fig. 5.** Plot of the logarithm of the lifetime in seconds versus the reciprocal of the thermodynamic temperature, assuming $f = 5.5 \times 10^9$ dynes cm.$^{-2}$.

Figure 4 shows a plot of $\Delta F^*$ versus $T$ (in degrees Kelvin). The radii of the circles are equal to the probable errors in $\Delta F^*$ caused by the probable errors attributed to $a$ in Table I. It appears that throughout the range of $T$ studied, $\Delta F^*$ is a constant. Indeed, a least squares calculation has given for Equation 9:

$$\Delta F^* = 48.6 \pm 10.0 + T(0.0091 \pm 0.028) \quad (14)$$

Here, $\Delta F^*$ is in kcal. and $T$ in degrees Kelvin; the indicated limits are probable errors. The standard error of estimate for Equation 14 was 3.72. Thus, we have as our best estimates, $\Delta H^* = 48.6 \pm 10$ kcal. and $\Delta S^* = -9 \pm 30$ eu. (cal. deg.$^{-1}$). We conclude that for 66 nylon $\Delta S^*$ makes a negligible contribution to $\Delta F^*$. This explains the approximate equality of our estimate of $\Delta H^*$ and the average of the values of $\Delta F^*$ in Table II.

A test of the prediction of Equation 11 that a plot of $\log_{10} t_B$ versus $1/T$ should yield a straight line is shown in Figure 5. A particular value of $f$, $f = 5.50 \times 10^9$ dynes cm.$^{-2}$, was selected for this test. At each of the values of $T$ listed in Table I, the experimentally determined values of $a$ and $b$ were used to calculate $\log_{10} t_B$ for that $f'$ which, at the temperature considered, corresponds to $f = 5.50 \times 10^9$ dynes cm.$^{-2}$. For $T \geq 100°$ C. this method of obtaining $\log_{10} t_B$ represented little more than an averaging of the dead-loading data. For $T < 100°$ C., however, the values $f'$ involved in the calculations were outside of the ranges investigated in the experiments (see Figures 2 and 3); thus, for these cases, the values plotted in Figure 5 represent extrapolations which assume the validity of Equation 6. The straight line obtained in Figure 5 covers seven decades in time; thus it confirms both the functional form of Equation 11 and the validity of the use of Equation 6 for extrapolations to large $t$.

A least squares analysis of the plot shown in Figure 5 has given the following result:

$$\log_{10} t_B = 17.85 \pm 0.75 + (8.45 \pm 0.26)\frac{10^3}{T} \quad (15)$$

with a standard error of estimate of 0.281. A comparison of Equations 15, 11, and 12 yields, for the apparent enthalpy of activation at $f = 5.50 \times 10^9$:

$$\Delta H^* = 38.7 \pm 1.2 \text{ kcal.}$$

where the indicated precision corresponds to the probable error shown for the coefficient of $1/T$ in Equation 15. If we add to $\Delta H^*$ the contribution

of the second term on the right in Equation 12, assuming that $\alpha \sim 235$, we obtain $48 \pm 11$ kcal. as an estimate for $\Delta H^*$. The large probable error in $\alpha$ contributes over 9 kcal. to the error associated with the value of $48 \pm 11$ kcal. for $\Delta H^*$. This second estimate for $\Delta H^*$ is in very good agreement with the value of $49 \pm 10$ kcal. obtained from Equations 9 and 14. Arguments given earlier in this paper indicate that the estimate for $\Delta H^*$ obtained from Equations 9 and 14 should be superior to that based on $\Delta H^*$ and Equation 12. Considering the spread in the raw data and the heuristic nature of the assumptions involved in the two calculations (such as the use of Equation 10 and the identification of $\gamma_B/\lambda$ with $E_B$), the very close agreement obtained is probably partly fortuitous.

**Acknowledgment**

The authors are grateful to Mrs. Nancy W. Seitz for assistance in the numerical calculations presented here.

**Literature Cited**

1. Coleman, B. D., *J. Polymer Sci.* **20**, 447–455 (1956).
2. Coleman, B. D., *J. Appl. Phys.* **27**, 862–866 (1956); *ibid.* **28**, 1058–1064 (1957).
3. Coleman, B. D. and Knox, A. G., TEXTILE RESEARCH JOURNAL **27**, 393–399 (1957).
4. Illingworth, J. W. and Kilby, W. F., TEXTILE RESEARCH JOURNAL **26**, 243–254 (1956).
5. Margenau, H. and Murphy, G. M., *The Mathematics of Physics and Chemistry*, D. Van Nostrand, New York, 493–502 (1943).

*Manuscript received November 14, 1957.*

# A Two-Dimensional Load-Extension Tester for Fabrics and Film

**P. B. Checkland, T. H. Bull, and E. J. Bakker**

*Imperial Chemical Industries Limited, Fibres Division, Harrogate, Yorkshire*

**Abstract**

Fabrics in use are rarely subjected to extensions in only one direction, though fabric load–extension testing is normally done in this way. A two-dimensional tester has been constructed with which load–extension curves for both weft and warp directions (or any other mutually perpendicular directions) are recorded simultaneously. The internal strain within the homogeneously strained portion at the center of the fabric is also recorded. The instrument is suitable for making measurements on both knitted and woven fabrics and on plastic film.

## Introduction

The determination of the breaking load and ultimate extension of fabrics and the nature of the load–extension curve provide useful information concerning the quality of the basic material of the fabric and give guidance as to the suitability of the material for any particular end use.

The normal determination of the load–extension characteristics of a fabric consists either of tests on a constant rate of extension tester (e.g., the Instron Tensile Tester) or a constant rate of load tester (e.g., the Scott Inclined Plane Strength Tester). These methods usually consist of tests in either the warp or weft directions of the fabric, or both, but not in warp and weft directions simultaneously. In actual service, fabrics are rarely subjected to an unrestricted extension in one direction. In some particular application a load applied in, say, the warp direction of a fabric may induce a considerable load in the weft direction if the weft threads are restricted at some arbitrary boundary. As a result of such restraints, a considerable cross-straining is set up in the fabric and the warp appears to be considerably stiffer, in the sense that the load–extension curve has an increased slope compared with that determined in a one-dimensional test.

In order to investigate the effects of cross-straining in both woven and knitted fabrics, an apparatus has been constructed which permits the determination of the dynamic load–extension curve of a fabric in two mutually perpendicular directions simultaneously.

Multidirectional test devices (mainly for rubberlike materials) have been developed by Ariano [2], Anderson [1], Boonstra [3], and Treloar [5]. A two-dimensional load–extension tester for woven fabrics has been described by Reichardt, Woo, and Montgomery [4] and used in an investigation of mechanical properties of formaldehyde-treated cellulosic fabrics by Woo, Dillon, and Dusenbury [6]. Their tester consists of a modification to the Instron Tensile Tester in the form of an additional pair of fabric grips plus a strain-sensing element. The strain-measuring device indicates the strain in the homogeneously strained region of the fabric as a function of the dynamically varying load. The disadvantage of this tester is that there is no simultaneous measurement of warp and weft loads and warp and weft strains; also, the strain is indicated over a very limited region.

The apparatus described overcomes the limitation of the tester mentioned above and may be used for the two-dimensional testing of knitted and woven fabrics, rubberlike materials, and plastic films.

## Apparatus

### *Two-Dimensional Straining Device*

The straining device consists of a Pratt 24-in. four-jaw self-centering lathe chuck. The fabric is gripped between special jaws attached to the original chuck jaws. The chuck is mounted horizontally on a rigid table and is driven at a constant speed by a ¼-h.p. motor suspended beneath the chuck. The linear speed of each fabric grip is 1 in./min. A plan of the straining device is shown in Figure 1.

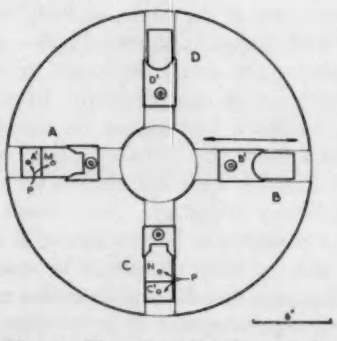


**Fig. 1.** Plan view of straining device.

Blocks D and B, which contain the fabric grips $D^1$ and $B^1$, are moved either outwards or inwards by the motion of the chuck scroll. Blocks A and C are divided into two parts. Parts $A^1$ and $C^1$ are driven by the scroll. Parts M and N, which actually contain the fabric grips, slide freely in grooves in the chuck bed and are linked to $A^1$ and $C^1$ respectively by two Langham Thompson dynamometers of either 200-lb. or 500-lb. maximum load, which fit on metal pegs P. Figure 2 shows a side view of one of the jaws which carries a dynamometer.

Thus, when a fabric is extended between the four jaws, the loads in the fabric in mutually perpendicular directions are transmitted to and registered by the dynamometers.

The fabric is gripped between two flat surfaces Q and R (Figure 2), each 2 in. × 1½ in. The fixed surface Q is of plasticized PVC, while R is of hardened steel. R is forced onto Q by the screw V, the shaft of which is in two parts. These are connected by a collar of nylon polymer in order to lessen the very real possibility of producing a spurious load signal by overtightening the grips, with consequent deformation of the chuck jaws.

The movement of the jaws is limited by two microswitches fixed at the limit of their traverse. When closed the microswitches cut off the power to the driving motor. The full limit of traverse of each jaw is 9 in., and the distance of nearest approach of opposite jaws is 3.75 in.

### *The Dynamometers*

The dynamometers are made by J. Langham Thompson Ltd. Each comprises a ring of beryllium copper with four active resistive elements cemented on the inner surface at opposite ends of longitudinal and transverse diameters. The load is applied by means of diametrically opposite lugs, which make a good sliding fit on the metal pegs on the chuck jaws.

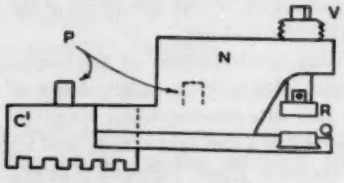


**Fig. 2.** Side view of Jaw C.

The resistive elements are connected to form a Wheatstone Bridge, the output of which can be fed directly to an indicating meter. Sensitivities of the 200-lb. and 500-lb. dynamometers are 0.015 mV/applied volt/lb. and 0.006 mV/applied volt/lb. respectively.

*Load Indication*

The outputs of the dynamometers are recorded separately on Honeywell-Brown Electronik strip recorders having a full scale deflection of 10 mV. The input voltage for the dynamometers is provided by a series of Nife cells, the appropriate voltage being selected by a rotary switch. A variable resistor is placed across one arm of the bridge; it is used to balance out any signal from the dynamometer at zero load or to give any required arbitrary zero setting.

The dynamometers were calibrated both statically and dynamically. For static calibration the dynamometer was suspended vertically and loaded successively with known loads, the output for a given load and input voltage being recorded on the strip-chart recorder. The output was also recorded during unloading. The loading and unloading curves were identical and linear.

For dynamic calibration the dynamometers were fixed in special constructed links between the upper jaw and crosshead of the Instron Tensile Tester. A load was impressed upon the dynamometer by movement of the crosshead, this load being recorded on the Instron recorder. The dynamometer output was fed to a Honeywell-Brown recorder and compared with the Instron record. This procedure allowed a greater load range to be covered than did static loading. Where the load ranges overlapped, static and dynamic calibration curves were found to be identical. Figure 3 shows the calibration curves for one of the dynamometers. The curves are identical and linear during both loading and unloading up to the maximum loading claimed by the manufacturer.

*Measurement of Strain*

A photographic technique is used for measuring the strain in the fabric or film during loading. A camera is supported over the center of the chuck on a rigid stand. It is focused on a series of grid lines on the specimen under test. As this is extended, a series of exposures can be taken of the displacements of the grid lines at any instant. The camera, an electrically controlled one made by Shackman and Sons, permits a series of exposures to be made in rapid succession, the depression of the control key opening the camera shutter and then transporting the film for the next exposure after the first exposure has been completed. The camera takes 20 ft. of 35-mm. film, providing 200 1 × 1-in. exposures without reloading.

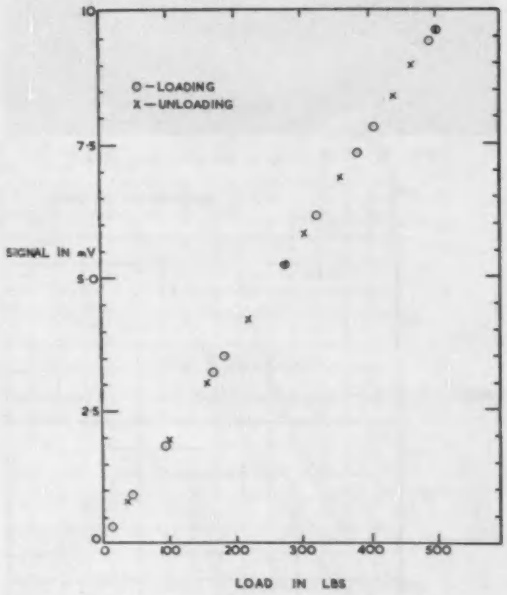


**Fig. 3.** Dynamic calibration curve.

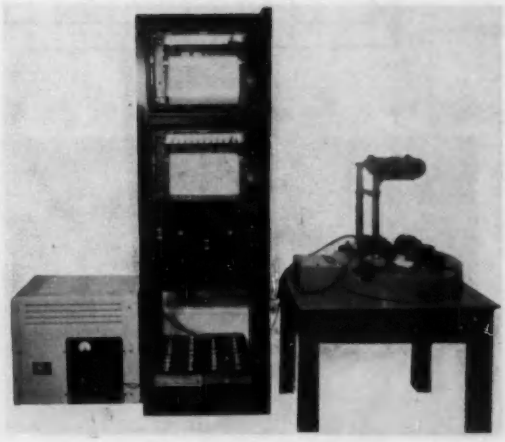

**Fig. 4.** The complete instrument.

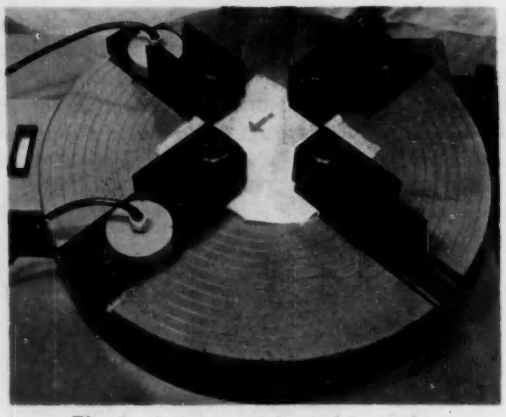

Fig. 5. A close-up of the straining device.

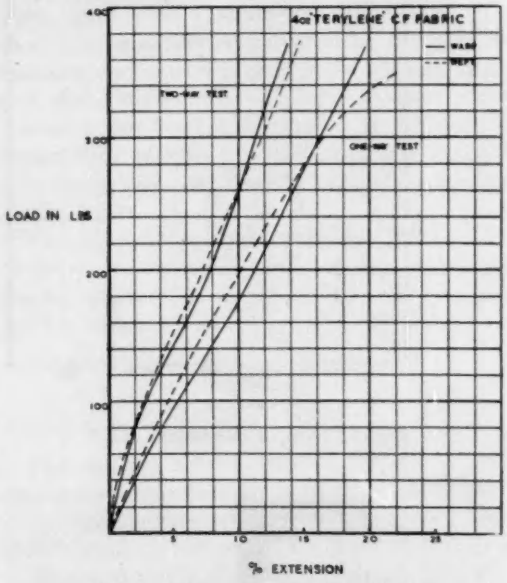


Fig. 6. Test results, Terylene fabric.

Grid lines may easily be drawn on film specimens. The method of putting grid lines on the fabrics depends upon the fabric construction and the warp and weft yarn deniers. The grid lines may be drawn upon the fabric or put in in the form of contrasting threads. To obtain a good contrast between the grid lines and the fabrics (most of which are usually white or off-white) bright red grid lines can be used in conjunction with an orthochromatic recording film. The specimen is given top illumination from a single photoflood bulb and reflector at about 2 ft.

To determine loads in mutually perpendicular directions at the instant each photograph is taken, an additional pen is attached to each recorder, each pen being attached to the moving core of a miniature solenoid. On depressing the key of the camera control unit, an electrical pulse actuates a relay in each solenoid circuit. This results in the application of a short voltage pulse to the solenoid, the spring-loaded core of which drives the pen a short distance across the chart. The extra pens are fixed at the high-reading side of the chart, hence do not interfere with the normal pen of the recorder. Figure 4 shows the complete instrument; Figure 5 shows a close-up of the straining device.

## Typical Results

Figure 6 shows load–extension curves for a 4-oz. plain weave Terylene fabric made from continuous filament yarn. In both cases the fabric weft is stiffer than the warp except at high extensions, and the effect of cross-straining is apparent in the displacement of the "two-way" curve.

Figure 7 shows three typical photographs taken during the testing of a fabric woven from woolen-spun yarn. Figure 7a shows the unstrained fabric.

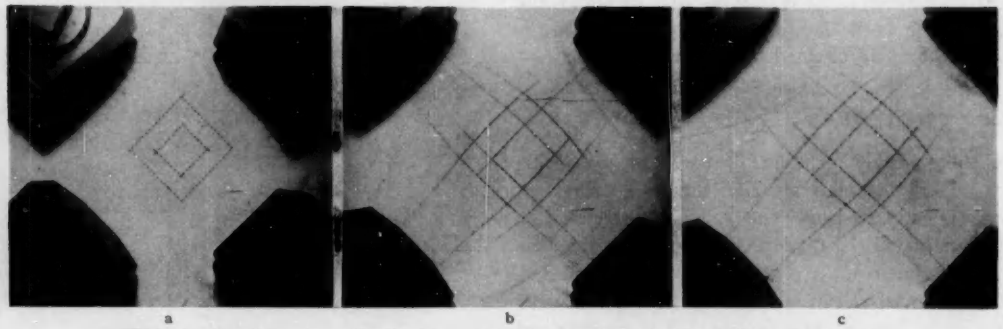


Fig. 7. (a) Unstrained fabric; (b) strained fabric; (c) fabric just before the break.

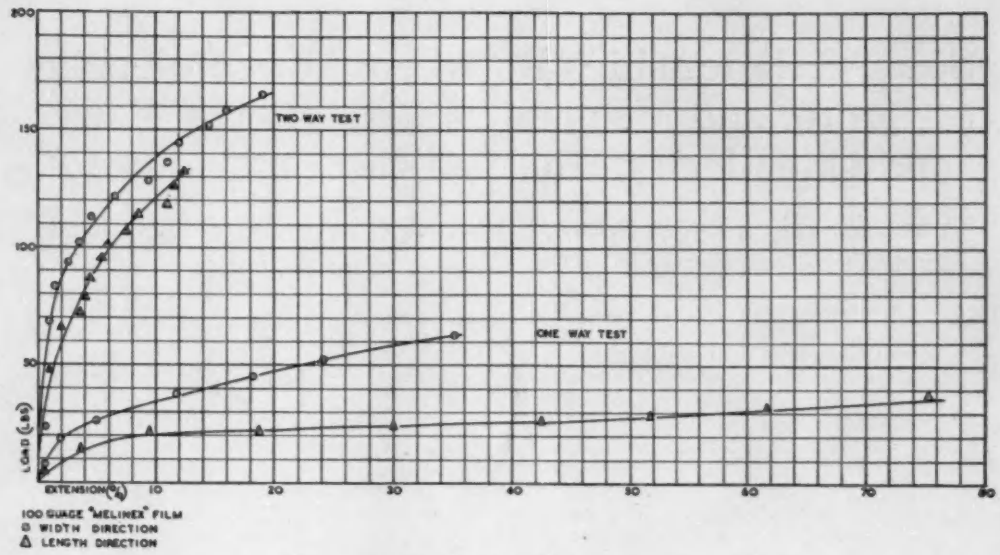


**Fig. 8.** Test results, Melinex film.

In this case the grid lines were put in with red sewing thread. The photographs of the strained fabric show clearly the heterogeneity of the strain pattern across the fabric, only a central portion being homogeneously strained.

Figure 8 shows load–extension curves obtained during the two-dimensional stretching of a plastic film. Comparison of these curves with those obtained under one-dimensional stretching shows very clearly the large extent to which "waisting" of the film inhibits the rise in load during extension.

## Literature Cited

1. Anderson, S. L., *J. Sci. Instruments* **24**, 25 (1947).
2. Ariano, R., *Rubber Chem. and Technol.* **13**, 92 (1942).
3. Boonstra, B. B. S. T., *J. Appl. Phys.* **21**, 1098 (1950).
4. Reichardt, C. H., Woo, H. K., and Montgomery, D. J., Textile Research Journal **23**, 424 (1953).
5. Treloar, L. R. G., *Trans. Faraday Soc.* **46**, 783 (1950).
6. Woo, H. K., Dillon, J. H., and Dusenbury, J. H., Textile Research Journal **26**, 761 (1956).

*Manuscript received November 20, 1957.*

# Some Relationships Between Supermolecular Structure and Mechanical Behavior of Native and Chemically Modified Cotton Cellulose[1]

**Verne W. Tripp, Rollin S. Orr, Hilda M. Ziifle, and Carl M. Conrad**

*Southern Regional Research Laboratory,[2] New Orleans, Louisiana*

**Abstract**

Cotton fibers are constructed principally of macromolecules of cellulose. These are disposed in the fiber in such a way as to display a number of aspects, which collectively may be referred to as the "supermolecular structure." It includes such features as molecular chain length, polymolecularity, natural cross-linkage, crystallinity, crystal modification, crystallite size, orientation, accessibility, and chemical modification. Superimposed on these structural aspects is the gross morphology of the fiber itself. Many of these aspects have an influence in one way or another upon the response which the fiber makes when subjected to a variety of mechanical forces, which collectively may be referred to as "mechanical behavior." Among the responses considered are strength, elongation, stiffness, toughness, elasticity, and resilience. Selected examples are presented, showing how the mechanical behavior is conditioned in various ways by the supermolecular structure.

THE mechanical behavior of the cotton fiber is considered to express the supermolecular structure of which it is composed. Mechanical behavior, of course, refers to the response of the fibers and their products when subjected to any one of a variety of forces. By supermolecular structure is meant the physical arrangement resulting from the multiform association and organization of molecules in the fiber. Thus, supermolecular structure, as used in the present report, is not limited to the macromolecular structure of Staudinger [36] or to the so-called fine structure, which, as Ranby [25] explains, represents the microscopical morphology discernible between the lower limits of optical and electron microscopic resolution (2500 and 30Å) but includes the entire range of morphology. The gross structure of the fiber itself plays an important part in determining fiber properties and is also considered.

A considerable number of the important textile properties of cotton are influenced by mechanical forces; some only slightly, others more extensively. Some of the more important of these, although by no means all, are listed below. Some of these basic properties have different important subdivisions. Several of the properties are especially important in mechanical fabrics. Others are important in apparel and household fabrics. The six properties considered include strength, elongation, stiffness, toughness, elasticity, and resilience. As Smith [34] has pointed out, these mechanical properties in textiles, like those of other engineering materials, are basic, and all other mechanical properties, such as creep, drapeability, flex endurance, crease recovery, abrasion resistance, etc., can be related to one or more of these six.

## Some Structural Features Responsible for Mechanical Behavior of Cotton Fibers

The macromolecular structural features responsible for the peculiar behavior of cotton when subjected to mechanical forces is a subject which has received much attention in recent years and even yet is only partially explored. The structural factors given below, although not a complete list, are believed to be important.

The gross morphology of cotton, which refers to the relatively large structural elements visible in the

[1] Presented at the 132nd Meeting of the American Chemical Society, New York, New York, September 8–13, 1957.

[2] One of the laboratories of the Southern Utilization Research and Development Division, Agricultural Research Service, U. S. Department of Agriculture.

fiber by microscopy, undoubtedly plays an important role in determining the mechanical properties of the fiber. In nearly every part of the fiber this structure is characterized by an ordered microfibrillate texture (Figure 1), giving rise to pores, channels, and cavities through which vapors and liquids can move. The arrangement of fibrils in the fiber follows a spiral pattern, in which reversals are frequent. It is marked by structurally weak points [8, 43]. This arrangement of fibrillate bodies thus is superimposed upon and contains the other structural features present in cotton.

Molecular chain length in undegraded cotton cellulose probably averages 5,000 anhydroglucose units (DP) or more. The molecular weight may exceed 1,000,000. By action of various degradative agents, this chain length decreases progressively to lower values. In strong mineral acid the chain length decreases in a few minutes to about 220 anhydroglucose units, and thereafter hydrolyzes only very slowly to the oligosaccharides and to glucose.

Polymolecularity or variability of molecular weight of cellulose is normally expressed in terms of degree of polymerization, or some function of it. In undegraded cotton cellulose the chain length is normally most uniform and becomes less uniform as degradation or depolymerization takes place.

Cross-linkage in native cellulose is considered to be due to hydrogen bonding [24, Vol. 1, p. 230] through the hydroxyl groups and to van der Waals forces along the macromolecules. In the crystalline regions bonding is highly regular, to such an extent that the unit cell can be determined easily with the aid of X-ray diffraction. In the poorly crystallized or noncrystalline regions, on the other hand, the bonding is considered to be more or less sparse and random. Van der Waals forces are considered to cross-link along the chains perpendicular to the glucose rings.

Crystallinity, which is often referred to as lateral order, represents the state of arrangement of the macromolecules in many parts of the cellulose microstructure. The order of arrangement in the crystalline regions (crystallites or micelles) is considered to be equal to the order in crystals of small molecules, but due to the linear nature of the macromolecules and their intermingling, crystallization of the cellulose can never be very complete. Degree of crystallinity is commonly used to indicate the proportion of the cellulose by weight which is arranged in regular lattice structure.

Cotton in the native state appears to be remarkably uniform in the degree to which its cellulose chains are organized laterally. With few exceptions, neither species nor variety shows characteristic variation of this structural parameter. Significant reduction of the crystalline component of cotton may be accomplished in a number of ways.

Crystal modification or polymorphism of cotton cellulose is represented by at least four forms, identified as celluloses I, II, III, and IV. All native cellulose is in the I modification, with the possible exception of the marine plant *Halicystis*, in which II has been reported to occur [24, Vol. 1, p. 236]. Cellulose II, often called hydrate cellulose or regenerated cellulose, is produced in the process of mercerization by a rearrangement of the space lattice of native cellulose. Cellulose III is formed from native cellulose by treatment with liquid ammonia or ethylamine [30] followed by evaporative removal of the liquid. Cellulose IV can be prepared [14] from cellulose III by heating the latter in glycerine to 250° C.

The crystallite size, i.e., size of the crystalline regions in cellulose, is still in a rather unsatisfactory state of elucidation. Since cellulose macromolecules from beginning to end presumably pass through many crystalline regions, it is obvious that the latter can have no clearly demarked surface, at least at the ends, in the sense of conventional macrocrystals.

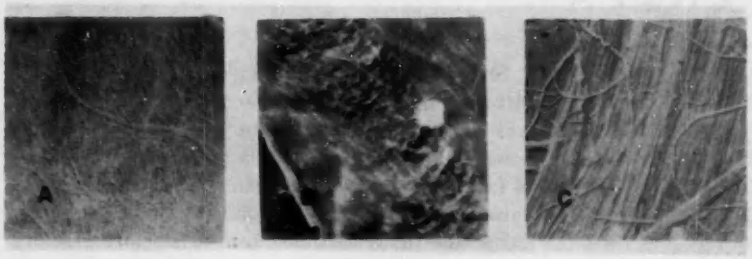


**Fig. 1.** Gross structure of cotton fiber cell wall. (A) Primary wall; (B) winding layer; (C) secondary wall. Distance between marks in each electron micrograph is 1μ.

From X-ray diffraction, electron microscope, and acid hydrolysis studies it is concluded [24, Vol. 1, pp. 255 *et seq.*] that the crystalline regions in native cellulose are roughly 1500 Å long and perhaps 40 × 50 Å in cross section.

The orientation of crystallites, sometimes referred to as the "X-ray angle," is well established and easily determined by X-ray [4] and other means. In cotton cellulose the azimuthal angle of half maximum intensity about the 002 band varies from about 20 to 45° [1, 4]. Most of this is due to the spiral arrangements of the fibrils. The orientation is highly dependent on variety of cotton and conditions of growth. In certain other natural cellulosic fibers such as flax, ramie, and hemp, according to Morey [21] the orientation deviates only a few degrees if at all from the fiber axis. As will be shown below, orientation in cotton is highly correlated with strength.

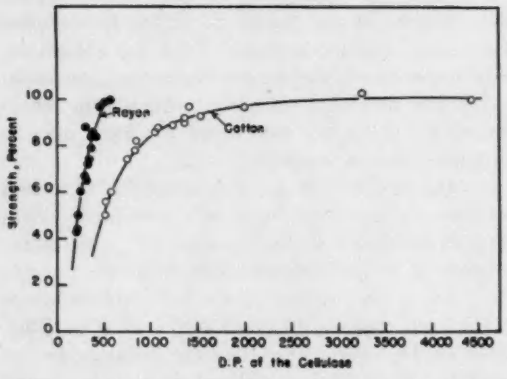


**Fig. 2.** Relation between relative strength retained after heat degradation of cotton and rayon tire cords and degree of polymerization.

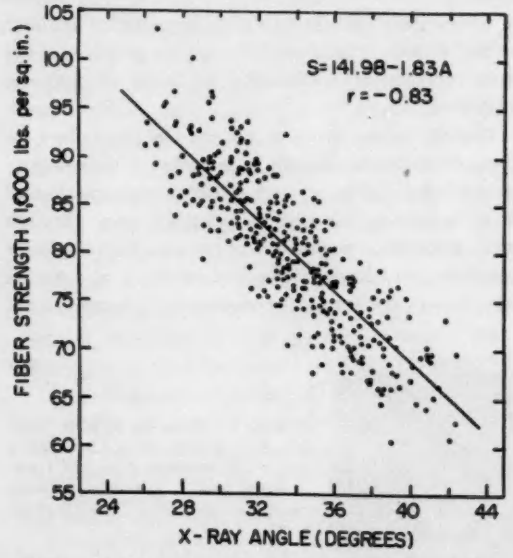


**Fig. 3.** Relation of cotton fiber strength and crystallite orientation; Berkley et al. [1].

Accessibility is often confused with the converse of crystallinity, but it is very distinct in a number of ways. Actually, accessibility refers to the availability of macromolecules to participate in chemical reactions. A polycrystalline aggregate, containing no amorphous material, still could display a large amount of accessibility, depending on the total amount of available crystal surfaces. Accessibility depends, too, on the nature of the reactant in question. Small molecular reactants often will disclose much more accessibility than will larger molecular reactants. In cellulose the accessible regions are considered to include most, if not all, of the amorphous cellulose plus the lateral surfaces of the crystalline regions.

Chemical modification of cotton cellulose has considerable effect on mechanical properties. Under chemical modification may be included such modifications as partial acetylation, partial carboxymethylation, partial cyanoethylation, partial methylation and ethylation, and many other esterifications, etherifications, and hydroxyl replacement reactions. In all cases the degree of substitution (DS) may be slight, moderate, or extensive.

## Fiber Properties Responsive to Mechanical Forces

Various properties of cotton fiber respond in one way or another to mechanical forces due to the supermolecular structure of the fiber. It will be the purpose of this section to deal with a number of specific cases, indicating in each case what important features of the structure are probably involved and in what way.

### *Strength*

Strength is commonly thought of as the maximum force per unit area of cross section which a material will support without rupture. In textile materials, however, it is customary to express strength in terms of force per unit of linear density. In this form, as tenacity, it represents the number of unit lengths of the textile material which can be supported before

rupture. Strength is related to a number of supermolecular structural factors, but especially to molecular chain length and orientation.

Gross morphology may be expected to affect tenacity to the extent that fibril alignment deviates from the fiber axis, and that the voids and pore system permit distribution of forces during unloading. The effects of spiral reversals in the fibril system of cotton have been stressed recently by Wakeham and Spicer [43].

The effects of molecular chain length have been deduced almost entirely from the results of heterogeneous degradation studies, and as such may not give a valid picture of the relationships involved. Thus, Staudinger and Jurisch [37] report that the strength of cotton cellulose whose chain length has been reduced by oxidative and hydrolytic treatments decreases almost imperceptibly from DP 3000 to about DP 1000, then rapidly to about DP 200, below which it is lost entirely. Similar results were observed by Conrad et al. [3]. Regenerated celluloses go through similar changes in tenacity at the lower DP range, but do not display the prominent intermediate DP range where strength is only slightly affected.

According to Sookne and Harris [35] little increase in the strength of cellulose acetate films occurs above DP 150. Flory [6] has shown that if the tensile strength data of Sookne and Harris are plotted against the reciprocal of the number average DP, a straight line results. Hermans [10, p. 491] also has demonstrated that the tenacity of viscose filaments produced under comparable conditions increases with DP of the cellulose.

The relation between DP and retention of strength of cotton and rayon tire cords subjected to heat degradation is shown in Figure 2. It is seen that the curves of cotton and rayon do not overlay, i.e., do not fall on different ends of the same curve.

It has been shown by Conrad et al. [3] in a study of degradation of cotton tire cords by heat that as little as 0.3% of the total primary bonds between anhydroglucose units need be ruptured under typical degrading conditions for all sensible tenacity to be lost and that the residual strength is an exponential function of the number of bonds broken. Orr et al. [23] found a similar relationship for the strength of cotton yarns and fibers degraded by heat.

The relation of strength to polymolecularity of cotton cellulose is quite unknown. It is often assumed that high polydispersity is unfavorable to high strength, especially when considerable proportions of low polymeric components are present [15, 35]. However, Scherer and McNeer [28] recently have found contradictory results in the case of certain cellulose derivatives.

Natural cross-linkage undoubtedly plays some part in cotton cellulose tenacity. In the crystalline regions the hydrogen bonding and van der Waals forces presumably are sufficient to prevent completely any slippage of chains. However, due to the noncontinuous nature of the crystalline regions, tenacity must be principally dependent on primary valence bonds and on some cross-linkage existing in the amorphous areas. Additional cross-linking achieved by chemical modification usually causes severe reduction of tenacity, probably because the cellulose chains are no longer free to move and thus to relieve imposed stress. This will be discussed further in connection with chemical modification.

The effect of degree of crystallinity on tenacity has been mentioned above under cross-linking because of the nature of the crystallizing forces involved. In cotton, these effects are not readily demonstrated and are largely deduced from theoretical considerations. It was observed by Susich [38] that reduction of the crystallinity of a 20s ($30 \times 1$ tex) cotton yarn from 90 to 30%, approximately, by amine treatment resulted in an increase of tenacity from 14.7 to 15.3 g./tex. The crystal modification was unchanged. If crystalline regions are actually a discontinuous phase, it is quite possible that crystallinity has little or no effect on tensile strength.

Orientation of crystallites is one of the more important supermolecular factors in determining cotton fiber strength. The relationship between strength and orientation, in terms of X-ray angle, is shown in Figure 3, taken from a paper by Berkley et al. [1]. Similar results were observed by Rebenfeld and Virgin [26]. The low orientation in cotton as compared to many other cellulosic fibers is due principally to the spiral angle which the fibrils in cotton make with respect to the fiber axis.

Little is known of the influence of crystal modification or crystallite size on tenacity as such. But the effects of these structural parameters, as well as degree of crystallinity and accessibility, appear important in determining the rate of strength loss in degradation. It is a frequently observed phenomenon

that different celluloses exhibit varying rates of strength loss under similar conditions of degradation. A cellulose whose molecular chains are more accessible to the attacking reagent will suffer more frequent chain scission. Thus, Conrad et al. [3] found that when cotton and rayon were heated for equivalent periods, only 0.12% of the links in cotton were destroyed, while 0.24% of those in rayon were broken. However, under these conditions, the cotton lost 30% of its strength and the rayon 40%. Sippel [32, 33], in considering the effects of photolysis on the strength of manmade polymers, also has attacked this problem. He has shown that the logarithm of the tenacity is linearly related to the reciprocal of the DP of the degraded polymer. It can be shown that the strength retained by a fiber element when a given fraction of the bonds has been broken is inversely proportional to the distance between centers of regions of high lateral order. This may be expressed approximately by the following equation:

$$T = T_0 e^{-BL}$$

in which $T$ and $T_0$ are the tenacities at any given time and at zero time, respectively, $B$ is the fraction of total bonds broken, and $L$ is the average distance between crystallite centers. This equation may be tested empirically by noting strength losses at equivalent bond breakages for celluloses whose lateral order distribution is known. Table I presents strength and DP data on a number of cellulosic fibers which have been degraded by various means, together with values of $L$ calculated from the above equation. The fraction of bonds broken, $B$, was calculated from the relation

$$B = 1/P_t - 1/P_0$$

where $P_0$ and $P_t$ are the DP of the original cellulose and the degraded cellulose respectively.

Table I shows that the four fiber types examined fall into two groups. Cotton and ramie underwent strength losses of 25–50% when the fraction of bonds broken ranged from 0.06% to 0.10%. Mercerized cotton and viscose rayon, on the other hand, lost 25–40% of their tenacity when 0.15–0.25% of their

**TABLE I. Molecular Properties, Breaking Strength, and Distance $L$ Between Crystallite Centers of Celluloses Degraded in Various Ways**

| Fiber and means of degradation | Degree of polymerization (viscosity) | Bonds broken, % of original | Breaking strength, % of original | $L$, from equation (DP) | Approximate leveling-off DP by acid hydrolysis |
|---|---|---|---|---|---|
| Cotton fibers, hydrolyzed | 5200 | 0.000 | 100 | — | 220 |
| Same | 1060 | 0.075 | 65 | 580 | |
| Same | 850 | 0.100 | 59 | 520 | |
| Cotton cord, hydrolyzed | 4700 | 0.000 | 100 | — | 220 |
| Same | 1170 | 0.064 | 67 | 620 | |
| Same | 1050 | 0.074 | 55 | 810 | |
| Cotton yarn, heated 150–160° C. | 5000 | 0.000 | 100 | — | 220 |
| Same | 1200 | 0.060 | 69 | 620 | |
| Same | 850 | 0.100 | 50 | 690 | |
| Ramie fibers, hydrolyzed | 2700 | 0.000 | 100 | — | 230 |
| Same | 880 | 0.077 | 76 | 360 | |
| Same | 740 | 0.098 | 67 | 410 | |
| Mercerized cotton, hydrolyzed | 5000 | 0.000 | 100 | — | 150 |
| Same | 560 | 0.159 | 75 | 180 | |
| Same | 400 | 0.230 | 61 | 220 | |
| Viscose filaments, hydrolyzed | 450 | 0.000 | 100 | — | 60 |
| Same | 270 | 0.148 | 74 | 220 | |
| Same | 210 | 0.255 | 61 | 195 | |

bonds were broken. The calculated values of $L$ are about 700 DP for cotton, 385 for ramie, and 200 for the cellulose II fibers. These results indicate that the frequency of successive regions of high lateral order is greatest for mercerized cotton and viscose. Table I also lists the approximate crystallite lengths derived from measurements of the "leveling-off DP" in acid hydrolysis. While the values of $L$ differ from the crystallite lengths by factors of 2 or more, there is general parallelism between the results for each fiber type.

Insofar as degradation affects loss of strength, it is obvious that a cellulose which has more frequent, i.e., small, regions of high lateral order will be superior to one which has relatively few, large crystallites. Mercerization of cotton apparently accomplishes this effect. However, the advantage is gained at a cost of increasing the rate of bond breakage significantly. How these two parameters of structure, accessibility and crystallite size, which are mutually opposed in this respect, may be controlled to best advantage is not yet known.

Chemical modification of cotton appears to have diverse effects on tenacity. The esterification of cotton with acetic anhydride at lower degrees of substitution lowers the tenacity of fibers and yarns. This effect is shown in Figure 4, where tenacity is plotted against acetyl content of partially acetylated cottons of three varieties. The loss of strength noted at low DS does not continue as acetylation proceeds, and at DS 1.0 and higher the trend is reversed. As Honold et al. [12] have shown, breaking strength increases above that of the unacetylated cotton at DS 1.5. The loss of strength at low DS may arise from several sources. Since moisture regain is reduced as acetylation proceeds, the loss of tenacity noted may be similar to that observed when cotton is stressed in drier atmospheres. The effect of humidity on the strength of acetylated cotton is shown in Figure 5, where the tenacity of a cotton of DS 0.6 at 81% RH is higher than that at 65% RH and even equal to that of unacetylated cotton at 65% RH. A second factor, according to Tripp et al. [41], which enters into consideration of the decrease of tenacity at low DS is the observed nonuniformity of extent of reaction at the fiber level. Inequalities of composition of the partial esters formed would lead to poor stress distribution and lower breaking strength. An additional point which deserves mention in connection with the effects of derivative formation on strength is the reduction of the number of regions of inherently poor stress distribution by swelling during reaction. Another consideration of importance is the distribution of the substituent groups in the derivative. As Reeves et al. [27] have shown, methylation with ethereal diazomethane and with dimethyl sulfate gives products of widely differing mechanical properties at equivalent DS.

The impregnation and curing of cotton with melamine-formaldehyde resin-forming agents improve its

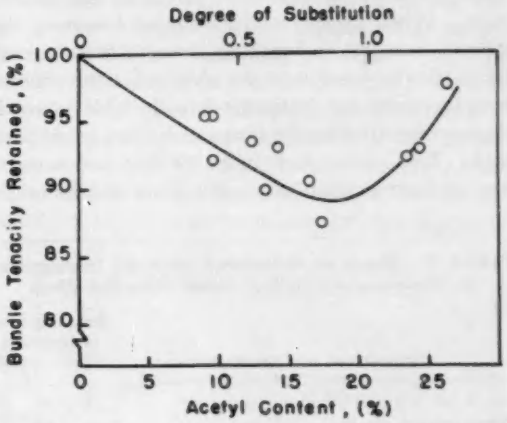


Fig. 4. Relation of fiber bundle tenacity to acetyl content of partially acetylated cottons of three varieties.

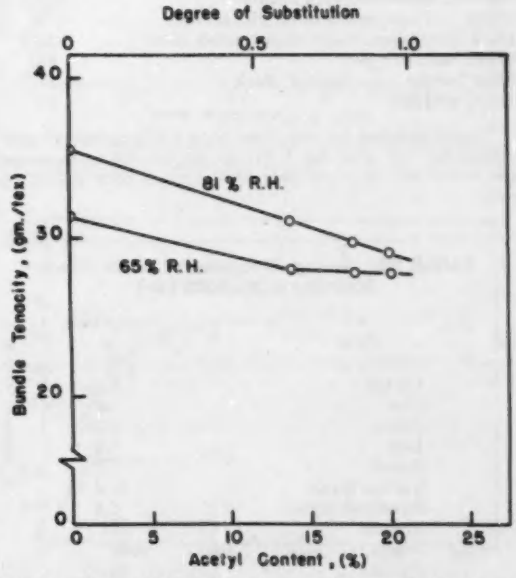


Fig. 5. The relation of bundle tenacity to acetyl content of partially acetylated cottons at two moisture conditions.

dimensional stability markedly. It is generally believed that the cellulose chains in regions of low lateral order are cross-linked through the resin molecule in these treatments. The resulting effects on the tenacity are striking and serve to throw light on the behavior of fibers in tension. Table II presents observations on the strength and tenacity of yarns and fiber bundles impregnated with such a resin and the effect of resin removal on this property. Severe reduction in the strength of yarns and fibers is noted when the resin is applied to cotton in the relaxed state. When applied under tension, however, significant increases in breaking strength are obtained. Of particular interest is the observed restoration of tenacity when the melamine-formaldehyde phase is removed by stripping the fibers with dilute phosphoric acid. This observation indicates that the strength loss on impregnation of relaxed fibers had its origin in mechanical sources rather than degradation accompanying curing of the resin with acid catalysis.

**TABLE II. Effects of Melamine-Type Resin Impregnation on Mechanical Strength of Cotton Yarns and Fibers**

| Sample and treatment | Breaking load or tenacity, % of control |
|---|---|
| 14s/3 (42 × 3 tex) Yarn, untreated | 100 |
| Resin-treated, slack | 23 |
| Control, wet-stretched | 119 |
| Resin-treated with tension | 129 |
| Control, mercerized with tension | 149 |
| Mercerized and resin-treated with tension | 178 |
| 16s/2 (37 × 2 tex) Yarn, resin-treated, slack | 53 |
| Same, resin stripped* | 87 |
| Fiber bundle, resin-treated, slack | 27 |
| Same, stripped | 84 |

* Resin removed by treatment with 1.5% phosphoric acid containing 5% urea for 1 hr. at 80° C. All resin-treated specimens had approximately 10% add-on (dry weight) of resin.

**TABLE III. Average Elongation of Textile Fibers According to Meredith [19]**

| Fiber | Elongation, % |
|---|---|
| Cotton | 7.3 |
| Flax | 3.0 |
| Hemp | 2.2 |
| Jute | 1.8 |
| Ramie | 3.7 |
| Viscose rayon | 21.0 |
| Stretched rayon | 5.8 |
| Acetate | 29 |
| Silk | 26 |
| Nylon | 26 |
| Wool | 38 |
| Casein | 25–60 |

The retention of strength when resin cross-links are introduced with the fiber in tension is also significant. Immobilization of the structural elements in their positions when the fiber is relaxed undoubtedly places a severe restriction on their ability to shift and distribute imposed stresses. In tension, the elements have already moved to positions they would occupy in the stressed state, and in this condition any added strength which the resin component may lend due to cross-linking can be fully realized.

### *Elongation*

This is a property of textile fibers which is easily and commonly measured. Elongation represents the extension of a material when stressed to the point of rupture. Although it may be expressed in absolute units it is commonly expressed as a fraction of the unstressed length. The elongation of cotton is high among the natural cellulosic fibers, being on the average, according to Meredith [19], nearly twice that of its nearest competitor, ramie. The average values given by Meredith are shown in Table III. Only silk and wool, of the natural textile fibers, exceed cotton in elongation. On the other hand, most of the regenerated fibers show high ultimate elongation. In the case of cotton the relatively high elongation is believed to be associated with the spiral arrangement of the fibrils, which is essentially absent in the other cellulosic fibers.

The relation of elongation to DP in cotton and rayon tire cords degraded by heat [3] is presented in Figure 6. It is evident that as degradation of the cotton cord proceeds, elongation increases slightly and then decreases rapidly at the lower end. This is even more emphasized in the rayon cord. The point of intersection of the curves with the DP axis is not zero, but somewhere in the region of 100–300 DP.

The slight increase in elongation at the early stages of degradation has been noted before [3] and is thought to be associated with chain breakage in the amorphous regions, accompanied by relief of stress on some of the cellulose chains.

From the standpoint of the relation of polymolecularity to elongation, very little is reported in the literature. Sookne and Harris [35] noted some tendency of very short chains, introduced into cellu-

lose acetate films, to reduce elongation. On the other hand, Scherer and coworkers [28, 29] found surprisingly little effect of polymolecularity on the elongation of cellulose nitrate or ethyl cellulose films, provided the average DP was above a certain minimum (100–200 DP). There was some increase of elongation with increase in sharpness of the distribution curve at all ranges of DP.

Cross-linking can only be expected to restrict elongation; this expectation is borne out in fact, as is indicated by results of Cameron and Morton [2], among many.

Since crystallinity may be interpreted as a type of cross-linking by hydrogen bonds and van der Waals forces, we may justly expect that cellulosic fibers with higher crystallinity may have lower elongation and vice versa. This is confirmed by observations of Segal et al. [31] on the effect of reduction of crystallinity of cotton. Also, Susich [38] observed that elongation at break of 20s/1 (30 × 1 tex) cotton yarn was increased 90% (from 9.1 to 17.3%) as the crystallinity decreased from 90 to 30%.

No satisfactory information is available on the effects of crystal modification or crystallite size on elongation. However, Hertel and Craven [11] as well as Rebenfeld and Virgin [26] have demonstrated amply that elongation increases as axial orientation decreases.

The effect of partial chemical modification of cotton cellulose on ultimate elongation is shown in Figure 7. The increase in elongation due to acetylation is taken from Honold et al. [12] and that due to carboxymethylation from Daul et al. [5]. These treatments both bring about increases of elongation at break, due probably to decrease of rigidity and relaxation of chemically modified cellulose chains. In the case of carboxymethylation, reaction conditions involving mercerization of the cellulose undoubtedly are responsible for the effect.

*Stiffness*

Stiffness may be defined as resistance to deformation, and for textiles is commonly defined as ratio of breaking stress to breaking strain. It is also referred to as secant modulus. The stiffness of cotton, like that of other cellulosic fibers, is relatively high among the textile fibers. According to Smith [34] the average stiffness of cotton in grams/tex is 570, compared with glass at 2900, flax at 2700, ramie at 1670, high tenacity viscose at 230, silk at 150, acetate at 50, and wool at 40. Factors involved in the stiffness of cotton are the molecular weight, the natural rigidity of the cellulose molecule, the high degree of

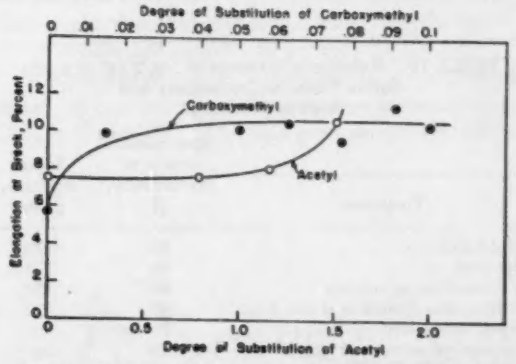
Degree of Substitution of Carboxymethyl
0 .01 .02 .03 .04 .05 .06 .07 .08 .09 0.1
Carboxymethyl
Acetyl
Elongation at Break, Percent
0 2 4 6 8 10 12
0 0.5 1.0 1.5 2.0
Degree of Substitution of Acetyl

**Fig. 7.** Relation of elongation at break of partially acetylated and partially carboxymethylated cotton to degree of substitution.

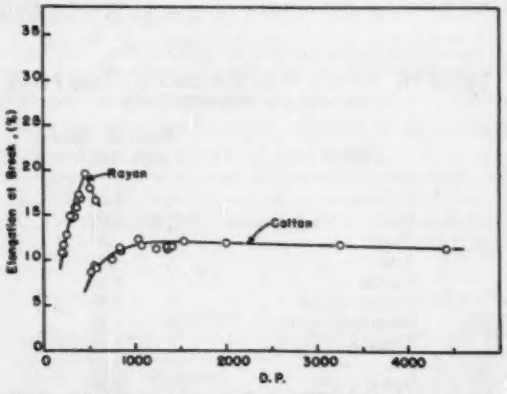


**Fig. 6.** Relation of elongation to DP of cotton and rayon tire cord degraded by heat.

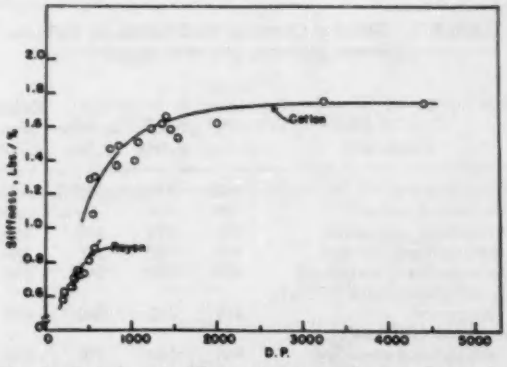


**Fig. 8.** Relation of stiffness of cotton and rayon tire cord to DP in heat degradation.

crystallinity conditioned by hydrogen bonding and van der Waals forces, and the orientation of the cellulose chains.

The relation of stiffness of cotton and rayon tire cord to molecular weight is shown in Figure 8. The change in DP was brought about by heat degradation.

The relation of X-ray angle to stiffness of cotton has been demonstrated recently by Rebenfeld and Virgin [26]. Tension applied to cotton while in a swollen state can improve the orientation and presumably the hydrogen bonding in the amorphous regions. The changes in stiffness (secant modulus) accompanying the treatments which affect the lateral order of the cotton cellulose (Table IV) reflect the trends noted for elongation. The amine-decrystallized and slack mercerized yarns have lower slopes in their load–elongation curves than the untreated cottons, while mercerization at normal length produces a significantly stiffer yarn.

In the case of chemical modification by acetylation, extensibility decreases more rapidly than tenacity in the lower DS range, so that average stiffness increases up to 20% or more and a noticeable harshness of hand of the fabrics occurs. The effect of certain chemical modifications on the stiffness of cotton fibers is shown in Table V [7]. It is seen that large relative changes are produced by the various treatments.

**TABLE IV. Relation of Stiffness of 16s/2 (37 × 2 tex) Cotton Yarns to Crystallinity and Type of Treatment**

| Treatment | Approximate degree of crystallinity,* % | Secant modulus, g./tex |
|---|---|---|
| Untreated | 86 | 170 |
| Scoured | 90 | 170 |
| Ethylamine, no tension | 40 | 120 |
| Ethylamine, boiled in water 1 hr. | 60 | 120 |
| Slack mercerized | 70 | 80 |
| Mercerized at normal length | 80 | 280 |
| Cellulose III slack (20s/1 yarn) | — | 110 |

* Estimated from acid hydrolysis rate measurements.

**TABLE V. Effect of Chemical Modification on Stiffness (Secant Modulus) of Cotton Fibers**

| Treatment | Stoneville 2B, g./tex | S×P, g./tex | Rowden g./tex | Deltapine, g./tex |
|---|---|---|---|---|
| None (control) | 440 | 430 | 350 | 360 |
| Mercerized, relaxed | 220 | 230 | — | 230 |
| Mercerized, restrained | 460 | 510 | 430 | 450 |
| Decrystallized, relaxed | 300 | 330 | 280 | 280 |
| Decrystallized, restrained | 480 | 450 | 360 | 380 |
| Carboxymethylated (DS 0.1), restrained | 470 | 470 | 380 | 420 |
| Aminized (DS 0.04), relaxed and stretched | 560 | 440 | 370 | 440 |
| Acetylated (DS 1.2), restrained | 560 | 440 | 370 | 440 |

*Toughness*

Toughness represents the ability of a material to absorb work. It is also called work of rupture, energy to break, etc., and may be measured by the area under a stress–strain curve carried to rupture. More frequently, toughness is computed as one-half of the product of the stress by the strain at rupture on the premise that the curve is sufficiently well represented by a straight line. This is roughly true for cotton. This property is important in many mechanical fabric applications. In cords for reinforcing automobile tires, high toughness may be thought of as a margin of safety against sudden thrusts or large impacts when a tire climbs a high curb or passes over large sharp objects.

Cotton stands relatively high among natural cellulosic fibers in toughness but is inferior to most regenerated fibers and to silk and wool. This can be seen in Table VI, which is taken from an investigation by Meredith [19]. Toughness is closely related to DP, as can be seen in Figure 9, representing cotton and rayon tire cord degraded by heat. Work of rupture rises slightly at first and then falls off almost linearly as elongation and strength are lost.

The influence of the different supermolecular structural factors is still inadequately understood. Poly-

**TABLE VI. Average Work of Rupture of Textile Fibers According to Meredith [19]**

| Fiber | Work of rupture, gm. cm./tex |
|---|---|
| Cotton | 1.21 |
| Flax | .99 |
| Hemp | .66 |
| Jute | .33 |
| Ramie | 1.32 |
| Viscose rayon | 2.86 |
| Stretched rayon | 1.87 |
| Acetate | 2.75 |
| Silk | 9.02 |
| Nylon | 9.46 |
| Wool | 3.96 |
| Casein | 2.86 |

molecularity can lead to increased complexity of the manifold relaxation processes. Cross-linkage presumably opposes secondary creep and improves elastic recovery. Although cotton cellulose has a large component of crystalline cellulose it does not, as outlined by Mark and Press [17], show the short range elongation and instantaneous recovery of crystalline materials within their elastic limits. Rather, it displays a certain amount of instantaneous crystalline recovery, superimposed on a certain proportion of long range primary and secondary creep. All of this elongation, coupled with intermolecular forces of considerable magnitude, contributes improved toughness. The improvement in toughness of 20s/1 (30 × 1 tex) cotton yarn brought about by ethylamine and hexylamine "decrystallization" is shown in Table VII, computed from data of Segal et al. [31]. The 156% improvement is seen to be due largely to increased elongation, the strength decreasing only slightly. Presumably much longer segments of cellulose chains are available for extension after the ethylamine and combined ethylamine and hexylamine treatments. Susich [38] observed similar improvements in work of rupture due to ethylamine decrystallization of 20s/1 (30 ×1 tex) cotton yarn.

Increase of orientation normally brings about increased tenacity and reduced elongation. Changes in toughness as a result of chemical modification will, of course, depend on the concomitant effects on tenacity and elongation. Acetylation, for example, which reduces both of these properties in the lower ranges of substitution, gives increased toughness at higher DS [12]. Similarly, reactions which involve swelling of the fiber, such as carboxymethylation [5], improve the toughness of cotton through gains in tenacity, elongation, or both properties.

In all of the foregoing discussion elongation, or strain, has been considered without any implications as to tendency to recover. In the discussion which follows attention will now be directed to mechanical behavior involving recovery from strain.

*Elasticity*

The ability to recover from deformation is one of the most important properties of textiles. Elasticity provides the stability needed to maintain the size and shape of clothing and to retain the dimensions of mechanical fabrics. It represents the ability of a material to return to its original dimensions after removal of an applied stress, and is always time-dependent. In textile usage it may refer to recovery from tensile stress or from bending (crease recovery). Elasticity is normally divided into three classes: (1) immediate elastic recovery, (2) delayed elastic recovery, or primary creep, and (3) nonrecoverable elongation, or secondary creep.

Elasticity of textiles varies with the stress or strain imposed. Consequently, to understand elastic behavior it is advantageous to express elastic recovery in terms of the stress. This has been done in Figure 10, taken from a study by Meredith [20]. It is seen that with stress up to 50 g./tex flax has the greatest elasticity, ramie next, and cotton least. Furthermore, cotton would not support 50 g./tex.

Elasticity also may be expressed as a function of strain, as has been done for the same measurements [20] in Figure 11. This plot gives us quite a differ-

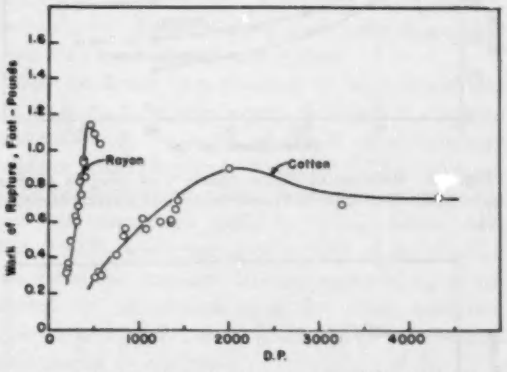


**Fig. 9.** Relation of work of rupture to DP of cotton and rayon cellulose in tire cords degraded by heat.

**TABLE VII. Improvement in Toughness Associated with Ethylamine "Decrystallization" of 20s/1 (30 × 1 tex) Cotton Yarn**

| Treatment | Crystallinity, % | Tenacity, g./tex | Elongation, cm./cm. | Toughness, g. cm. / tex cm. | Toughness, % |
|---|---|---|---|---|---|
| Bleached and scoured, control | 89 | 17.0 | 0.058 | 0.50 | 100 |
| Ethylamine, no tension | 38 | 16.0 | .133 | 1.06 | 212 |
| Ethylamine, plus hexylamine, no tension | 46 | 15.0 | .171 | 1.28 | 256 |
| Same as above, then in boiling water 2 hr. | 52 | 15.0 | .143 | 1.07 | 214 |

ent picture. Now it is seen that for a given strain the elasticity of cotton exceeds that of flax and ramie. Actually it was possible to measure recovery after twice as great strain in cotton as in flax and ramie.

As has been ably discussed by Mark and Press [17], the forces which cause retraction of elongation of linear high polymers are at least four in number. Primary covalent bonds, hydrogen bridges, and van der Waals bonds permit only small extensions (0.1–1.5%) but impart immediate elastic recovery within the range of the elastic limit. On the other hand, kinetic elasticity of flexible long chain amorphous molecules involves large extension (up to 1000%) and induces delayed recovery.

In the release of stress of a textile material, normally all types of retractive forces operate simultaneously. Primary, hydrogen, and van der Waals bonds retract instantaneously and give rise to immediate elastic recovery. The mechanism of elasticity due to hydrogen bonding in the amorphous regions has been discussed recently by Nissan [22]. On the other hand, segments of cellulose chains of a range of magnitudes will have moved from their original equilibrium position a greater or lesser distance depending on their individual masses, their relaxation times, the period and magnitude of the stress, etc. A certain number of weak bonds in the amorphous regions will be broken and new ones will be established in the stressed state. Upon release of the stress, retraction will set in, and movement of many of the chain segments will proceed at similar rates in the opposite direction depending on their mass, activation energy, entropy, etc. However, this slow or delayed recovery will be incomplete to the extent that many segments will be moved far enough that the restoring forces never exceed the forces tending to hold them in the new positions.

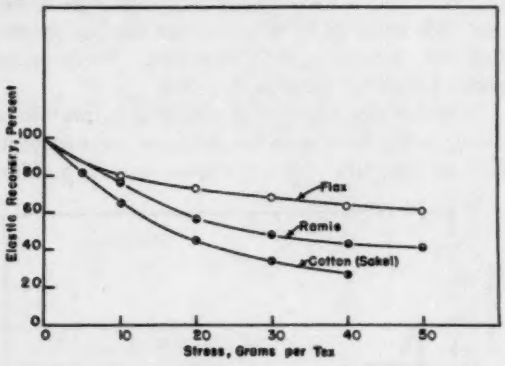


**Fig. 10.** Relation of elastic recovery of samples of flax, ramie, and cotton after different degrees of stress (Meredith [20]).

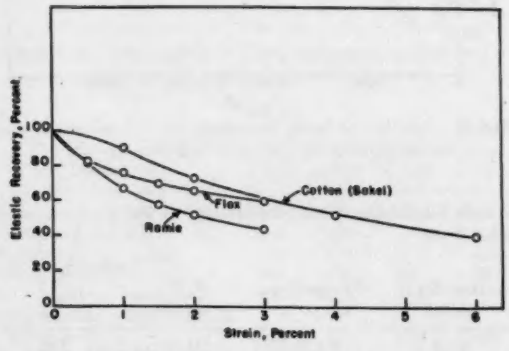


**Fig. 11.** Relation of elastic recovery of samples of flax, ramie, and cotton after different degrees of stress (Meredith [20]).

With the above considerations, what may we expect from the various elements of our supermolecular structure? There is little or no information as far as molecular chain length is concerned. However, when a certain necessary minimum length has been exceeded, we should expect little effect. Because of the high crystallinity in cellulose fibers (particularly flax and ramie), the long chains may be considered as extending through many crystalline areas, and are thus much longer than necessary for maximum effect. Swanson and Williams [40] concluded that low molecular weight additions to cellulose acetate improved the recoverable elongation and reduced the permanent set. Therefore, neither chain length nor polymolecularity may be an important factor in elasticity of native fibers, except in seriously degraded samples where many breaks occur between crystallites. On the other hand, by introduction of cross-links into the amorphous regions of rayon, molecular flow is prevented and elastic recovery can be increased greatly. Thus Gruntfest and Gagliardi [9] could increase elastic recovery of rayon yarn from 20% (control) to 95% and the wrinkle recovery of cotton sheeting from 51% (control) to 87%.

While crystallinity of cotton cellulose must contribute to the small ($<1.5\%$) immediate elastic recovery, normally it does not vary greatly in cotton, and its effect is greatly masked. On the other hand, Susich [38] showed that in terms of absolute values ethylamine decrystallization of 20s/1 ($30 \times 1$ tex)

cotton yarn increased the immediate elastic recovery from 1.2 to 1.5% and the delayed elastic recovery from 2.5 to 2.8%. The permanent set was increased from 5.4 to 13.0% under the conditions used, thus indicating that a large proportion of the increased elongation imparted by decrystallization was not useful for improving the elastic recovery. Pertinent recovery data for 16s/2 (37 ×2 tex) cotton yarns treated to reduce their crystallinity or change their crystalline modification are presented in Table VIII. The total recovery of amine-decrystallized and mercerized yarns treated in the slack condition is significantly higher than the control, when measured after stretching to 2% strain. At 50% of the breaking strain, however, the reverse is true. When treated under conditions of restraint, the yarns achieved no change in relative recovery. Mauvisseau [18] has concluded that fatigue resistance of regenerated cellulose fibers is improved by having as large a portion of the cellulose as possible in the amorphous state.

The effects on elasticity of crystal modification and crystallite size are completely unknown. Also, very few results seem to be recorded on the relation of elasticity to orientation in cotton fibers, although Mauvisseau [18] recommends high orientation to improve fatigue resistance of regenerated celluloses. Kumm [13] found in polyacrylic fibers stretched at 160° C. that elastic recovery increased with degree of stretching (orientation) as follows:

| Stretching ratio | 1 : 3.1 | 1 : 4.0 | 1 : 6.0 | 1 : 7.6 |
|---|---|---|---|---|
| Elastic recovery, % | 51.1 | 63.0 | 75.0 | 82.4 |

In view of the large variation of orientation in cotton, this relationship may be very important and should be studied.

There are no data on relation of elasticity to accessibility, although the effects of accessibility should largely parallel those of crystallinity. So far as is known, no studies have been made of the relation of elasticity to partial chemical modification of cotton cellulose.

*Resilience*

Resilience refers to the ability to absorb work without suffering permanent deformation. In textiles it is commonly measured as the ratio of the work recovered to the work expended at any stress below rupture. Resilience involves no new factors from those already discussed other than use of integrated areas beneath the stress–strain curve, *not* carried to rupture. It is assumed for actual energy computations that both stress and strain are expressed in absolute units. The recovery curve, of course, does not follow the initial curve. The energy recovered is usually expressed as a percentage of the energy expended. Like elasticity, resilience is time-dependent and can be divided into immediate elastic recovery, delayed elastic recovery, and permanent set. A thorough discussion of methods of dealing with such measurements has been published by Susich and Backer [39]. Resilience has some advantage over elasticity alone since both strain and stress are considered simultaneously.

**TABLE VIII. Recovery Properties of 16s/2 (37 × 2 tex) Cotton Yarns**

| Treatment | Sum of immediate and delayed elastic recovery*, %, at strains of 2% | Sum of immediate and delayed elastic recovery*, %, at strains of 50% of ultimate |
|---|---|---|
| Untreated | 82 | 67 |
| Decrystallized slack† | 90 | 58 |
| Decrystallized restrained† | 83 | 66 |
| Mercerized slack | 93 | 42 |
| Mercerized restrained | 81 | 69 |

* Yarns allowed to relax for 1 hr.; % of total strain.
† By treatment with ethylamine.

Since resilience is a resultant of both stress and strain, it may be considered to entail a complex combination of the same effects of supermolecular structure which influence elasticity. The resilience of heat degraded cotton and rayon tire cords in the previously mentioned study by Tripp, Mares, and Conrad [42], when measured at 50% of the residual tenacity of the degraded sample, appeared to be unaffected by degradation over the range observed. Little or nothing is known about the effects of polymolecularity on resilience.

Since crystallinity in cellulose is a cross-linking mechanism, it serves to increase stiffness and prevent long range flow. The elasticity per unit stress may be expected to go up as crystallinity increases. This appears to be exemplified in Figure 10, where decreasing elasticity seems to be in the order of decreasing crystallinity of flax, ramie, and cotton. At the same time the elasticity per unit of strain decreases in the inverse order, as shown in Figure 11. Therefore, the total expended and recovered energy

may be higher, the same, or even lower as crystallinity increases. Mark [16] emphasizes the need of occasional "fix points" but great localized mobility, i.e., low crystallinity or low intermolecular attraction in localized areas, as a basis for high resilience. The introduction of artificial cross-links may be expected to improve the resilience, provided they do not impede the localized mobility too much, i.e., Mark's "Micro-Brownian Motion."

Little or nothing is known about the effects of crystallite type or orientation, although it may be anticipated that resilience will increase as orientation increases. This should follow from the greater opportunity for anchor points along the chains and consequent less slippage of molecular chains on one another. Similarly, very little is known about the effects of crystallite size or degree and type of chemical modification. Rich opportunities for profitable research are open here for the scientist who will give of his time and effort.

Obviously, it has not been possible within the narrow confines of the present report to cover many aspects of the mechanical behavior of textiles. Only the high points, the scope of the subject, have been indicated. Many other aspects of mechanical behavior are of great interest to the advanced textile technologist together with corresponding interpretations in terms of supermolecular structure and mechanism.

## Literature Cited


1. Berkley, E. E., Woodyard, O. C., Barker, H. D., Kerr, T., and King, C. J., *U. S. Dept. Agr. Tech. Bull.* No. 449, 64 pp. (1948).
2. Cameron, W. G. and Morton, T. H., *J. Soc. Dyers Colourists* **64**, 329–336 (1948); *Am. Dyestuff Reptr.* **38**, 575–581 (1949).
3. Conrad, C. M., Tripp, V. W., and Mares, T., TEXTILE RESEARCH JOURNAL **21**, 726–739 (1951).
4. Creely, J. J., Segal, L., and Ziifle, H. M., TEXTILE RESEARCH JOURNAL **26**, 789–795 (1956).
5. Daul, G. C., Reinhardt, R. M., and Reid, J. D., TEXTILE RESEARCH JOURNAL **22**, 787–792 (1952).
6. Flory, P. J., *J. Am. Chem. Soc.* **67**, 2048–2050 (1945).
7. Grant, J. N., private communication.
8. Grant, J. N. and Morlier, O. W., TEXTILE RESEARCH JOURNAL **18**, 481–487 (1948).
9. Gruntfest, I. J. and Gagliardi, D. D., TEXTILE RESEARCH JOURNAL **18**, 643–650 (1948).
10. Hermans, P. H., "Physics and Chemistry of Cellulose Fibers," p. 491, New York, Elsevier Publishing Co., Inc. (1949).
11. Hertel, K. L. and Craven, C. J., TEXTILE RESEARCH JOURNAL **26**, 479–484 (1956).
12. Honold, E., Poynot, J. M., and Cucullu, A. F., TEXTILE RESEARCH JOURNAL **22**, 25–29 (1952).
13. Kumm, A. W., *Faserforsch. u. Textiltech.* **5**, 497–501 (1954).
14. Loeb, L. and Segal, L., *J. Polymer Sci.* **14**, 121–123 (1954).
15. Mark, H., *Am. J. Phys.* **13**, 207–214 (1945).
16. Mark, H., TEXTILE RESEARCH JOURNAL **16**, 361–368 (1946).
17. Mark, H. and Press, J., *Rayon Textile Monthly* **24**, 297–299; 339–341; 405–407 (1943).
18. Mauvisseau, P., *Bull. inst. textile France*, No. 51, 47–78 (1955).
19. Meredith, R., *Shirley Inst. Mem.* **19**, 5–28 (1944–45); *J. Textile Inst.* **36**, T107–T130 (1945).
20. Meredith, R., *J. Textile Inst.* **36**, T147–T164 (1945); *Shirley Inst. Mem.* **19**, 29–45 (1944–45).
21. Morey, D. R., TEXTILE RESEARCH **4**, 491–512 (1934).
22. Nissan, A. H., *Trans. Faraday Soc.* **53**, 710–721 (1957).
23. Orr, R. S., Weiss, L. C., Humphreys, G. C., Mares, T., and Grant, J. N., TEXTILE RESEARCH JOURNAL **24**, 399–406 (1954).
24. Ott, E., Spurlin, H. M., and Grafflin, M. W., eds. "Cellulose and Cellulose Derivatives," 2nd ed., 3 vols., 1601 pp. New York, N. Y., Interscience (1954).
25. Rånby, B. G., Inaug. Diss., Inst. of Phys. Chem., Univ. of Uppsala, Sweden; Grafiska Konstantalten Tryckeri A B, Stockholm, 1952.
26. Rebenfeld, L. and Virgin, W. P., TEXTILE RESEARCH JOURNAL **27**, 286–289 (1957).
27. Reeves, R. E., Armstrong, A. C., Blouin, F. A., and Mazzeno, L. W., Jr., TEXTILE RESEARCH JOURNAL **25**, 257–261 (1955).
28. Scherer, P. C. and McNeer, R. D., *Rayon and Synthetic Textiles* **31**, No. 2, 53–55; No. 4, 54–56 (1950).
29. Scherer, P. C. and Rouse, B. P., *Rayon and Synthetic Textiles* **30**, No. 11, 42–44; No. 12, 47–49 (1949).
30. Segal, L., Loeb, L., and Creely, J. J., *J. Polymer Sci.* **13**, 193–206 (1954).
31. Segal, L., Nelson, M. L., and Conrad, C. M., *J. Phys. and Colloid Chem.* **55**, 325–336 (1951).
32. Sippel, A., *Kolloid Z.* **112**, 80–84 (1949).
33. Sippel, A., *Kolloid Z.* **127**, 79–82 (1952).
34. Smith, H. DeW., *Am. Soc. Testing Materials Proc.* **44**, 543–592 (1945).
35. Sookne, A. M. and Harris, M., *J. Research Nat. Bur. Standards* **30**, 1–14 (1943)
36. Staudinger, H. and Fritschi, J., *Helv. Chim. Acta* **5**, 785–806 (1922).
37. Staudinger, H. and Jurisch, J. *Zellwolle, Kunstseide, Seide* **44**, 375–377 (1939).

38. Susich, G., *Am. Dyestuff Reptr.* **42**, 713–718 (1953).
39. Susich, G. and Backer, S., U. S. Quartermaster Corps Military Planning Div. Research and Development Branch. Textile Ser. Rep. No. 64, 53 pp. (1950); TEXTILE RESEARCH JOURNAL **21**, 482–509 (1951).
40. Swanson, D. L. and Williams, J. W., *J. Appl. Phys.* **26**, 810–815 (1955).
41. Tripp, V. W., Guiffria, R., and deGruy, I. V., TEXTILE RESEARCH JOURNAL **27**, 14–24 (1957).
42. Tripp, V. W., Mares, T., and Conrad, C. M., TEXTILE RESEARCH JOURNAL **21**, 840–846 (1951).
43. Wakeham, H. and Spicer, N., TEXTILE RESEARCH JOURNAL **21**, 187–194 (1951).

*Manuscript received January 10, 1958.*

# Changes in the Weight Distribution of Fiber Lengths of Cotton as a Result of Random Fiber Breakage[1]

**W. J. Byatt[2] and J. P. Elting**

*Kendall Company Research Laboratories, Paw Creek, North Carolina*

**Abstract**

An integro-differential equation is derived; it describes the time rate of change of the weight distribution of lengths for cotton fibers. A solution to the equation is found. Comparison between theory and experiment is made. Agreement is satisfactory.

## Introduction

This note discusses changes which occur in the weight distribution of cotton fiber lengths as a consequence of random fiber breakage. The changes considered are those which can be produced by microbial deterioration or by the action of saws, as in ginning. A discussion of these questions may be found in the literature [2, 4, 5, 7, 9, 10]. The mathematical representation derived should be applicable in all instances where the causal agent produces a random collection of weakened or ruptured spots. In this treatment, a weight rather than a number distribution is used, since the total weight remains constant in the process, while the number of fibers increases if breakage occurs.

An integro-differential equation governing the change in the weight distribution function (WDF) is developed and a solution given. Examples are presented which compare theory with experiment. Evidence is found in the examples shown, assuming an average fiber length of 1 in., that one or two in every ten fibers is broken.

[1] Presented at the spring meeting of The Fiber Society, Clemson, S. C., May 1, 1958.

[2] On leave of absence from the Physics Department, University of Mississippi, University, Mississippi.

## Development of Equation

Designate a weight–length distribution function as of a particular time by $W(l, t)$. Such a function can change with time in two ways. Its value for some particular length can decrease due to fibers of that length being broken into shorter segments. Its value can increase for the same length interval if fibers of length $l' > l$ are broken such that some of the resulting segments are of length $l$. The change in the (WDF) in time $\Delta t$ can then be written

$$W(l, t + \Delta t)\Delta l = W(l, t)\Delta l - f(W_{\text{out}}) + g(W_{\text{in}}) \quad (1)$$

where $g(W_{\text{in}})$ and $f(W_{\text{out}})$ are the weights into and out of the interval $\Delta l$ about $l$, respectively, in time $\Delta t$. To find the function $f(W_{\text{out}})$, assume that the weight decaying out of $\Delta l$ about $l$ is proportional to the weight initially present. Take the constant of proportionality to be the probability that a fiber of length $l$ will decay in time $\Delta t$. Thus

$$f(W_{out}) = W(l, t)\Delta l(kl\Delta t) \quad (2)$$

The constant $k$ is the number of decay (or rupture) events per unit length per unit time due to some arbitrary external cause. For $g(W_{in})$, analogous to Equation 2, write

$$g(W_{in}) = \int_l^\infty W(l', t)p(l' \to l, \Delta t)dl' \quad (3)$$

where $W(l', t)$, the weight of fibers of length $l'$, is multiplied by the probability that a fiber of length $l'$ will break such that one of its segments will fall into $\Delta l$ about $l$; since this process can occur for all $l' > l$, the sum over $l'$ must be taken. For $p(l' \to l, \Delta t)$, assume the following holds:

$$p(l' \to l, \Delta t) = (kl'\Delta t)(\Delta l/l') \quad (4)$$

The term $kl'\Delta t$ is the probability that a fiber of length $l'$ will break in time $\Delta t$. The second term is the independent probability that if the first occurs, one of the resulting segments will be in $\Delta l$ about $l$. Using Equations 2, 3, and 4, Equation 1 becomes

$$W(l, t + \Delta t)\Delta l = W(l, t)\Delta l - klW(l, t)\Delta l\Delta t + k\Delta l\Delta t \int_l^\infty W(l', t)dl' \quad (5)$$

Note that as $\Delta t \to 0$, Equation 5 is identically satisfied. On transposing $W(l, t)\Delta l$, dividing by $\Delta l$, and passing to the limit $\Delta t \to 0$, there results

$$\frac{\partial W(l, t)}{\partial t} = -klW(l, t) + k\int_l^\infty W(l', t)dl' \quad (6)$$

This is the basic integro-differential equation governing the change in the weight distribution function with time. Equation 6 is, in a sense, a linearized Boltzmann transport equation. It is capable of describing phenomena involving changes in distribution functions of widely divergent kinds. Thus, for example, Thompson and Holmes [8] have used an equation similar to Equation 6 in a discussion of neutron irradiation effects on the distribution of pinned lengths in copper crystals.

To solve Equation 6, assume that $W(l, t)$ has a Laplace transform with respect to $t$. If it be denoted by $\phi(l, s)$, the transformed equation is

$$(s + kl)\phi(l, s) = W(l, 0) + k\int_l^\infty \phi(l', s)dl'$$

Differentiating both sides of this equation with respect to $l$ and multiplying each term by $(s + kl)$ produces

$$\frac{\partial}{\partial l}[(s + kl)^2\phi(l, s)] = (s + kl)\frac{\partial W(l, 0)}{\partial l}$$

On integrating over $l$, the result is

$$\phi(l, s) = -\int_l^\infty \frac{(s + kl')}{(s + kl)^2}\frac{\partial W(l', 0)}{\partial l'}dl'$$

where a constant of integration has been put equal to zero. The inverse Laplace transform of the last equation is

$$W(l, t) = -e^{-klt}\int_l^\infty [1 + kt(l' - l)] \times \frac{\partial W(l', 0)}{\partial l'}dl' \quad (7)$$

Integrating Equation 7 as it stands, one finds

$$W(l, t) = e^{-\mu l}\left\{W(l, 0) + \mu\int_l^\infty W(l', 0)dl'\right\} \quad (8)$$

where $\mu = kt$ is a constant having the dimension of a reciprocal length. If Equation 8 is to be interpreted as a fractional weight distribution for finite length intervals, it will be properly normalized when the second term within the brackets on the right hand side is multiplied by interval width.

It is often convenient to have an analytical representation for $W(l, 0)$. It turns out that in all cases thus far examined in these laboratories a sufficiently accurate ($\pm 0.02$ of total area) representation of $W(l, 0)$ is given by a series of normalized Gaussian curves; i.e.,

$$W(l, 0) = \sum_k \frac{A_k}{\sqrt{2\pi}\sigma_k}e^{-(l-l_k)^2/2\sigma_k^2} \quad (9)$$

If Equation 9 is substituted into Equation 8, the result is

$$W(l, t) = e^{-\mu l}\left\{W(l, 0) + \frac{\mu}{2}\sum_k A_k\left(1 - \text{erf}\left(\frac{l - l_k}{\sqrt{2}\sigma_k}\right)\right)\right\} \quad (10)$$

The notation $\text{erf}(x) \equiv \frac{\sqrt{2}}{\pi}\int_0^x e^{-t^2}dt$; the function is tabulated [3]. The normalization of this expression already is accomplished.

The magnitude of the essential parameter $\mu$ can be estimated in the following manner. Calculate

the average length at time $t$, denoted by $\bar{l}(t)$. It is given by

$$\bar{l}(t) = \int_0^\infty lW(l, t)dl$$

where, for example, $W(l, t)$ is given by Equation 8. The result of carrying out the indicated integrations is

$$\bar{l}(t) = \int_0^\infty W(l, 0)\left[\frac{1 - e^{-\mu l}}{\mu}\right] dl \qquad (11)$$

Thus, the average length at time $t$ is the average of $\left[\frac{1 - e^{-\mu l}}{\mu}\right]$ over the initial distribution. If $\mu l \ll 1$, the exponential under the integral sign can be approximated by $e^{-\mu l} = 1 - \mu l + \mu^2 l^2/2 + \cdots$; the result is

$$\bar{l}(t) = \frac{1}{\mu}\left[\mu \bar{l}(0) - \mu^2 \frac{\overline{l^2(0)}}{2}\right]$$

The value for $\mu$ is then given, in first approximation, by

$$\mu = 2[\bar{l}(0) - \bar{l}(t)]/\overline{l^2(0)} \qquad (12)$$

The quality $\overline{l^2(0)}$ is related to $\overline{l(0)}^2$ and $\sigma$, the standard deviation of the array, by

$$\sigma = (\mathrm{CV})\bar{l}(0) = \sqrt{\overline{l^2(0)} - \overline{l(0)}^2} \qquad (13)$$

where CV is the coefficient of variation of $W(l, 0)$.

### Comparison of Theory with Experiment

The assumptions regarding probability of fiber damage made above are (1) there is equal probability for the decay to occur at any point along the fiber length; (2) the probability of fiber decay is directly proportional to the first power of fiber length; (3) the probability of one break per fiber in time $\Delta t$ is much greater than the probability of two or more breaks per fiber in time $\Delta t$. These assumptions led to a simple picture of the change in the WDF in time. The shortcomings of such a simple theory are readily apparent. Nonetheless, they lead to a theory which accounts for the general trend of fiber degradation adequately.

Examples are presented in this section of the change in the WDF of so-called cavitomic cotton, and a comparison between hand pulled and saw ginned cotton is made. Both Equations 8 and 10 will be employed to estimate the $W(l, t)$, given the initial distribution and a value of the parameter $\mu$.

**TABLE I. Experimental and Theoretical Weight Distribution for Cotton ADOC 672 on November 28, 1955 and August 20, 1956**

| Length units of 1/8 in. | Fractional weight per interval: Observed November 1955 | Observed August 1956 | Predicted $W(l,t)$: $\mu$=0.12 | $\mu$=0.20 |
|---|---|---|---|---|
| 0– 1 | .0071 | .0040 | .0220 | .0314 |
| 1– 2 | .0102 | .0129 | .0246 | .0314 |
| 2– 3 | .0248 | .0379 | .0378 | .0458 |
| 3– 4 | .0253 | .0365 | .0373 | .0455 |
| 4– 5 | .0288 | .0445 | .0395 | .0460 |
| 5– 6 | .0368 | .0735 | .0459 | .0510 |
| 6– 7 | .0749 | .0837 | .0788 | .0805 |
| 7– 8 | .1153 | .1332 | .1120 | .1098 |
| 8– 9 | .1973 | .2263 | .1800 | .1694 |
| 9–10 | .2668 | .2027 | .2350 | .2150 |
| 10–11 | .1693 | .1069 | .1447 | .1310 |
| 11–12 | .0412 | .0379 | .0346 | .0314 |
| 12–13 | .0022 | | | |
| Mean length | 1.04 | .97 | | |
| Upper quar. | 1.23 | 1.18 | | |
| CV | 27 | 30 | | |

The first example is typical of a cavitomic cotton. Fiber arrays[3] made in November 1955 and August 1956 furnished the data of Table I.

In Table I there are also two columns giving computed values of $W(l, t)$ for the values of $\mu$ shown thereon. The first value of $\mu$ was computed from Equations 12 and 13. It turns out that this method usually underestimates $\mu$, so that there is included a histogram for the value $\mu = 0.2$. Generally, the agreement between theory and the experimentally determined histogram is fair. The value $\mu = 0.12$ yields better agreement at small $l$, while the larger value of $\mu$ makes the agreement better at large $l$.

The second and third examples employ the analytical representation (Equation 10) to $W(l, t)$. The first of these examples is again of a cavitomic cotton. An equation of the form of Equation 9, namely

$$W(l, 0) = 0.212\, e^{-12.2(l-1.04)^2} + 0.035\, e^{-12.8(l-.8)^2} \qquad (14)$$

fits the initial histogram adequately. This corresponds to constants $A_1 = 0.1076, \sigma_1 = 0.202; A_2 = 0.0173; \sigma_2 = 0.1975$. Note that $A_1 + A_2 \cong 0.125$, the length of the interval (in inches) on which the histogram is plotted. In Figure 1, the initial and final histograms, the smooth curve given by Equation

[3] All experimental data used herein were furnished us by the USDA Fiber and Spinning Laboratory, Clemson, South Carolina.

14 above and two curves $W(l, t)$ for the assumed values of $\mu$ shown thereon are plotted. Again, note that the smaller value of $\mu$ results in better agreement at low values of the length, while the higher value of $\mu$ causes the upper end of the histogram to be in better agreement.

The final example concerns a cotton which was treated as follows. One sample of this cotton was pulled by hand from the seed and arrayed. The second and third samples from the same cotton were ginned in saw and roller gins respectively and then arrayed. The roller gin operates in a manner such that the first and second assumptions listed above do not apply. Actual computations involving the roller gin distribution functions showed large deviations between theory and experiment. In Figure 2 the hand pulled and saw ginned histograms are plotted; the smooth curve superimposed on the hand pulled histogram is of the form of Equation 9 and has constants

$$\left.\begin{aligned} A_1 &= 0.019 \quad l_1 = 0.70 \quad \sigma_1 = 0.252 \\ A_2 &= 0.089 \quad l_2 = 1.25 \quad \sigma_2 = 0.129 \\ A_3 &= 0.0140 \quad l_3 = 1.00 \quad \sigma_3 = 0.112 \end{aligned}\right\} \tag{15}$$

The curve $W(l, t)$ found from Equation 10 is plotted in Figure 2 for a value $\mu = 0.15$. The agreement between the saw ginned histogram and $W(l, t)$ is good.

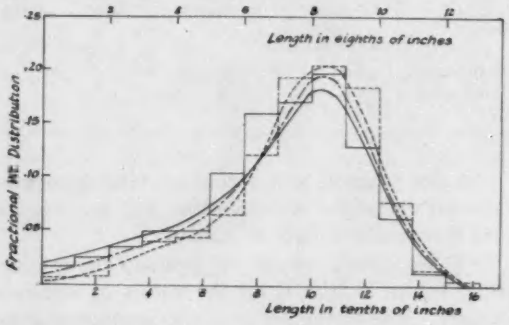


**Fig. 1.** The dotted line whose segments are of equal length is a plot of the empirical Equation 14. The remaining two curves were plotted from Equation 10; the values of the parameter $\mu$ are $\mu = 0.10$ (in.)$^{-1}$ for the broken line and $\mu = 0.2$ (in.)$^{-1}$ for the solid line.

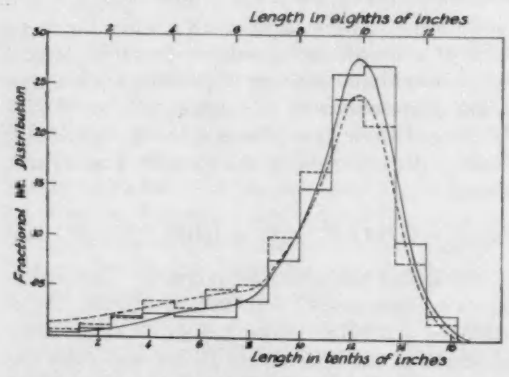


**Fig. 2.** The smooth solid line is an empirical fit to the hand pulled WDF; its equation is given by Equation 9, with the constants having the values shown in Equation 15. The dotted line is the predicted distribution, to be compared with the observed distribution given by the histogram whose line is also broken. The value of the parameter $\mu$ is 0.15.

## Discussion and Conclusions

To find $W(l, t)$ it has been shown that it is necessary to know the parameter $\mu$. According to the assumptions made in developing the theory, $\mu$ should be a constant. The examples above show that $\mu$ cannot be a constant if agreement with experiment is to be obtained over the entire range of lengths. As the length increases, $\mu$ increases, according to the examples mentioned above. This contradiction must be regarded as evidence of a defect in the linear theory developed, although the loss of short fibers when arraying or ginning may be adduced as a cause.

Attempts have been made to incorporate assumptions different from the first two above. For example, it is natural to assume, in view of the dependence of $\mu$ on length, that the probability of decay of a fiber of length $l$ is proportional to $l^p$

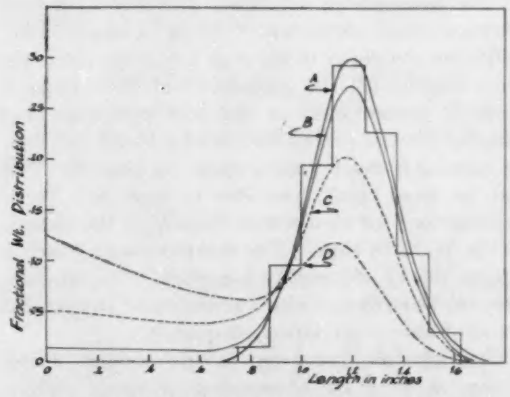


**Fig. 3.** This illustrates the behavior of the solution (Equation 10) as the value of the parameter $\mu$ increases. Curve A is an assumed fit to the histogram shown. Curves B, C, and D were computed from Equation 10, using values of $\mu$ equal to 0.10, 0.40, and 1.0, respectively.

where $\rho$ is a number greater than unity, and not necessarily an integer. This leads to serious mathematical difficulties when one attempts to take an inverse Laplace transform.

The assumption that the probability of decay (or breakage) is a rectangular distribution is in error for roller ginning; it may be incorrect for saw ginning. But attempts to modify the second assumption again led to no fruitful results.

Faced with the obvious shortcomings of a linear theory, it is still possible to obtain useful information. According to Equations 12 and 13, the value of the parameter $\mu$ can be found from a knowledge of average fiber length before and after degradation and the coefficient of variation of the initial fiber distribution. The parameter $\mu$ provides a useful criterion of fiber damage. The interpretation of $\mu$ as the number of breaks per unit length per unit time introduced in time $t$ permits the assignment of a quantitative measure of fiber breakage to a given ginning (or bacteriological decay) process. The larger the value of $\mu$, the greater is the number of breaks sustained by the fibers. Thus, if $\mu = 0.1$ $(\text{in.})^{-1}$, the interpretation is that there has been one break somewhere in ten lineal inches of fibers.

It is of interest to study the behavior of the solution $W(l, t)$ as the parameter $\mu$ increases. For simplicity, imagine that the initial fiber distribution is a single Gaussian, the equation of which is

$$W(l, 0) = 0.30\, e^{-18.1(l-1.20)^2}$$

This corresponds to constants $A_1 = 0.125$ and $\sigma_1 = 0.167$. In Figure 3, $W(l, t)$ is shown for several different values of $\mu$. As the value of $\mu$ increases, the original distribution function is, in effect, destroyed. Finally, in the limit as $\mu \to \infty$, all fibers would be in the cell of length $\frac{1}{8}$ in. or less. This type of behavior, the transition from an initial (sharp) distribution function to a final sharp distribution function, has been found by other writers in the study of hydrolysis and other random chain-scission processes [1]. The fact that the rate equations for change in molecular size distributions with time lead to solutions of a form similar to Equation 8 or 10 is not surprising. As Montroll [6] points out, some of the aspects of depolymerization follow from the solutions to corresponding problems in radioactive decay. To put it another way, Equation 5 and radioactive decay equations are both, in probabilistic interpretation, examples of Markov chain equations.

**Acknowledgment**

The authors wish to thank Dr. Wayne A. Bowers, Physics Department, University of North Carolina, for a careful review of the manuscript and for several helpful suggestions.

**Literature Cited**

1. Grassie, Norman, *The Chemistry of High Polymer Degradation Processes*, London, Butterworth (1956); especially Chapter 3 and References 19–24 in that chapter.
2. Heyn, A. N. J., *Tex. Industries*, **120**, No. 5, 137 (1956).
3. Jahnke and Emde, *Tables of Functions*, Berlin, B. G. Tuebner, (1933).
4. Leitgeb, D. J. and Wakeham, H., TEXTILE RESEARCH JOURNAL **24**, 1047 (1954).
5. Montgomery, R. A. and Nissing, T. J., The Cotton Gin and Oil Mill Press, March 9, 1957.
6. Montroll, E. W., *J. Am. Chem. Soc.* **63**, 1215 (1941); esp. p. 1219.
7. Moore, V. P., USDA Circular 922, July 1953.
8. Thompson, D. O. and Holmes, D. K., *J. Appl. Phys.* **27**, 713 (1956).
9. Wakeham, H., Stickley, H., and Spicer, N., TEXTILE RESEARCH JOURNAL **24**, 1037 (1954).
10. Webb, R. J., USDA Preliminary Report on Problems and Methods in Cotton Ginning, April 1929.

*Manuscript received November 4, 1957.*

# The Reliability of the Soil Burial Method for Evaluating Textile Preservative Treatments[1]

**J. M. Ashcroft**

*Materials Branch, U. S. Army Engineer Research and Development Laboratories, Fort Belvoir, Virginia*

**Abstract**

The variability in the degradation rate of a fabric treated with each of two rot-inhibiting treatments was measured after burial in a biologically active soil for varying periods of time under controlled conditions. The purpose of the experiment was to determine what limits of reliability might be expected in average strength measurements as a consequence of random variations inherent in the soil burial procedure employed under practicable measures of control. The experiment utilized a random block design, which permitted estimation of the effect of soil variations among the several blocks. The design also made possible an analysis of the results as 5 replicate measurements of 10 observations, or, when combined, as a single measurement of 50 observations.

The results showed that the variability in fabric strength measurements increased as deterioration progressed, reaching a maximum when 40–60% of the original strength was lost. The increase was greater in the treated than in untreated fabric, and for one treatment than for the other. The degradation rate of untreated fabric in the several soil blocks showed highly significant differences. But a similar block effect on the treated fabric could not be detected in 8 of the 10 exposure periods. The increased variability and reduced rate of deterioration resulting from the treatment evidently tended to mask the smaller effect of soil variation. At the stage corresponding to the greatest variability, the 95% confidence range for measurements based on 10 observations was for one treated fabric 43.8% of the original strength, and for the other, 22.4%. This degree of precision does not justify the high confidence often placed in soil burial test data based on 10 or fewer observations per sample. The variability measurements indicate several measures that can be taken to increase the precision of the test procedure by reducing the random variations.

The shortcomings inherent in the general practice of reporting the results of soil burial tests as the average percentage of the original strength lost or retained are discussed. A novel method of presenting test data in the form of a histogram of the cumulative frequency distribution is proposed as a means of overcoming most of the disadvantages of the conventional methods of reporting data.

## Introduction

The effectiveness of rot-inhibiting preservative treatments for cotton textiles usually is determined by a biological test. The procedure followed generally is to apply the treatment to cotton cloth, expose a sample of the cloth to conditions which favor deterioration by rot, and compare the strength of the sample under standardized conditions with the strength of another sample which has not been so exposed. The results are usually recorded as the percentage of strength lost or retained after the exposure. Comparison with the results obtained with the same fabric but without the treatment provides a measure of the effectiveness of the treatment.

The type of exposure may be varied in a number of ways, but one which has found considerable favor in the past is that of burying the treated cloth in the soil. This is a very severe exposure, because the material is subjected to a wide spectrum of degrading organisms at once. A detailed description of a soil burial test is given in Federal Specification CCC-T-191, "Textile Test Methods." The procedure described apparently was intended as an acceptance test for use in connection with the purchase of finished textile materials treated by industrial

[1] The subject matter of this report was presented as part of the program of the Society of Industrial Microbiology at the annual meeting of the American Society of Biological Sciences, Leland Stanford University, California, August 26–29, 1957.

processing methods. Variations of the method have been employed rather extensively, however, as an investigative tool for such purposes as comparing the effectiveness of fungitoxic compounds or evaluating treatments in the process of development.

In more recent years, the soil burial method has been the target of considerable adverse criticism, especially among laboratories of the Department of Defense. This stems from inconsistencies among the results obtained by different laboratories which have used the method to evaluate the same treatments. The inconsistencies usually have been attributed to the variability of the different soils used, but the results obtained with the soil burial procedure are affected by a number of random variables other than those of the soil. For example, variations incidental to the spinning and weaving of the fabric, in the application of the treatment to the fabric, and in the process of selecting and measuring a representative sample all have effects in addition to those of the soil.

This investigation is an attempt to estimate the magnitude of these several random variables and of their combined effect on the efficacy of soil burial technique as commonly employed to distinguish real differences among preservative treatments. It was also expected to provide a guide to practicable modifications which would serve to increase the reliability with which such differences might be detected.

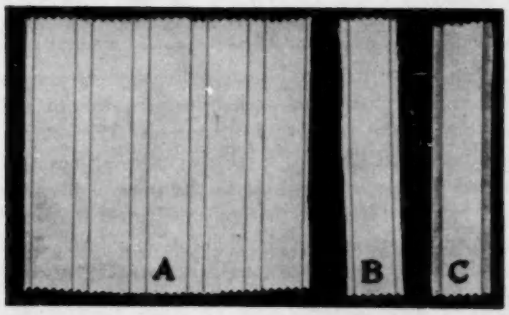


**Fig. 1.** The test fabric showing (A) spacing of colored warp yarns, (B) break specimen formed by cutting between narrowly spaced colored yarns, and (C) break specimen reduced to standard size by raveling warp to colored yarn along both edges.

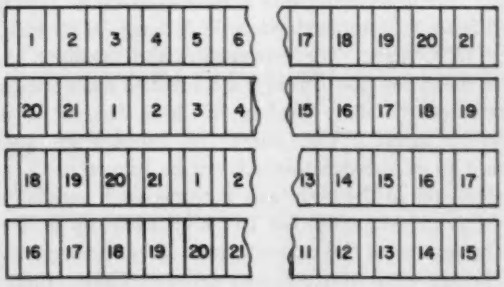


**Fig. 2.** Scheme for numbering break specimens.

## Procedure

Since the description of the soil burial method given in Federal Specification CCC-T-191 was modified for this investigation, a brief description of the modifications will be given.

### *The Fabric*

The fabric used was a cotton duck, weighing approximately 10 oz./yd.$^2$ with dark colored yarns woven at regular intervals in the warp. These are shown in Figure 1, which also illustrates how the break specimens are cut and raveled. The advantage of the colored yarns, other than economy, is that all of the specimens have the same number of warp yarns despite any dimensional changes which may result from varied treatment. The breaking strength of the fabric as received had a standard deviation of 8.5 lb.

### *The Sampling Plan*

One hundred strips of this fabric, 6 in. in length and the width of the roll, were cut from a single piece of stock and numbered serially as cut. The sequence of the strips was then changed to a random one by the use of a table of random numbers, and the strips were renumbered in serial sequence. The first 40 strips, numbered 1 to 40, were then impregnated with copper naphthenate; the second 40, numbered 41 to 80, with G-4 [2, 2′ methylene bis (4 chlorophenol)]; and the last 20 strips were left untreated. The break specimens of the successive strips in a series which had received one of the preservative treatments were now numbered as shown schematically in Figure 2. After the specimens were cut, those with the same number (one from each of the strips in the series) were combined into bundles. In each bundle, the order of the specimens corresponded to the order of the strips. The several bundles of specimens were then combined in a single series, beginning with the bundle made up of specimens numbered 1 and ending with those num-

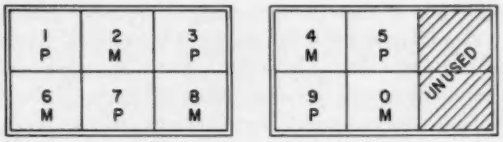


**Fig. 3.** Arrangement of block areas in soil beds; (P) used for preliminary run, (M) used for main run.

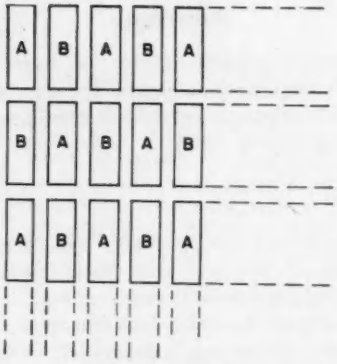


**Fig. 4.** Arrangement of break specimens in each block.

bered 21. Consequently, any considerable number of specimens taken in sequence would be an unbiased sample of the treated fabric which it represented.

*Application of Treatment*

The treatment was applied to the fabric by immersing it in a solution of the fungitoxic compound, passing the wet cloth between the rolls of a laboratory padding machine under pneumatic pressure to remove the excess solution, and then drying it by means of a forced draft of air. During the drying period the fabric was stretched in a horizontal position to reduce migration of the solution. The deposition of the treating compound on the fabric was controlled by means of the pressure on the padder rolls and the concentration of the treating solution. The nominal strength of the G-4 treatment was 0.5%; that of the copper naphthenate treatment was the equivalent of 0.6% copper. Both of these figures are based on the dry weight of the fabric.

*The Experimental Design and Burial Technique*

To reveal the effect of soil variation, a block design was employed in burying the samples. Two large soil boxes (82×44 in.) were divided into 10 equal-sized blocks, which were numbered as shown schematically in Figure 3. The odd-numbered blocks were used for a preliminary run. The results of this run do not appear in the final analysis. They were used, however, to determine when the harvesting of samples from the even-numbered blocks should begin and to estimate the time lapse between the taking of successive samples. The specimens making up the preliminary run were buried 1 week prior to the burial in the even-numbered blocks, which were used for the main experiment.

Fifty specimens of each treated fabric were buried in each of the 10 blocks in the alternating pattern shown in Figure 4. When the specimens were harvested, 10 specimens of each treated fabric, chosen from scattered locations within each of 5 blocks, were removed at one time. Immediately after the last of the treated fabrics had been harvested, 50 untreated specimens were buried in each of the 5 blocks used for the main experiment. These were harvested at the rate of 10 specimens/day from each block from the third to the seventh day of burial inclusive.

The method of burying the specimens differed from either of the methods recommended in the Federal Specification previously mentioned. In our laboratory, we have had some unsatisfactory results with the recommended burial method due to the fact that, quite often, the maximum deterioration would occur at the end of the specimen. Since this part of the specimen is held in the jaws of the machine during breaking, the recorded break does not measure the strength at the point of maximum degradation. For this reason, the specimens in this experiment were buried with only the middle in the soil, both ends protruding above the surface.

*The Soil Beds*

The soil beds were located in a tropical test chamber. The interior of this chamber, which is shown in Figure 5, is approximately 32 ft. long, 20 ft. wide, and 14 ft. high. The temperature and humidity inside the room pass through a controlled cycle which simulates the daily cycling of these factors in a tropical forest. The ranges of temperature and humidity of the cycle are shown in Figure 6.

The soil in the beds was not prepared especially for this investigation, but had been made up in the early months of the current year. It was composed of humus derived from well decayed leaves, sand, and a natural sandy loam soil. All components were

screened through a ¼-in. screen before mixing, which was effected in a concrete mixer. During the mixing, calcium carbonate equivalent to 2% of the dry weight of the soil was added. The resultant soil mixture was porous, well aerated, and biologically active, with a moisture content between 25 and 27.5%, a pH between 6.2 and 6.6, and with little tendency to lump under pressure.

## Results and Discussion

*Untreated Fabric*

The soil burial results given in Table I show that the untreated fabric lost, on the average, 49% of its strength in 3 days and 77% in 5 days (see "mean" for all blocks). This indicates that the biological activity of the test soil was fairly high. The arithmetic mean strength declined progressively for each succeeding burial period. Moreover, comparison with the standard error (SE) [2] indicates that the difference between the mean for any period and that for the succeeding period were statistically significant at the 5% level.[3] The period means for all blocks may be taken, therefore, as a reasonably accurate measure of the degradation resulting from the difference in the exposure time.

An analysis of variance [4] test applied separately to each of the burial periods shows that the results obtained from the several blocks were different at a significance level of 0.1%. Therefore, despite the

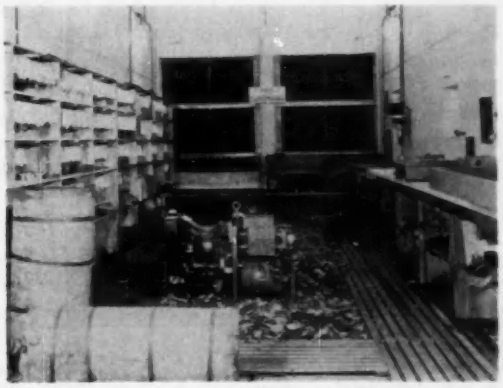

**Fig. 5.** The tropical test chamber.

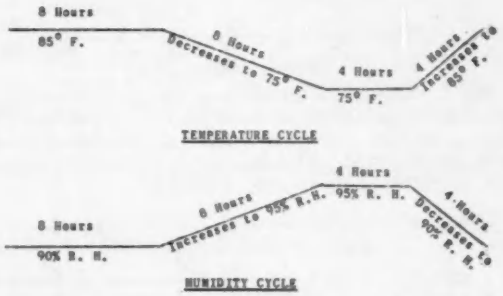


**Fig. 6.** Temperature–humidity cycle of the tropical test chamber, Engineer Research and Development Laboratories, Fort Belvoir, Va.

[2] The standard error is a measure of the deviations, about a population mean, of sample means of a given number of observations selected at random from the population. If each of the sample means is the average of an equal number of observations (such as breaking strength measurements), and the number of observations is four or more per mean, the distribution of the sample means will approximate a normal curve with a standard deviation which is estimated by the standard error of each sample. The sample mean and the standard error may therefore be used to estimate the probability that a deviation of any magnitude will occur by chance. For example, deviations from the population mean equal to or greater than ±1 standard error may be expected with a frequency of approximately 30%; ±2 standard errors, 5%; and ±3 standard errors, 0.26%.

[3] This statement implies that a difference as large as the one observed would not be expected to occur by chance more often than once in twenty replications (or 5%) on the average, if the two samples means were estimates of the same population mean.

[4] For a discussion and description of this test the reader is referred to a standard textbook of statistical methods, such as "Introduction to Statistical Methods," Dixon, W. J. and Massey, F. J., McGraw-Hill, N. Y., 1951.

**TABLE I. Percent Strength Retained and Standard Error of Untreated Fabric After Soil Burial**

| Soil burial period, days | Block number 2 | | 4 | | 6 | | 8 | | 0 | | All blocks | |
|---|---|---|---|---|---|---|---|---|---|---|---|---|
| | Mean | SE | Mean | SE | Mean | SE | Mean | SE | Mean | SE | Mean | SE |
| 0 | | | | | | | | | | | 100 | 0.88 |
| 3 | 40 | 1.89 | 56 | 5.15 | 43 | 4.91 | 50 | 2.10 | 67 | 1.25 | 51 | 2.03 |
| 4 | 15 | 1.40 | 22 | 2.09 | 34 | 2.22 | 37 | 2.91 | 48 | 1.13 | 31 | 1.89 |
| 5 | 15 | 1.13 | 22 | 1.44 | 21 | 1.48 | 20 | 1.91 | 34 | 1.17 | 23 | 1.08 |

attempt made to prepare a homogeneous test soil, variations remained which were detectable in the results obtained with untreated fabric. This effect of the soil blocks does not affect the period means for all blocks combined, since each block was represented equally in each period mean.

The period means within individual blocks reveal a number of anomalies. For example, in blocks 2 and 4 the results for the fourth and fifth day were no different, and in block 6 the difference between the third and fourth day is of questionable significance. Thus, of the 10 possible comparisons of results differing in exposure time by one day, 3 yielded inconclusive results.

Additional discrepancies appear between blocks. A comparison of the results for blocks 4 and 6 shows, for example, that on the third day the results from the former block were significantly higher in strength than those from the latter; on the fourth day the results indicate the strengths were reversed; and on the fifth day the difference was not significant. No explanation of this can be given other than to suggest that the soil variations noted between blocks may be operative within blocks, although perhaps to a lesser degree.

The standard errors for all blocks in Table I indicate that the variability in strength of the sample increases with the stage of deterioration to a maximum and then declines. This is shown in graphic form much more clearly by Figure 7, in which the cumulative frequency (probability) is plotted against the strength of the specimens for each period sample of 50 observations. The variability is reflected by the range of breaking strengths of the 50 specimens included in the histogram. This range is greatest in the sample exposed for 3 days, and decreases for each succeeding exposure.

All of the causal factors involved in the increase cannot be identified, but soil variations are undoubtedly responsible in part. It is also conceivable that variations in the inherent resistance of the different cotton fibers could also be a factor.

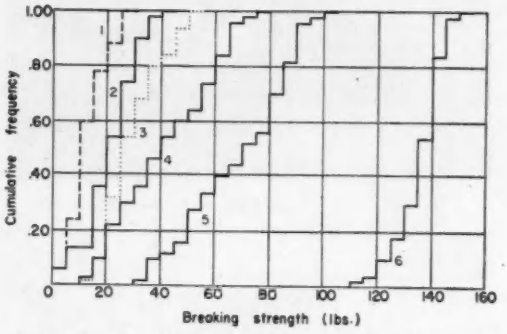


**Fig. 7.** Distribution of breaking strengths of untreated fabric after exposure to soil burial for varying periods. (1) 7 days SB, $\overline{X} = 14.02$; (2) 6 days SB, $\overline{X} = 23.06$; (3) 5 days SB, $\overline{X} = 30.84$; (4) 4 days SB, $\overline{X} = 42.68$; (5) 3 days SB, $\overline{X} = 69.98$; (6) 0 days SB, $\overline{X} = 136.96$.

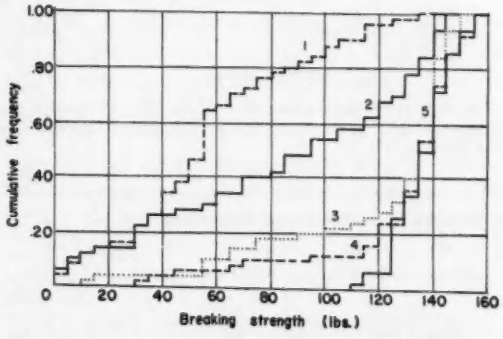


**Fig. 8.** Distribution of breaking strengths of fabric treated with G-4 after various soil burial periods. (1) 40 days SB, $\overline{X} = 59.52$; (2) 31 days SB, $\overline{X} = 88.90$; (3) 25 days SB, $\overline{X} = 123.72$; (4) 21 days SB, $\overline{X} = 131.06$; (5) 0 days SB, $\overline{X} = 138.36$.

*Treated Fabrics*

The soil burial results for the treated fabrics are given in Table II. The most noticeable effect of the treatments is the greatly reduced rate of deterioration. The untreated fabric lost a greater percentage of strength in 4 days than the G-4 fabric lost in 40 days or the copper naphthenate fabric in 49 days. Almost as prominent as the reduction in

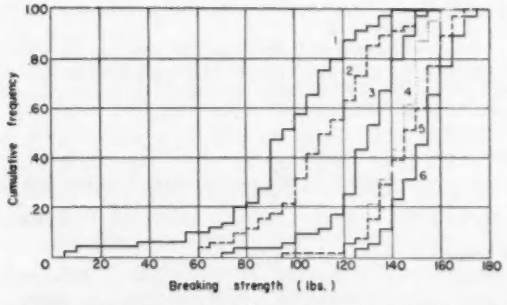


**Fig. 9.** Distribution of breaking strength of fabric treated with copper naphthenate after various soil burial periods. (1) 49 days SB, $\overline{X} = 97.18$; (2) 42 days SB, $\overline{X} = 113.58$; (3) 35 days SB, $\overline{X} = 130.56$; (4) 28 days SB, $\overline{X} = 143.66$; (5) 21 days SB, $\overline{X} = 147.60$; (6) 0 days SB, $\overline{X} = 154.06$.

deterioration rate is the considerable increase in the standard error of the treated fabrics. This represents a further increase in the variability, with respect to the rate of deterioration, of treated compared to untreated fabric at corresponding stages of degradation. As in the case of the untreated fabrics, the maximum variability appears to be reached when the loss of strength is approximately 50% of the original strength. The change in the variability with time of exposure is shown by the histograms of the cumulative frequency distribution for the G-4 fabric in Figure 8 and for the copper naphthenate fabric in Figure 9.

It appears probable that this increased variability is related to the degree of uniformity of the treatment applied. Any nonuniformity would afford varying levels of protection at different points on the surface of the fabric. As the protective material weathers or is leached away on exposure, the differences due to nonuniformity of the treatment would be accentuated, since subminimal levels of protection would be reached at different points at different times. The effect of all such increases in variability is to decrease the precision of the test, because they increase the range of values which are probable from random fluctuations.

In Table II, the period means measure the differences in deterioration of the copper naphthenate fabric in uniform increments of 7 days after the first 21 days. In the column for all blocks, the mean of each succeeding period is lower than that of the preceding period by an amount which is significant at the 5% level or lower. The samples of 50 observations (10 from each block) is, therefore, a fairly reliable measure of the degradation which occurs in this fabric in increments of 7 days soil burial. The reliability of the means of the samples of 10 observations within blocks is, as a measure of the same quantity, however, manifestly low. The results obtained in blocks 4 and 8 after 28 days burial, in block 2 after 42 days, and in blocks 8 and 0 after 49 days are too high to be significant at the 5% level. Thus the means of 10 observations give inconclusive results in 5 of 20 possible comparisons. Even when the difference in the soil burial period is increased to 14 days, 1 of 15 comparisons was inconclusive (compare the means for 21 and 33 days in block 8).

The period means given in Table II for the G-4 fabric measure the degradation after varying increments of exposure time (4, 6, 2, and 7 days). Reference to the means in the column for all blocks shows a difference significant at the 5% level in each succeeding period except that for 33 days. In this case, however, the increment of exposure time over the preceding period was only 2 days. The data indicate, therefore, that the means of 50 observations provide a reliable measure of the degradation of this fabric, if the difference between burial periods is 4 days or more.

If the means of the 10 observations for successive periods within blocks are examined, the same unreliability encountered in the copper naphthenate fabric results may be noted. None of the blocks show, for the 33-day period, a significant difference from the 31-day period. This is, however, not surprising, since the sample of 50 observations in the

**TABLE II. Percent Strength Retained and Standard Error of Treated Fabrics After Soil Burial**

| Treatment | Soil burial period, days | Block number 2 | | 4 | | 6 | | 8 | | 0 | | All blocks | |
|---|---|---|---|---|---|---|---|---|---|---|---|---|---|
| | | Mean | SE | Mean | SE | Mean | SE | Mean | SE | Mean | SE | Mean | SE |
| | 0 | — | — | — | — | — | — | — | — | — | — | 100 | 1.0 |
| | 21 | 100 | 1.4 | 100 | 1.9 | 92 | 5.6 | 75 | 10.2 | 100 | 2.1 | 95 | 2.7 |
| G-4 | 25 | 87 | 9.1 | 93 | 3.8 | 87 | 10.1 | 87 | 6.9 | 93 | 6.2 | 89 | 3.3 |
| 0.5% | 31 | 53 | 11.4 | 62 | 8.9 | 62 | 11.9 | 55 | 12.0 | 89 | 7.9 | 64 | 4.9 |
| | 33 | 46 | 9.8 | 62 | 9.8 | 46 | 10.1 | 69 | 9.1 | 95 | 2.5 | 64 | 4.6 |
| | 40 | 48 | 6.7 | 39 | 6.5 | 34 | 8.3 | 40 | 8.6 | 55 | 9.5 | 43 | 3.6 |
| | 0 | — | — | — | — | — | — | — | — | — | — | 100 | 1.1 |
| Cu | 21 | 100 | 3.4 | 96 | 2.2 | 97 | 1.8 | 89 | 4.2 | 97 | 2.4 | 96 | 1.3 |
| Naph | 28 | 92 | 2.6 | 94 | 1.8 | 92 | 2.5 | 96 | 1.7 | 92 | 2.2 | 93 | 1.0 |
| 0.6% | 35 | 86 | 3.5 | 85 | 4.6 | 85 | 2.8 | 85 | 2.7 | 83 | 3.3 | 85 | 1.5 |
| Cu | 42 | 81 | 3.9 | 73 | 3.0 | 71 | 4.6 | 68 | 5.2 | 75 | 5.1 | 74 | 2.1 |
| | 49 | 58 | 5.5 | 63 | 3.4 | 54 | 8.6 | 67 | 5.2 | 69 | 3.2 | 63 | 2.5 |

all block column is likewise not significant. Exclusive of the 33-day results, however, those for 25 days in blocks 6 and 8, 31 days in block 0, and 40 days in blocks 2 and 6 are not significantly different at the 5% level from those for the preceding period. The number and percentage of inconclusive results among the G-4 fabric results for the several increments in the exposure period are, therefore, as follows:

| Exposure increment, days | Inconclusive results | Percent inconclusive |
|---|---|---|
| 2 | 5 | 100 |
| 4 | 2 | 40 |
| 6 | 1 | 20 |
| 7 | 2 | 40 |

From the foregoing it should be clear that, while samples of 50 observations will estimate with reasonable accuracy the degradation which occurs between successive periods of exposure under the conditions of this experiment, the same statement cannot be made for samples of 10 observations. While interesting, this information is not very useful, since the comparison involves the period of exposure which may be varied at will. A comparison of the efficiency of samples of 50 and 10 observations independent of the exposure period is, therefore, desirable. The recorded standard errors of the various samples permits such a comparison.

The best available estimates of the variability at the several stages of deterioration are given by the standard error in the column for all blocks in Table II. For the G-4 fabric the maximum variability (SE=4.9) is that of the exposure for 31 days. This, then, is the determination which would be expected to be the least precise. It shows that the mean obtained when the variability is greatest may be expected to lie outside of the range $64 \pm 9.8\%$ with a probability of 5%. The 95% confidence range extends, therefore, from 54.2 to 73.8%, or 19.6% of the original strength.

The corresponding range for a sample of 10 observations may be computed. If the standard error ($SE_0$) for a sample of $N_0$ observations is given, the standard error ($SE_1$) for a sample of any number of observations ($N_1$) is given by the relationship

$$SE_1\sqrt{N_1} = SE_0\sqrt{N_0} \qquad (1)$$

The computed standard error for a sample of 10 observations is 10.95. Estimates of the mean based on 10 observations would be expected to lie outside the range $64 \pm 21.9\%$ with a frequency of 5%. The 95% confidence range for such estimates would, therefore, be 43.8% ($\pm 2 \times 10.95$) of the original strength. In the same way the confidence range at any level and for any number of observations per sample may be computed. The 95% ranges for the G-4 and copper naphthenate fabric for samples of 5 to 100 observations are shown in Figure 10. The greater precision obtained with the latter fabric is due to its much lower variability.

Under given experimental conditions and with a given procedure, the results of an experiment can be made as precise as desired by the experimenter. This can be done, however, only by increasing the number of observations per sample. Suppose it were necessary to obtain results which would be accurate to within 5% of the original strength with a confidence level of 99%. Then, since 99% corresponds to a deviation from the mean of 2.576 times the standard error (SE)

$$SE = \frac{5}{2.576} = 1.941$$

If this value is substituted for $SE_1$, and 4.9 and 50 for $SE_0$ and $N_0$ respectively in Equation 1, the number of observations required may be estimated by solving for $N_1$. This gives the number 319 for the G-4 fabric. The corresponding number for the copper naphthenate fabric is 83. One measurement of the latter fabric is, therefore, equivalent to 3.84 measurements of the former fabric. The difference represents an increase in efficiency equal to 284% for the copper naphthenate fabric. This greater efficiency is due entirely to the lower standard error for the copper naphthenate fabric.

Variance analysis tests applied to the treated fabric indicated that the effect of the soil in different blocks was not significant at the 5% level for the copper naphthenate fabric in any exposure period. For the G-4 fabric, the same tests yield a positive answer for the periods of 21 and 33 days only. These results are, therefore, in striking contrast with the results obtained with the untreated fabric, but the difference is not necessarily contradictory. The block effect is no doubt real, but, in the results for the treated fabric, it is much reduced in relative importance as a cause of the observed variations, being masked by the much larger effect of the treatment. This decreased importance is probably due

to the reduction in the overall deterioration coupled with the increase in the variability. Both of these effects result from the treatment.

*Suggestions for Increasing Precision*

The results of this investigation emphasize the need in soil burial tests for techniques and procedures which will reduce the random variability of such tests to a minimum. In fact, such techniques are an absolute necessity if any major improvement in the precision of soil burial results is to be effected without resorting to much more extensive testing. Consequently, investigations aimed at reducing variability in the overall procedure probably will be quite rewarding in the long run. Any improvement in the procedure will, in all probability, be brought about, however, by reducing the variability of specific techniques employed in the overall procedure. This investigation points out a number of directions which such attempts at improvement might take with considerable promise of success. One of these is in the basic fabric used in the evaluation of treatments. The art, skill, and science of the spinning and weaving industry should be employed to the maximum practical extent to obtain a fabric in which variability has been reduced to a minimum. A second is in improved design of experiments. The random block design used in this experiment is an effective way of nullifying the effect of soil variability. It is not necessarily the best, however, and other designs should be investigated for greater efficiency. A third direction would be in the improvement of the technique of applying the treatment. The present investigation provides an indication that this might prove to be very rewarding indeed.

Comparison of the histograms for the G-4 fabric in Figure 8 with those for the copper naphthenate fabric in Figure 9 reveals that the variability of the former is much greater than that of the latter at comparable stages of degradation. The upper fourth of the G-4 histograms indicates, however, a rot-inhibiting potential for this treatment not greatly different from that of copper naphthenate. This suggests that the observed differences between the two treatments may not be due to any appreciable differences in the potential of the two treatments but rather to the degree of uniformity, or to the persistence, of the treatment. If this be essentially correct, the poorer results obtained with the G-4 treatment could reflect properties inherently faulty for

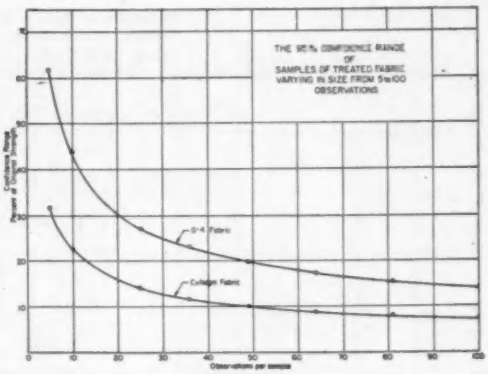


**Fig. 10**

the intended purpose. On the other hand, they could be caused by an application technique which was less favorable for depositing a uniform, adherent coating than was achieved in the copper naphthenate treatment.

The latter conjecture is made to appear more plausible by the fact that different solvents were used to apply the treatments. The solvent for copper naphthenate was toluol, and for G-4, alcohol. Toluol is an effective solvent of waxes, oils, and fats; alcohol is rather ineffective in this respect. The behavior of the two solvents towards the natural waxes, fats, and oils in cotton fibers may account in part for the different results obtained with the two treatments.

*Suggested Method of Reporting Data*

The general practice of reporting the results of soil burial tests conducted to evaluate preservative treatments as the average percentage of the original strength lost or retained is unfortunate from a number of viewpoints. Although the serviceability of a fabric depends largely on strength, preservative treatments are applied usually to preserve some minimum level of strength. In evaluation of such treatments, interest should be principally focused on how long, at least in a relative sense, the treatment may be expected to preserve this minimum strength. This interest would be better satisfied if the results were expressed in terms which represent time.

Coupled with this primary interest is a secondary one. This stems from the fact that failure of the treatment can result in consequences of varying degrees of seriousness. Thus a natural concern with

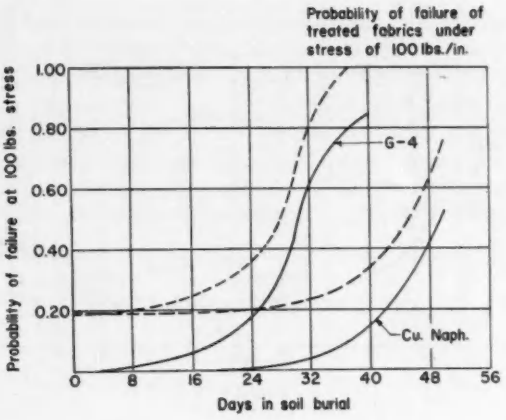


**Fig. 11**

the probability of failure of the treatment arises. Because of these two interests, evaluation results are in the most generally useful form when they satisfy the desire to know how long a treatment will preserve a given level of strength with a given level of confidence.

The greater precision of answers given in accord with the latter form may be exemplified by two different answers to the question: What was the relative effectiveness of the copper naphthenate and the G-4 treatments shown in this experiment? This could be answered with data taken from Table II by stating that fabric treated with G-4 retained 43% of its original strength after 40 days burial and that fabric treated with copper naphthenate retained 63% after 49 days. This answer would indicate that the latter treatment is better but would furnish at best only a very imprecise measure of how much better. Note, however, how much more precise the following answer would be: fabric treated with G-4 failed at 100 lb. stress with a frequency of 20% after 25 days exposure; whereas the same fabric treated with copper naphthenate failed at the same stress with the same frequency after 42 days exposure. In the latter answer the ratio of the exposure time (42/25 = 1.7) is a direct measure of the relative effectiveness at the same confidence level, provided the fabrics were tested under the same conditions.

If soil burial exposure results are recorded in the form of cumulative frequency histograms similar to those in Figures 7, 8, and 9, such comparisons are made very simply, even though the original data are obtained from tests in which the exposure periods were unequal or irregular. To illustrate, the probabilities of the G-4 fabric failing at 100 lb. stress after the several periods of exposure can be obtained from Figure 8. These probabilities are given by the ordinates of the several histograms at the abscissa representing 100 lb. If the probabilities are plotted as ordinates against the soil burial period as the abscissa, the curve labeled G-4 shown in Figure 11 is obtained. Similar data obtained from Figure 9 yield the curve for the copper naphthenate fabric labeled Cu Naph. in Figure 11. The relative effectiveness of the treatments at any probability level is now obtained by the ratio of the abscissas of the two curves. At the 20% level this is as 42 days are to 25 days, or 1.7. By a similar process, any treatment might be ranked on a single scale, if the treatment and a standard treatment were applied to the same fabric and compared after exposure to the same test conditions. In Figure 11, the broken line curves represent the lower limits of the 95% confidence band for the solid line curves. Comparison of the two treatments on the basis of the broken lines would indicate a greater superiority on the part of the copper naphthenate treatment. For example, at the 20% probability level, the abscissas for the treatments are 23 days and 8 days for copper naphthenate and G-4 respectively. The ratio of these periods gives a factor of 2.9.

The presentation of data in the form of a cumulative frequency histogram has other advantages. It shows at a glance the range and distribution of values which are hidden in an average value. This range and distribution is the key to the limits of reliability of the estimated mean, and enables the reader to interpret the data independently of the interpretation of the reporter. This graphic form of presentation may also indicate causes of observed differences between treatments other than primary causes. For example, comparison of Figure 8 with Figure 9 suggested that observed differences may be due to differences in application technique, as previously discussed.

## Acknowledgments

The author gratefully acknowledges the assistance of Samuel Shapiro and Robert W. Ragland in preparing the specimens and in making the many measurements required in this investigation.

*Manuscript received December 5, 1957.*

# Punched-Card Methods for Studying Fiber-Yarn Relationships[1]

**Helmut Wakeham[2] and La Dean Steward[3]**

*Textile Research Institute, Princeton, New Jersey*

**Abstract**

Methods of applying punched-card computing to a study of the relationships between fibers and yarns are described. Various factors such as fiber property distributions, fiber arrangements, the interaction of fiber properties with yarn structure, and the yarn breakage mechanism are considered. Some informational needs which may lead to a better comprehension of the problem and ultimately to a valid prediction of yarn properties are discussed.

## Introduction

Recently developed fiber tests have permitted the definition and evaluation of many "new" fiber properties. By these new tests it is possible to determine accurate means and variations for many properties of single fibers within a sample and also to explore interrelationships between fiber properties for the same fiber. The basic information needed to obtain an estimation of yarn (and fabric) properties from fiber data is, therefore, obtainable.

The predictions from these data should be considerably improved over those made from empirical or correlation procedures [22], provided methods can be set up for handling the masses of fiber data necessary to describe adequately a fiber sample. Fortunately, such methods are available with high speed data processing machines. The present paper describes one approach to the application of punched-card computing equipment to the problem of translating fiber properties into yarn characteristics. While the method is still far from complete, considerable progress has been made in understanding the problem.

Although the methods herein described should be applicable to all types of staple and filament yarns, this work has been concerned only with cotton yarns. Actually this restriction is no limitation of the field. Staple yarns present many complexities not present in filament yarns. Some of these complexities are considerably more involved in cotton yarns than in yarns of other materials. It seemed, therefore, that application to cotton of the methods herein described would provide a most rigorous test of their usefulness and generality. Subsequent modification, for other yarn structures, of those methods found successful with cotton should then be a relatively simple matter.

[1] A report of work done under a contract with the Office of Naval Research, Organic Materials Branch.

[2] Present address: Ahmedabad Textile Industry's Research Association, Ahmedabad 9, India.

[3] Present address; Wayland College, Plainview, Texas.

## The Problem

A generalized statement of the problem considered here might be made in the form of a question: Under the conditions of yarn structure, how do the properties of the constituent fibers manifest themselves to impart to the yarn its observed behavior? The various factors relating to this problem may be classified into several groups, enlarged upon below.

### *Fiber Properties*

These properties include fiber length, cross-sectional area and shape, crimp, and stress-strain derived parameters in tension, torsion, and bending. It is important to remember that individual fibers may vary greatly in the values for the property parameters. Part of this variation may be overcome by using distributional indices as well as mean values [14], but in many cases the property values are not distributed normally, and the use of conventional indices such as standard deviations may give misleading results. This situation may be illustrated by the cotton fiber length distribution, which is usually bimodal for uncombed cotton samples [18].

*Distribution of Fibers in the Yarn*

In staple yarns the number of fibers in the yarn cross section usually varies considerably from point to point, as indicated by conventional unevenness measurements. If the average number of fibers in the yarn cross section is small, there may also be appreciable differences in average properties of the fibers found in different locations. At some points in the yarn the fibers may be predominately long, or strong, or stiff, or flat, or kinky. Thus there may be all sorts of heterogeneities in fiber distribution along the length of the yarn. Cross-sectional variations in fiber properties may also occur. For example, there is some evidence that in spinning a mixture of fibers the stiff ones remain in the center of the yarn and the flexible ones tend to migrate out to the periphery of the yarn [11].

*Arrangement of Fibers in the Yarn*

In the twisted filament yarn the fibers generally follow a helical path along the length of the yarn. Morton and Yen [11, 12] have shown this is not exactly the case with staple yarns. Here the fibers "migrate" or "dart" from one level to another in the yarn cross section; that is, the radius of the helical path varies along the length of the yarn. Fiber ends, and occasionally loops, protrude from the body of the yarn. With highly crimped fibers this fiber migration might be more pronounced than in yarn of low crimp fibers. The extent to which crimp will affect migration probably depends upon the amount of twist imposed upon the fibers, and this will in turn depend upon the number of fibers in the yarn cross section, since it is a fact that the twist is greater in the thin sections of yarn than in the thick portions.

*Influence of Yarn Geometry on Fiber Properties*

In some fibers, especially cotton, the strength and elongation exhibited by the individual fibers depend upon the gauge length (or distance between clamps holding the fiber) used in the test [2, 6, 7, 19]. This effect is due to the large number of relatively weak "links" found per unit length of the cotton fiber. As a result of these, the average fiber strength at a 10-mm. gauge length is only half that at a 1-mm. gauge length.

When a loose yarn is stretched, the twisted structure gives rise to lateral pressures between the fibers which build up from the outer layers of the yarn to the inner core. The greater the stretch, the greater the pressure and the greater the friction. As a result of the friction, the tensional force on the yarn is borne by the fibers, which are now stretched as if held between clamps. The effective gauge length of the "clamped" fiber in the yarn thus probably depends upon its location in the yarn cross section, the yarn twist, the tension on the yarn, etc. The properties of the fiber in the yarn hence are appreciably affected by the yarn structure and the conditions imposed upon the fiber in the process of stretching and breaking the yarn.

*Factors in the Mechanism of Stress Transfer and Yarn Breakage*

Some movement of fibers takes place as the yarn is initially stretched. This is especially true if the yarn twist is low and the fibers are rather kinky. To what extent does this movement take place, and is it desirable or undesirable for good yarn strength? This question is related to those involving the mechanism of yarn breakage when tension is applied. Do the fibers merely slip out or do they break? Do some break first and then the others slip out when the yarn structure disintegrates? The factors of fiber friction and entanglement and the contribution these make in stress transfer also relate to yarn behavior.

It is evident from these considerations that the translation of fiber properties into staple yarn behavior is a rather complex problem. Many of the factors mentioned above cannot be investigated separately but must be considered together. It is for this reason that automatic computing methods such as those employing punched-card techniques seem ideally suitable for studying these factors in staple yarn systems.

## General Approach

Methods employed by previous investigators may be classified as empirical, analytical, and statistical. In the empirical method, one simply makes standard yarns of different kinds of fibers and tries to relate the yarn properties with the fiber properties. The results from these experiments may be analyzed statistically by multiple correlation methods to find out which of the fiber properties tested are most important to yarn behavior [17, 22]. In the analytical approach, various assumptions regarding yarn geometry and fiber properties are used to set up equa-

tions for predicting yarn behavior [1, 6, 13, 14, 15, 16]. This last approach to the problem is generally most fruitful in explaining the mechanism whereby fiber properties produce the properties observed in the yarn.

Each of these methods generally has the failing that the relationships between fibers and yarns are based on average values of fiber properties rather than upon the distributions of fiber properties existing in the sample. Under special circumstances where the distributions of fiber properties are normal and the various properties are interrelated in the recognizable ways, the use of average property values and even of standard deviations in characterizing the sample is often justifiable and profitable [13]. In other cases, such as cotton for example, a valid picture of fiber properties is not always obtained from simple statistical means and standard deviations, and the entire fiber property distribution must be taken into account.

With wide variations in fiber properties possible, the translation problem becomes one in which the yarn property under consideration is the result of superposition of a large number of variables, the values which these variables take being governed by probability laws. Previous methods also generally have not taken the probability considerations into account. In the broad sense, the staple yarn problem is thus a stochastical problem, that is, one governed by probabilistic laws.

The approach to the fiber–yarn translation problem employed in this investigation is essentially a stochastical method in that a mathematical abstraction is used to represent the yarn situation. Combinations of fiber properties corresponding to actual fibers are used as raw materials for the computations, so that the distributions of fiber properties dealt with are similar to those found in reality. These fiber property combinations are inserted into punched cards, which are then assigned positions along a hypothetical yarn axis. Various probability conditions of fiber arrangement and interaction are then imposed upon the yarn and calculations of the resulting yarn properties are made. Assumptions concerning the mechanism of fiber–yarn relationships thus are applied without actually making yarns. In the final examination of the assumptions, calculated yarn properties are compared with those observed for yarns made of the fiber sample originally tested.

## Punched-Card Procedures

The following punched-card machines of the types available from the International Business Machines Corporation were used in this work. They have been described adequately in the literature [3, 8] and will only be listed here.

Card Punch—Type 024
Card Sorting Machine—Type 075
Reproducing Punch—Type 513
Card Collator—Type 077
Accounting Machine (Tabulator)—Type 405
Calculating Punch—Type 602-A

Because of limitations in space, only a broad outline of the punched-card procedures used in this study are given herein. Detailed procedures may be found in the final report of the Office of Naval Research [21], which sponsored the work. It should be emphasized that in work of this sort many alternate procedures to those described are possible, depending only on the ingenuity of the investigator and the limitations of the punched-card machines.

### *Fiber Properties*

In order to obtain the basic data for computation, several hundred single cotton fibers from a representative sample were tested for length, cross-sectional area, breaking strength, and elongation. The last two properties were measured at a gauge length of 2.5 mm. between tabs holding the fibers. Descriptions of the test methods used in these determinations already have appeared in the literature and will not be repeated here [20].

From the measured strength and elongation data, estimated strengths and elongations at 1-, 2-, and 3-mm. gauge lengths were calculated by the use of factors derived from the data of Grant and Morlier [6]. Their results showed that for 1-, 2-, and 3-mm. gauge lengths the fiber strengths were, respectively, 1.20, 1.04, and 0.96 times the strength at 2.5 mm. Since the cotton fiber stress–strain curve is approximately linear, it was assumed that, on the average, elongations at various gauge lengths are proportional to fiber strengths.

From the fiber test data, a deck of punched cards was then prepared to represent the fiber sample in the yarn calculation. In this deck each fiber is represented by a card containing the fiber length, cross-sectional area, strength, and elongation. The

distribution of fiber property values punched in this deck is then the same as that in the original data.

The deck of fiber cards was next expanded to provide enough fibers to make a 100-cm. length of the yarn to be studied. For example, in one case 391 fibers were tested. From the average fiber size it was calculated that approximately 4700 such fibers would be required for 100 cm. of a 36's cotton count yarn. The original deck of 391 cards was, therefore, expanded 12 times by making 11 more cards identical with each of the original ones. With punched cards this operation is very simply and quickly done in the reproducing punch by a "gang punching" procedure. In making the expansion this way, it is assumed that the tested fibers are representative of similar fibers in the larger sample. This assumption is valid if the original selection is properly made and large enough.

*Distribution of Fibers in the Yarn*

A hypothetical yarn axis is set up with 1000 coordinate positions (CP) representing locations on the axis 1 mm. apart. The CP numbers run from 000 to 999 along the 100 cm. of yarn. The fibers are distributed along this hypothetical yarn axis by assigning a three-digit random number to each card in the expanded deck of fiber cards. This number is taken as the CP for the left-hand end of the fiber, the position of the right-hand end being determined by the fiber length.

Various nonrandom distributions of fibers along the yarn axis also may be made. For example, the random number table may be modified to take into account periodicities in yarn size, such as drafting waves, etc. The assignment of yarn CP to the fiber may also be selective to take into consideration the fact that the shorter fibers tend to aggregate in the thick portions of the yarn. These variations in the procedure may all be made quite easily with the punched-card machines.

*Total Number of Fibers and Effective Fibers*

The distribution of fibers along the hypothetical yarn axis next is examined to determine the number of fibers in the yarn cross section at various CP's. Counts are made of the total number of fibers and of the number of effective fibers. A fiber is counted as being effective if it extends through the CP under consideration by at least some short distance; for example, 2 mm. The effective count thus corrects for the number of ineffective fiber ends at or near the CP being examined.

A plot of the total number of fibers in the yarn cross section versus the CP gives an "unevenness" curve similar to those obtained by the various testers being used commercially. The coefficient of variation of the total number of fibers for all the yarn positions is comparable with the unevenness values obtained with a quadratic type integrator on the commercial testers.

From a plot of effective count versus CP, yarn locations containing unusually low numbers of effective fibers may be selected for yarn strength calculations. This selection is based on the assumption that such locations are also weak places in the yarn.

*Assumptions for Calculation of Yarn Properties*

In the computation of yarn strength and elongation for the selected position, other assumptions must also be made. Since the estimated yarn properties will depend greatly on the nature of these assumptions, they will be listed below. Detailed discussion of their validity will be deferred to a later portion of the paper.

*Distribution of the fibers in the yarn cross section was assumed to be random.* If fibers are located preferentially near the yarn center or periphery depending upon some physical property, such as elastic modulus, the local yarn strength might be appreciably modified.

*The behavior of a given fiber at the local CP under consideration is assumed to be independent of the position of the fiber in adjacent yarn positions.* This situation generally is believed to be the case in filament yarns in which the filament makes a helix with respect to the yarn axis. In staple fiber yarns the fibers at various CP values are at various distances from the yarn axis.

*The effects of yarn twist or fiber obliquity on the relation between fiber and yarn extension are assumed to be defined by the following equation* [13]:

$$e_f = \frac{e_y}{1 + 4\pi^2 n^2 r^2} \qquad (1)$$

where $e_f$ is the fiber strain, $e_y$ is the yarn strain, $n$ is the yarn twist, and $r$ is the distance of the fiber from the yarn axis. For cotton staple yarns this may be transformed to

$$e_f = \frac{e_y}{1 + \frac{0.59\ (TM)^2}{F}\ \frac{r^2}{N}} = \frac{e_y}{C_t} \qquad (2)$$

where $(TM)$ is the twist multiple of the yarn, $F$ is the conventional cotton fiber fineness in micrograms per inch, $N$ is the number of fibers in the yarn cross section, and $C_t$ is the twist correction factor. It will be seen from these equations that since $C_t$ is greater than unity the effect of twist is to increase the fiber extension over the yarn extension for all fibers lying some distance from the center of the yarn. The result will be that the nonsimultaneity of fiber breaking due to differences in fiber strength and elongation will be spread even further by the geometrical factor introduced by fiber twist.

*A number of ways of taking into account the effect of gauge length on fiber strength and elongation have been assumed.* Preliminary calculations showed that the average effective gauge of the fibers in the yarn must be as low as 3 mm. or less in order to attain strength estimates comparable to that exhibited by singles cotton yarn. Three procedures have been used in selecting the fiber strength and elongation values to be used in computing yarn strengths.

1. A standard average gauge length of 2 mm. was assumed for all fibers, regardless of location, arrangement, and twist in the yarn.

2. The fiber gauge length was made to depend upon the total number of fibers and yarn twist at the CP under consideration. If the number of fibers is small, the yarn twist is higher (according to the Spinners' Rule) and the gauge length was assumed to be shorter. Conversely, for thick portions of the yarn, the average gauge length was assumed to be longer. Values such as 2, 3, and 4 mm. were used.

3. The effective gauge length and property values assigned to the fiber were based upon the local position of the fiber in the yarn cross section. Fibers near the center of the yarn, due to pressures from the outer fibers, were assumed to behave as if being stretched with short gauge lengths. The outer fibers, on the other hand, were assumed to be less tightly held and were treated as if their effective gauge lengths were longer.

### *Calculation of Yarn Properties*

In the final calculation the force contributions of individual fibers were calculated as strain is imposed on the yarn. Fiber stress–strain diagrams were assumed to be linear, a close approximation to the actual case. Thus,

$$f_f = ke_f \qquad (3)$$

where $f_f$ is the fiber load, $e_f$ is the fiber strain, and $k$ is the force–extension ratio based on the fiber breaking strength $S_f$ and breaking elongation $E_f$. Substituting from Equation 2 and using $k = S_f/E_f$

$$f_f = \frac{e_y S_f}{C_t E_f} \qquad (4)$$

where $C_t$ is the twist correction factor and $e_y$ is the yarn strain, as before. The load on each fiber is calculated for constant increments of yarn strain. This is continued up to the point where the fiber load $f_f$ equals the fiber breaking load $F_f$. Then, at each value of yarn strain, the load contributions of all the fibers are summed to give the total load on the yarn. The force–extension curve for the yarn was obtained by plotting the yarn extension versus the total fiber force. The maximum point of this curve was taken as the breaking point of the yarn.

## Results and Discussion

While the computing machines are capable of handling many different approaches to the problem outlined above, the decision as to the best approach must be made by the investigator on the basis of his understanding of the yarn situation. This understanding will guide him through the various assumptions which must be made in arriving at a solution of the problem. Therefore, the present study has been aimed primarily at a better comprehension of the problem without attempting to develop a successful prediction formula. In this case, then, the results will constitute observations on the assumptions being made in the course of the computations, and it is from this point of view that the following discussion is presented. Ultimately, it is hoped, a reasonable set of assumptions or conditions can be evolved which will permit a valid prediction of yarn properties to be made.

### *Fiber Distribution and Yarn Evenness*

When fibers are distributed simply at random along a hypothetical yarn axis, the yarn evenness is much better than that experienced from actual spinning processes. The extent of this difference is

illustrated in Figure 1, in which the fiber distribution of the random hypothetical yarn is compared with evenness curves for good and poor 36's carded cotton yarns. The corresponding yarn size coefficients of variation are 11%, 19%, and 34%. These values are to be compared with "standard" coefficients of variation of 19% for a "very even" carded 36's yarn and of 24% for an "average" yarn of the same size.

That actual yarns are even less uniform than expected from a random fiber distribution is well known [5, 10]. What is not clearly understood is how yarn evenness relates to yarn strength. Apparently many factors besides local yarn size affect local yarn strength. This is evident from Figure 2, in which the yarn strength at a clamp spacing of 1 in. is plotted against the local yarn size obtained by weighing the broken yarn ends between the clamps.

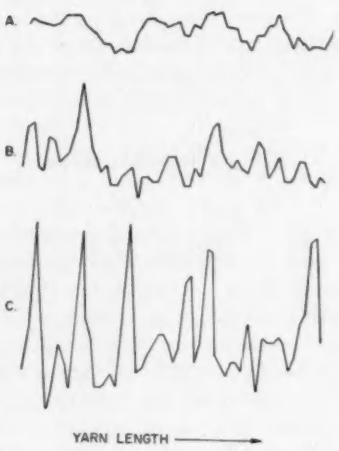


**Fig. 1.** Lengthwise yarn size variations: (A) random fiber distributions of hypothetical yarn, (B) a good 36's cotton yarn, (C) a very uneven 36's cotton yarn.

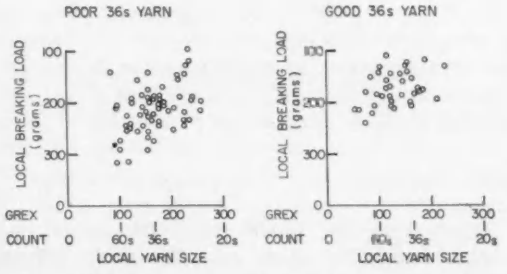


**Fig. 2.** Distribution of local yarn strength with local yarn size for a poor and a good 36's cotton yarn.

While there is a rough general relation between strength and yarn size, there appear also to be local strength coefficients of variation of about 30% and 12% for the poor and the good yarn, respectively, at any given yarn size.

A partial explanation for this observation may lie in the fact that as tension is applied to the yarn, twist "runs" from thick to thin places. If the yarn is generally undertwisted, it would seem altogether possible that thin places would be more nearly at optimum twist than thick places, and that the former might then be stronger than the latter. Other reasons for the failure of local strength to follow local yarn size must lie in the possibilities of finding local concentrations of fiber ends, aggregates of strong (or weak) fibers, etc. In other words, undoubtedly there are other nonuniformities in fiber distribution in the yarn than those which contribute to yarn size.

A successful computational method for the fiber–yarn problem must take into account these nonuniformities in fiber distributions. Many, such as those relating to fiber strength, elongation, etc., may be assumed to be randomly distributed. But others, such as the number of fibers at a given yarn point and fiber length, are definitely known not to be random due to the mechanics of the drafting process. For these the computational instruments must be instructed regarding the kind of a nonuniform fiber distribution pattern necessary to make the hypothetical yarn situation like a real one. It follows also that, for computational purposes, the description of the yarn to be considered must include a specification of the fiber distribution pattern in the yarn.

### *Effective vs. Total Fibers*

The number of effective fibers contributing to yarn strength at any given position along the yarn axis will be less than the total number of fibers at the same point for two reasons. First, a finite length of fiber from its end is required to bind the fiber sufficiently to develop tension in the remainder of the fiber when the yarn is stretched. The ends of the fibers are, therefore, not effective contributors to yarn strengths at those points where they are located. Secondly, there are on the yarn "wild fibers" which, over the greater part of their length, simply lap around the outside of the yarn without being securely anchored at any point. These fibers add weight to the yarn without adding strength.

The decision of what constitutes an effective fiber

depends first on the basic assumption that there is relatively little if any fiber slippage at the yarn breaking point. This situation will be expected to prevail particularly at twists giving maximum strength to the yarn and at higher twists. Shorter [15], in his theory of yarn structure and strength, has given fairly strong support to this view. At lower twists, fiber slippage probably does occur, and the number of effective fibers would be correspondingly reduced.

There is, unfortunately, no factual information regarding the critical distance which the fiber end in the absence of slippage must extend through a given yarn point if the fiber is to support a load and break rather than slip. Gregory [6] has defined half the fiber length as a critical length at which the fiber–fiber pressure in the yarn is just sufficient to cause the fiber to break when tension is applied. If one accepts that the majority of the fibers at the yarn rupture point are breaking, then Gregory's critical length must pertain to the outer fibers, where it will be a maximum. As the twist is increased, or as the fiber end is located away from the surface and closer to the core of the yarn, then the critical distance must become shorter and shorter. This is because both interfiber pressure and interfiber friction arise from the twist and build up from the surface to the core of the yarn. It would seem reasonable, then, to assume that the critical length of a fiber end in an optimum twist yarn may be considerably less than half the fiber length and, in fact, may not be related to fiber length at all, but rather to factors such as twist, tension, fiber arrangement, fiber crimp, fiber surface characteristics, fiber stiffness, etc. Certainly the fact that fiber length *per se* has a relatively minor effect on yarn strength would not be true if a very great length of bound fiber end is necessary to make the fiber an effective load bearer.

Nevertheless, even these general considerations provide little basis for deciding which fibers at a given yarn point are effective ones. Therefore, it was simply assumed in making the yarn calculations that fiber ends shorter than the assumed effective gauge length are ineffective for yarn strength. The importance of this assumption is reflected in the average ratio of effective fibers to total fibers. In a given hypothetical carded yarn the ratio was 0.78 when the effective fibers were assumed to be those extending 2.5 mm. or more through the yarn position being considered. This ratio increased to 0.91 by reduction of the required extension through the coordinate position to 1 mm. Theoretically the latter case would produce a 16% stronger yarn than the former. It is of interest to note that, even in the best situation of random fiber distribution, the range of ratios for the 2.5 mm. assumption was from 0.67 to 0.86. This variation is simply due to the chance of finding predominately long or short ends at any one yarn location.

Similar calculations also were made for a combed yarn situation in which 20% noils had been removed from the carded yarn cotton considered above. In combing, some of the shorter fibers in the cotton are preferentially removed. This should have the effect of reducing the frequency of fiber ends and of increasing the ratio of effective fibers at any given yarn position. The new ratio was calculated to be 0.80 for the 2.5 mm. case, barely more than the 0.78 value for the carded yarn. Apparently the very appreciable superiority (10–20%) of combed yarn strength over carded yarn strength is due to other factors, such as yarn evenness and improved fiber cohesion through crimp reduction, rather than to reduced fiber-end frequency.

The recent work by Morton and co-workers [11, 12] on the arrangement of fibers in yarns indicates that the blanket assumption of an average ineffective fiber-end length is in reality an oversimplification. As the yarn is spun, nearly all leading ends are tucked within the yarn, whereas trailing ends generally project out from the yarn structure. A refined method of calculation for yarn properties should take this effect into account.

The extent to which "wild" fibers appear on the surface of the yarn has not been measured. Therefore, it has not been possible to incorporate this factor into the computation of yarn behavior.

It is of interest to note that reduction in yarn strength because of "wild" fibers and protruding trailing ends has in a practical way been partially overcome in double creel spinning by the use of a double trumpet feed into the drawing zone of the spinning frame [9]. The yarns produced by this process are much less "hairy" and, it is claimed, 10 to 15% stronger than yarns produced by the single trumpet process.

### *Yarn Force–Extension Curves*

From the foregoing it is apparent that the force–extension relationship calculated by the methods outlined earlier will vary considerably, depending upon

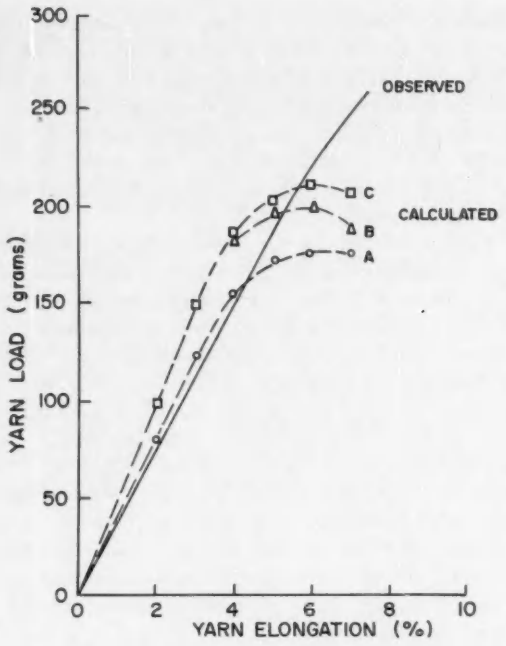


**Fig. 3.** Comparison of computed and observed force–extension curves for 36's cotton yarn. Effective fiber gauge length: (A) constant at 2 mm. for all fibers, (B) based on the number of fibers in the yarn cross section, (C) based on fiber position in the yarn cross section.

the assumptions made in setting up the problem. Furthermore, the fact that a given set of assumptions gives a computed force–extension curve similar to one experimentally determined is no assurance that the assumptions are all correct. With many factors to juggle, one can fairly readily obtain a desired result. The value of such curves in a hypothetical yarn study is mainly in observing the effect which changing one variable at a time has on the shape of the curve.

In Figure 3 are illustrated force–extension curves for three hypothetical 36's cotton yarn calculations, with the corresponding actual curve shown for comparison. All of these are for a twist multiple of 4.0. The hypothetical curves were calculated by the three methods of taking into account fiber gauge length effects outlined earlier. Specifically, in Curve *A* a standard average gauge length of 2 mm. was assumed for all fibers regardless of location, arrangement, and twist in the yarn. In Curve *B* the fibers in the yarn cross section were all assumed to have the same average effective gauge length depending on whether the yarn point was thick or thin; that is, of low twist or high twist, respectively. If the yarn cross section contained 89 or less fibers the gauge length was taken as 2 mm., 3 mm. for 90–110 fibers, and 4 mm. if there were 111 or more fibers. In Curve *C* the effective fiber gauge length was selected on the basis of the fiber position in the yarn cross section: the central 7 fibers were assumed to be at 2-mm. gauge, the next 57 at 3 mm., and the remaining at 4 mm. The force–extension curves are the average of 14 or more calculated positions in each case.

It is seen from Figure 3 that the three gauge-length bases for computation give quite different results and that one could change the calculated curve considerably simply by selecting a different set of effective gauge lengths. For example, by choosing a 1-mm. effective gauge length in Curve *A*, the straight portion of the curve would have been extended to 15% higher strength before bending toward the abscissa, simply because the 1-mm. fiber strength is 1.20/1.04 times the 2-mm. strength value. A further 10% rise would have resulted from the concomitant increase in number of effective fibers at the breaking point.

In the examination of force–extension curves two points were noted. One of these was that all computed yarn strengths fell short of the observed. Apparently in these twisted structures the effect of nonsimultaneity of breaks introduced by the helical structure assumed in Equation 2 causes such a large reduction in the hypothetical yarn strength that the calculated values of strength are less than the actual ones.

Looking again at the yarn structure, one is reminded that Morton and Yen [11, 12] have found that the path of a staple fiber in a twisted yarn is a helix of increasing and decreasing radii and that fibers do not generally remain in the same location "zone" with respect to the yarn axis. A fiber which at one point is on the surface of the yarn may in the next turn be at the core, although such a complete migration is, according to Morton, very rare. Nevertheless, it must be recognized that in a 36's cotton with 24 turns/in. (TM = 4.0) the length of a turn is only 1 mm., and that the fiber in this very short distance may migrate appreciably with respect to the yarn axis. Consequently, the effect postulated in the formulation of Equation 2 may be much less than that being applied in the computation.

Morton's observations also bear on the question of effective gauge length of the fibers in the yarn. If fibers are arranged in staple yarns as his results suggest, then the effective gauge length of an individual fiber probably varies from place to place along the fiber as it migrates into and out of the yarn. Since the migratory path is different for each fiber, the use of an average gauge length for all fibers in the yarn cross section should give a reasonable approximation of the yarn behavior. This would be comparable to the situation for Curve *A* in Figure 3.

A second item noted from this figure was that the actual yarn strength is not the maximum point of the integrated fiber force-extension curve, as computed by the present method, but some value on the curve prior to the region where the curve bends towards the extension axis. Apparently at some stage in the yarn extension process the failure of a relatively small number of fibers at the breaking position causes the yarn to snap long before the maximum integrated force of the effective fibers at that position has been reached. If this is the case, some suitable method of determining the practical end point of the curve must be found before a satisfactory calculation of yarn strength and elongation can be made.

*Variations in Fiber Strength*

If at any given yarn location the fibers by chance are all relatively weak ones, the yarn strength would be effected accordingly. In order to evaluate this factor, the variation of mean fiber strengths for a number of hypothetical 36's cotton yarn positions was computed. It was found that the coefficient of variation for mean fiber strengths was about 5.0%. This means that at about 5 of every 200 yarn locations the average fiber strength will be less than 90% of the overall fiber strength. For coarse yarns the probability of such aggregates of weaker fiber will be less than for fine yarns with fewer fibers in the cross section. Theoretically, the coefficient of variation for mean fiber strengths at random yarn locations is equal to the coefficient of variation for individual fiber strengths divided by the square root of the number of fibers in the yarn cross section. Thus, for example, with cotton in which the coefficient of variation of fiber strength is about 50%, the contribution of this factor alone in a 36's yarn with about 100 fibers in the cross section is represented by a yarn strength coefficient of variation of 5%, precisely the value actually found from the hypothetical yarn calculations.

*Effects of Fiber Elongations*

Individual fiber elastic moduli, breaking elongations, and breaking strength values vary widely in any given cotton sample. It would seem highly unlikely, therefore, that in a bundle of parallel fibers all will exert equal tensions at equal extensions, and that they will all break simultaneously when the yarn rupture occurs. What problably happens is that fibers of low extensibility and strength break at extensions less than the yarn breaking extension. Such fibers do not then contribute to the ultimate strength of the yarn. A very wide variation in fiber breaking elongation therefore would be expected to result in the production of a weaker yarn.

In order to check this effect computationally, comparable yarn situations were examined. In these the effective fibers were of the same average strengths and elongations, but the mean breaking elongations were distributed with different coefficients of variations. Strengths for idealized bundles and hypothetical yarns were calculated. It was estimated that an increase of the coefficient of variation for breaking elongation from 35% to 43% would result in a 20% loss in yarn strength. This observation confirms that of Platt, Klein, and Hamburger [14], who analyzed the influence of elongation variations on the efficiency of fiber–yarn strength translations. It is worthwhile to note in this connection that cotton samples may vary as much as from 30 to 50% in the value of breaking elongation coefficient of variation. In theory, at least, this difference would cause a large effect on yarn strength.

*Distribution of Fibers in the Yarn Cross Section*

Since the individual fibers in a given sample may vary considerably in extensibility and breaking elongation, and since, according to Equation 2, the extensibility expected of a fiber depends upon the fiber position in the yarn cross section, the radial distribution of fibers should influence local yarn strength. In order to evaluate this effect, ten permutations of fiber arrangement for each of two yarn locations were made and calculated for hypothetical strength. The range from the lowest to the highest yarn strength was about 20% of the mean yarn strength in each location.

It should be emphasized that a large part of the

estimated effect of fiber radial distribution on local yarn strength depends upon the assumption of a helical fiber configuration, which is the basis of Equation 2. If this holds, fibers near the center of the yarn are extended more than those near the periphery for a given yarn extension. A concentration of low elongation fibers near the yarn center therefore will result in yarn failure at lower extensions and strengths. If, in the other extreme, the fibers were not in a helical configuration but parallel, as in a bundle, the yarn strength should be appreciably greater than in the twisted arrangement assumed in Equation 2. In the bundle all fibers are, in theory, stretched to the same extent and therefore should work together better in carrying the yarn load. The results of Morton and Yen [11, 12] on fiber arrangements imply that in the real yarn the situation is probably somewhere between the helical arrangement in Equation 2 and the bundle.

## Conclusions

The stochastic method applied with punched-card computing machines appears to offer a new approach to the study of fiber–yarn relationships. The method permits the use of actual fiber property distributions in considerations of the problem. It also makes possible the exploration of various assumptions regarding fiber distributions and arrangements in the yarn, the effective gauge lengths of fibers in the yarn situation, and the effects of the dispersions of pertinent fiber properties such as length, breaking elongation, strength, and fineness on yarn strength.

Although the present investigation of the method has been a very preliminary one, it has revealed the need for additional knowledge regarding fibers and the yarn situation. These needs might be summarized as follows:

1. More accurate data on cotton fiber properties at low gauge lengths are needed to provide raw material for the yarn calculation. The present method of extrapolating from 2.5 mm. to 1 mm. is highly uncertain. The results of this study strongly indicate that the average effective gauge length of fibers in yarns is quite low and may be even less than 1 mm.

2. Additional information is required as to the most probable pattern of fiber distribution in actual yarns, particularly with respect to the relationship between local yarn size and fiber length. It is known in a general way from studies of fiber drafting that thick places in a yarn contain a predominance of short fibers. More precise data on this relationship would be helpful, especially since the average properties of fibers vary somewhat with the length group to which they belong.

3. The available information on fiber arrangement in staple yarns, while extremely valuable to a comprehension of the yarn situation, is inadequate to judge the correctness of Equation 2 for the effect of helical structure on nonsimultaneity of fiber breaking. What is needed is not only the arrangement of fibers in the slack yarn, but also some idea of how the arrangement may be changing as the yarn is being stretched to break. Possibly, with information of this type, Equation 2 may be modified to provide a more true picture of the structure effect for a staple yarn.

4. A theoretical study of the mechanics of staple yarn breakage might give useful criteria as to the point on the yarn extension curve at which yarn rupture might be expected to take place. How, when relatively few of the fibers are broken as a result of yarn stretching, does the resultant transfer of load to those remaining cause a sudden breakage of additional fibers and rupture of the yarn? Can the breakage process be treated as a chain reaction and so explain the final "snapping" of the yarn? Certainly more must be known of this process before satisfactory prediction of staple yarn strength and elongation can be made by analytical and computational methods.

## Acknowledgment

The authors sincerely appreciate the many helpful discussions and suggestions on this problem by Dr. James H. Wakelin and the aid of William P. Virgin on IBM techniques. We are grateful to the Office of Naval Research for a grant-in-aid to one of us (H. W.) for partial support of the work.

## Literature Cited

1. Braschler, E., "Die Festigkeit Von Baumwollgespinsten," Zurich (1935).
2. Brown, K. C., Mann, J. C., and Peirce, F. T., *J. Textile Inst.* **21**, T186 (1930).
3. Eckert, W. J., "Punched Card Methods in Scientific Computation," 136 pp., The Thomas J. Watson Astronomical Computing Bureau, Columbia University (1950).
4. Engineering Research Associates, Inc., "High Speed Computing Devices," 451 pp., McGraw-Hill, New York (1950).

5. Foster, G. A. R., *J. Textile Inst.* **41**, P357 (1950).
6. Grant, J. N. and Morlier, O. W., Textile Research Journal **18**, 481 (1948).
7. Gregory, J., *J. Textile Inst.* **41**, T1, T14, T30 (1950); **44**, T499, T515 (1953).
8. International Business Machines Corporation, "Bibliography on the Use of I. B. M. Machines in Science, Statistics and Education," 60 pp. (1956).
9. Landstreet, C. B. and Ewald, P. R., *Textile Industries* **117**, No. 5, 114 (1953).
10. Martindale, J. G., *J. Textile Inst.* **41**, P340 (1950).
11. Morton, W. E., Textile Research Journal **26**, 325 (1956).
12. Morton, W. E. and Yen, K. C., *J. Textile Inst.* **43**, T60 (1952).
13. Platt, M. M., Textile Research Journal **20**, 519 (1950).
14. Platt, M. M., Klein, W. G., and Hamburger, W. J., Textile Research Journal **22**, 641 (1952).
15. Shorter, S. A., *J. Textile Inst.* **48**, T99 (1957).
16. Sullivan, R. R., *J. Appl. Phys.* **13**, 157 (1942).
17. Virgin, W. P. and Wakeham, H., Textile Research Journal **26**, 177 (1956).
18. Wakeham, H., Textile Research Journal **25**, 422 (1955).
19. Wakeham, H. and Spicer, N., Textile Research Journal **21**, 187 (1951).
20. Wakeham, H., Virgin, W. P., and Spicer, N., Textile Research Journal **24**, 802 (1954).
21. Wakeham, H., Steward, L., Virgin, W., and Wakelin, J., "Research in Fiber-Yarn-Fabric Relations by Modern Statistical Methods," August, 1956, Final Report to the Office of Naval Research on Contract No. Nonr-391(00), Project NR330-021.
22. Webb, R. W. and Richardson, H. B., "Relation of Six Elements of Raw Cotton Quality to Strength of 22's and 50's Yarn (Long Draft)," Processed, 1950. 63 pp., U. S. Department of Agriculture, Production and Marketing Admin.

*Manuscript received March 4, 1957.*

---

## MIT Summer School Program
## Techniques in Textile Research

A one-week Special Summer Program, Techniques in Textile Research, will be given August 18–22 at the Massachusetts Institute of Technology. The course will emphasize the planning and analysis of experiments and will review current research techniques utilizing polarized light, modern instrumentation, variance analysis, differential geometry, and microscopy. There will be laboratory demonstrations covering the selection and handling of equipment and the integration of optical with physical and chemical techniques.

For further information write to the Textile Division, Department of Mechanical Engineering, Massachusetts Institute of Technology, Cambridge, Mass.

# Letters to the Editor

Short communications in the form of Letters to the Editor are intended to provide prompt publication of significant new research results and to permit an exchange of views on papers previously published in the JOURNAL. These communications are not submitted to formal review as are research papers, and the editors do not assume any share of the author's responsibility for the information given or the opinions expressed. When work previously published in the JOURNAL is the subject of critical comment, the authors of the original paper are given an opportunity to submit a reply, which will be published concurrently when possible.

## Micronaire Reading as a Close Approximation to Fiber Thickness

Agricultural Experiment Station
University of Tennessee
Knoxville, Tennessee
December 10, 1957

To the Editor
TEXTILE RESEARCH JOURNAL

*Dear Sir:*

It is most fortunate that there exists a scientifically defined scale of fiber fineness that is very closely approximated by the present micronaire scale. The proposed scientific scale values are shown in the third column of Table I. The closeness of the approximation is indicated by comparing Column III with Column I or II. Column I is an estimate of micronaire readings for the corresponding proposed readings based on the equation published by the Field Crops Research Branch of ARS–USDA [1] combined with the equation converting the linear scale to the curvilinear scale now widely used [2]. Column II is a similar empirical relation obtained in the Fiber Research Laboratory, University of Tennessee, using a single micronaire on several series of cottons by three different operators. It must be remembered that neither Column I or II is the best micronaire value obtainable. A better value should result by combining a number of instruments, operators, laboratories, and cottons under the best designed and controlled conditions. The values above were, however, serious independent attempts to relate micronaire readings to specific surface area. Other empirical correlations have been made, but there does not exist a universally accepted conversion of micronaire readings to any other fineness measurement.

**TABLE I. Comparison of Micronaire Reading with Equivalent Fiber Thickness and Specific Surface Area**

| Approximate micronaire readings | | Equivalent fiber thickness, $\mu$ | Specific surface area, $mm.^{-1}$ |
|---|---|---|---|
| I | II | III | IV |
| 6.9 | 7.3 | 6.7 | 300 |
| 6.0 | 6.3 | 5.7 | 350 |
| 5.1 | 5.3 | 5.0 | 400 |
| 4.4 | 4.5 | 4.4 | 450 |
| 3.7 | 3.8 | 4.0 | 500 |
| 3.2 | 3.3 | 3.6 | 550 |
| 2.8 | 2.9 | 3.3 | 600 |
| 2.5 | 2.7 | 3.1 | 650 |
| 2.4 | 2.5 | 2.8 | 700 |

The specific surface area of a cotton is defined as the ratio of the total external area of the fibers to their volume. This property is explicitly defined and can be determined by any one of a number of methods or combination of measurements that will give a measure of the total external surface of the fibers and of the total volume of the same fibers. The proposed scale in Table I is derived directly from specific surface area in $mm.^{-1}$ and is twice the reciprocal of specific surface area (Table I, Column IV) multiplied by 1000 to give the readings in microns. For want of a better name, the column might be headed "Equivalent Fiber Thickness."

Let us examine interpretations of the quantity,

"twice the reciprocal of specific surface area" (equivalent fiber thickness), both from the standpoint of the biologist and of the mill man. From the standpoint of the biologist the thickness of a fiber cell wall is especially significant. A fiber cross section in the uncollapsed state is represented diagrammatically in Figure 1a. In the final state, the fiber shrinks and the central lumen usually collapses, as shown in Figure 1b. It is probable that shrinking and collapsing occur simultaneously, but for purposes of simplification we can assume that Figures 1a and 1b represent the sections after shrinking. It can be shown that if the lumen ($2\pi r$) and external ($2\pi R$) perimeters as well as the area of cross section of fibrous material ($\pi R^2 - \pi r^2$) are preserved in collapsing from 1a to 1b, the thickness of the wall ($R - r$) is also preserved. If one divides the surface of lumen ($2\pi r$)$L$ plus exterior surface ($2\pi R$)$L$ by the volume of wall ($\pi R^2 - \pi r^2$)$L$ for a fiber segment of length $L$, one obtains $2/(R - r)$. Twice the reciprocal is then the wall thickness ($R - r$) of either 1a or 1b. The biologist and others would like nothing better than to be able to measure this wall thickness quickly and easily. In air flow instruments the lumen is not in contact with the flowing air and is therefore not directly involved as a part of the surface area. There is, however, a type of average wall thickness that can be read directly from an air flow instrument scale as proposed in Column III of Table I. In order to visualize this average wall thickness let us assume that the cell wall in Figure 1a uncollapsed or figure 1b collapsed is slit along the dotted line and then uncurled into a flat sheet with the length of both the lumen perimeter and the external perimeter unchanged. The thickest part of the sheet is $R - r$, or what is commonly considered the wall thickness. If, however, one takes the average thickness of the uncurled sheet, one obtains the equivalent wall thickness, which is the width of the rectangle (Figure 1b) having the same area. Twice this equivalent wall thickness is the equivalent fiber thickness and can be written as $2(\pi R^2 - \pi r^2)/2\pi R = R - (r/R)r$. The numerical values of equivalent fiber thickness are so near the present micronaire readings within the range of commercial cottons that it would require carefully designed and executed experiments to demonstrate a difference, if in fact one exists. Apparently real differences exist above and below the practical range where the present micronaire readings are already of questionable utility. The newly proposed scale would not only extend the present scale but would replace the empirical scale with a scientific scale easily defined and with only insignificant changes in the practical range.

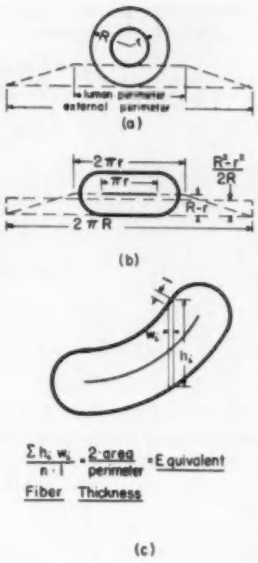


**Fig. 1.** Fiber cross section diagrams.

A second interpretation of equivalent fiber thickness is based on an average fiber thickness taken in a particular fashion. The average thickness might be obtained by taking the average distance across the cross section (Figure 1c) in parallel fashion at equal intervals. If these equal intervals are taken equidistant along the perimeter, some segments between parallels will be wider than others. It can be shown that the equivalent fiber thickness is the average distance across the cross section weighted according to the segment width. This method of weighting has the distinct advantage of giving a value independent of the direction of the parallels and hence is a measure of the fiber dimension regardless of orientation.

It should be noted that the double wall thickness $2(R - r)$ and the equivalent fiber thickness $R - (r/R)r$ are different but equally valid measurements of cell wall thickness. Their ratio is given in Table II for several values of $r/R$. Without some other measurement, such as perimeter or maturity, the idealized fiber cross section is not completely determined. The wide acceptance of micronaire reading indicates, however, that cell wall thickness or equivalent fiber thickness is an important property,

**TABLE II. Ratio of Equivalent Fiber Thickness to Twice Wall Thickness**

| Cotton | $\frac{r}{R}$ | $\frac{\text{Equivalent fiber thickness}}{\text{twice wall thickness}} = \frac{1+\frac{r}{R}}{2}$ |
|---|---|---|
| Very mature | 0.4 | 0.70 |
| Mature | 0.5 | 0.75 |
| Average | 0.6 | 0.80 |
| Immature | 0.7 | 0.85 |
| Very immature | 0.8 | 0.90 |

even though it gives only a part of the cross section information.

It is most fortunate that twice the cross-sectional area divided by the perimeter gives the equivalent fiber thickness directly and that this dimension is almost indistinguishable from the micronaire reading of wide practical usage. The adoption of the proposed scale would cause little difficulty in the market place and at the same time would give clarity and scientific standing to an otherwise practical but unclarified measurement.

### Literature Cited

1. *Comparison of Micronaire Readings and Arealometer Values,* USDA, ARS, December 1954, prepared in the Field Crops Research Branch, Beltsville, Maryland.
2. *Operating Instructions for the Sheffield Micronaire,* The Sheffield Corp., Dayton 1, Ohio, July 1, 1953, Catalog No. M01–753.

K. L. HERTEL

# The Occurrence of Myrothecium on Field Cotton

School of Textiles
Clemson Agricultural College
Clemson, South Carolina
January 20, 1958

To the Editor
TEXTILE RESEARCH JOURNAL

*Dear Sir:*

The fungi commonly found on normal field cotton and on cotton weathered before harvesting belong in large measure to only a few genera—*Alternaria, Cladosporium, Fusarium, Diplodia,* and sometimes *Colletotrichum*—and show much less variety than those found on stored raw cotton and on exposed cotton fabrics. A review of the species found is given by Marsh et al. [6, 7, 8], who introduced a simple method for identifying these fungi by placing small tufts of the cotton sample on a thin layer of 2% water agar and allowing a short period for incubation before examination. Using this method, the present author confirmed the above findings with field cotton from Clemson, S. C. and Athens, Ga. and found exactly the above-mentioned fungi [4]. In tightlock and boll rot of cotton, Arndt [1, 2] and Marsh [7, 8] found in addition to these fungi also a few other species (*Nigrospora, Rhizoctonia, Macrophominia, Rhinotrichum,* and *Curvularia*). These are to the author's knowledge the only fungi reported from field cotton.

In a bacteriological study of field cotton [5] the author used a substrate particularly suited for the growth of bacteria. It consisted of a sheet of purified cotton paper, placed on a thin layer of 1% agar, containing the following inorganic salts: $KNO_3$, 0.1 g.; $K_2HPO_4$, 0.1 g.; $MgSO_4$, 0.02 g.; $CaCl_2$, 0.01 g.; $FeCl_3$, 0.002 g.; tap water, 100 ml.; pH adjustment, 7.0–7.5. Although with this substrate mainly bacteria developed, also colonies of fungi were obtained. The most important of these were identified as *Myrothecium verrucaria* (Alb. & Schw.) Ditm. ex Fr. (= *Metarrhizium glutinosum* Pope) and *Stachybotrys atra* Corda. The occurrence of the first species appears to be of special interest, since it is considered to be the most powerful cellulose-destroying fungus known. It is actually more powerful than *Chaetomium,* and therefore has been widely introduced into the laboratory lately instead of *Chaetomium* in studies on preservation of cotton materials.

Although this fungus has been isolated a few times from exposed cotton cloth, it has not been found on raw cotton, and Siu remarks in his book [11], page 159, "It is not quite yet clear why Myrothecium verrucaria, which is about the most powerful cellulose-destroying species in the laboratory, is practically never observed fruiting or growing on cotton fabrics in the field . . ." On raw field cotton, the present author did not observe any fruiting either, but in filter paper cultures, conidia rapidly developed. A remarkable fact was that this fungus is often associated with a yellow *myxobacteria*. The author's identification was confirmed by comparison with standard material from USDA.[1]

With regard to taxonomy of this fungus, the reader is referred to the article by White and Downing [12], who first recognized its real nature, Preston [10], Pope [9], and Brian [3].

The other fungus, *Stachybotrys atra*, is also known to have a very high cellulose-destroying activity and has not yet been described to occur on field cotton.

A third interesting fungus, generally isolated from weathering cotton with this substrate, produced a deep purple *mycelium* on filter paper and destroyed the paper in a short time; under the microscope the hyphae show the same intense color, clearly contrasting with the affected fibers. It was not possible to obtain fructifications. Later on, commercial cotton samples were received from various mills, which samples showed spots of exactly the same purple color and which were found to contain the same purple *mycelium*.

The above observations show that by using other substrates than customary, cellulose-destroying fungi not reported so far can be isolated from field cotton.

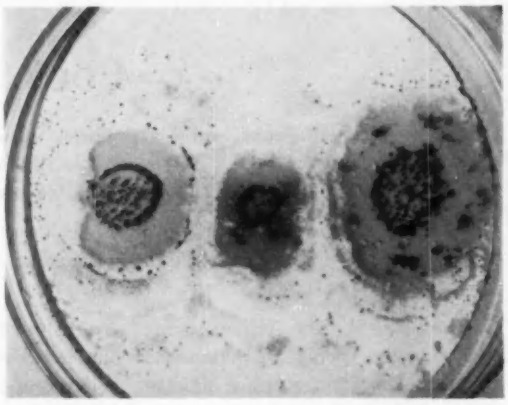

**Fig. 1.** Growth of *Myrothecium verrucaria* isolated from field cotton on filter paper substrate, showing typical glutinous, black, conidial masses and complete disintegration of paper around these centers.

## Literature Cited


1. Arndt, C. H., "Boll Rots of Cotton in South Carolina," *Plant Disease Reptr.* **34**, 176 (1950).
2. Arndt, C. H., "Tight Lock of Cotton, Associated Fungi and pH Values in South Carolina in 1952," TEXTILE RESEARCH JOURNAL **23**, 533–535 (1953).
3. Brian, P. W. and McGowan, J. C., "Biologically Active Metabolic Products of the Mold *Metarrhizium glutinosum* S. Pope," *Nature* **157**, 334 (1946).
4. Heyn, A. N. J., "Causes and Detection of Damage in Raw Cotton," *Textile Ind.* **120**, 137–145 (1956).
5. Heyn, A. N. J., "Bacteriological Studies on Cotton," TEXTILE RESEARCH JOURNAL **27**, 591–602 (1957).
6. Marsh, P. B. and Bollenbacher, K., "The Fungi Concerned in Fiber Deterioration. Art. I: Their Occurrences," TEXTILE RESEARCH JOURNAL **19**, 313–324 (1949).
7. Marsh, P. B., Guthrie, L. R., Bollenbacher, K., and Harrell, D. C., "Observations on Microbiological Deterioration of Cotton Fiber During the Period of Boll Opening in 1949," *Plant Disease Reptr.* **34**, 165–175 (1950).
8. Marsh, P. B., Merola, G. V., Bollenbacher, K., Butler, M. L., and Simpson, M., "The Effect of Weathering Prior to Harvest on Certain Properties of Cotton Fiber," *Plant Disease Reptr.* **38**, 106–119 (1954).
9. Pope, Seth, "A New Species of *Metarrhizium* Active in Decomposing Cellulose," *Mycologia* **36**, 343–350 (1944).
10. Preston, N. C., "Observations on the Genus Myrothecium Tode," *Brit. Myc. Soc. Trans.* **26**, 158–168 (1943).
11. Siu, R. G. H., "Microbial Decomposition of Cellulose," New York, Reinhold (1951).
12. White, W. L. and Downing, M. H., "The Identification of *Metarrhizium glutinosum*," Topical Report No. 20, Philadelphia, U. S. Army Quartermaster Biol. Laboratories, Dec. 1946; see also *Mycologia* **39**, 546 (1947).


A. N. J. HEYN

[1] The author wishes to express his thanks to Dr. P. B. Marsh, who kindly sent him an official USDA culture for comparison.

# Book Reviews

**Surface Active Agents and Detergents.** Vol. II. A. M. Schwartz, J. W. Perry, and J. Berch. New York, Interscience, 1958. 856 pages, 26 illust. Price $17.50.

*Reviewed by J. Edward Lynn, Colloid Chemical Engineer, Old Greenwich, Conn.*

Volume I, "Surface Active Agents," by Schwartz and Perry, has been an invaluable aid since 1949 to workers dealing with surface activity. When it was published, the authors planned to revise this volume periodically so that it would never be more than a few years out of date. Volume II is the result of the first attempt at revision and updating.

It was soon apparent that so much had happened in the surface agent field since 1949 that revision would result in either a very bulky volume, a two volume set, or inadequate coverage. The authors wisely chose to retain Volume I as the foundation and to use Volume II to cover new developments. Although owners of only Volume II may feel they are starting in the middle, a study of the ample references will allow them to cover the early ground or, preferably, Volume I can still be purchased for $12.00 a copy.

Volume II covers many diverse subjects, some of which might not appear to belong therein because we are not accustomed to think of their surface activity as being important. As the authors have ably demonstrated, especially in Part IV (200 pages) "Practical Applications of Surfactants," even these doubtful areas are germane.

References are ample and quite inclusive. However, the book is not a mere compendium of the literature, a class into which so many recent technical books seem to fall, but offers a good explanatory text which often becomes a conclusive critique of present knowledge.

The text type can be easily read and is set off from the page footnotes. While there are not many mechanical errors, this reviewer would be happier to see his name spelled the same way each time it appears. No technical errors were apparent in the sections of most interest to this reviewer.

"Surface Active Agents and Detergents," Volume II, can be recommended unequivocally as a definitive piece of literature which will never gather dust in a progressive laboratory. It should become the 'bible' and first reference source of workers in the field of surfactants, syndets, and surface phenomena.

---

**Handbook of Chemical Data.** F. W. Atack, Ed. New York, Reinhold, 1957. 629 pages. Price $6.75.

This compact reference book is an excellent compilation of chemical data, including physico-chemical constants, nomenclature of organic compounds, conversion tables, five-figure logarithm tables, mensuration formulae, a handy table of mechanical constants and their logarithms, etc.

Of special interest is the section on qualitative and quantitative analysis; concise yet comprehensive, it covers several schemes of analysis in an easy-to-follow format.

Containing the boiled-down data of a reference shelf of texts and weightier handbooks, this slim volume should be useful to chemists and chemical engineers in every field; it is of special value to the instructor or basic research worker as an accurate and timesaving source of information.